The Role of *CIL1* in *Brassica carinata* Lateral Meristem Development

A Thesis Submitted to the College of

Graduate Studies and Research

in Partial Fulfillment of the Requirements

for the Degree of Master of Science

in the Department of Biology

University of Saskatchewan

Saskatoon

By Shawn Gibson

PERMISSION TO USE

In presenting this thesis in partial fulfillment of the requirements for a postgraduate degree from the University of Saskatchewan, I agree that the libraries of this university may make it freely available for inspection. I further agree that permission for copying of this thesis in any manner, in whole or in part, for scholarly purposes may be granted by the professor or professors who supervised my thesis work or, in their absence, by the Head of the Department or the Dean of the College in which my thesis work was done. It is understood that any copying, publication, or use of this thesis or parts thereof for financial gain shall not be allowed without my written permission. It is also understood that due recognition shall be given to me and to the University of Saskatchewan in any scholarly use which may be made of any material in my thesis. Requests for permission to copy or to make other use of material in this thesis in whole or part should be addressed to:

Head of the Department of Biology

University of Saskatchewan

Saskatoon, Saskatchewan S7N 5E2

Canada

ABSTRACT

A cDNA sequence representing a *Brassica carinata* gene the expression of which is induced by copper chloride treatment, was isolated from a library constructed with mRNA from treated leaves, and designated *CIL1* (*COPPER CHLORIDE INDUCED* in *LEAVES*). A Basic Local Alignment Search Tool search revealed that *CIL1* has similarities to an auxin-induced gene, *AIR12* from *Arabidopsis thaliana*. Southern blot analysis of *CIL1* in *B. carinata*, *B. nigra* and *B. oleracea* indicated that it is a member of a small multigene family. Antisense *CIL1* transgenic plants were generated to investigate the function of *CIL1*, and the resulting transformants displayed increased secondary branching suggesting that *CIL1* has a role in regulating hormone content or plant architecture. Results of induction studies indicate that the auxin analog α-naphthalene acetic acid, the cytokinin 6-benzylaminopurine, and +/- abscisic acid increase expression of *CIL1*. Seven *CIL1* antisense lines were grown to the T_4 generation and were confirmed homozygous. Analysis of *CIL1* expression using real-time quantitative RT-PCR showed reduced expression in every examined line. Transgenic plants produced many leaves at the lateral meristems indicating a release of apical dominance. Additionally, the concentrations of auxins, cytokinins, and abscisic acid were altered in the roots and stems of transgenic plants compared to non-transformed plants. Therefore, *CIL1* has a role in regulating hormone content that affects lateral meristem activity, apical dominance, and leaf production.

ACKNOWLEDGEMENTS

I would like to take this opportunity to thank everyone who helped me throughout my Master's Degree study. I would like to thank my supervisor, Dr. Janet Taylor, for giving me this opportunity. I am grateful for her encouragement, financial support, and excellent supervision over the course of my research. I also want to express my thanks to Stephen Ambrose, who ran all of my samples for the phytohormone profiling portion of my thesis, his expertise and knowledge were invaluable, and to Sheila Chiwocha and Monica Lafond for help with the phytohormone extraction method. I appreciate the efforts of my advisory committee Dr. Peta Bonham-Smith and Dr. Sawhney who provided valuable input throughout the course of my research. I would also like to thank Dr. Gray for agreeing to be the external examiner for my defence.

Janet Condie, Carla Barber, Karl Schrieber, Sarah Steinbach, and Devin Polichuk were extremely helpful, both with assisting me with various techniques and interesting conversation to pass the time.

Most importantly, I thank my parents, David and Lorraine Gibson, and the rest of my family for financial support and putting up with my incessant ramblings regarding my project. My girlfriend, Sharla Lozinsky, deserves special thanks, as she was always a source of encouragement, love, support, and always believed in me.

TABLE OF CONTENTS

LIST OF TABLES

LIST OF FIGURES

LIST OF ABBREVIATIONS

α-NAA	α-Napthaleneacetic Acid
2,4-D	2,4-Dichlorophenoxyacetic Acid
2iP	2-Isopentenyladenine
7'-OH-ABA	7'-Hydroxy-Abscisic Acid
ABA	Abscisic Acid
ABA-GE	Abscisic Acid-Glucose Ester
ARF	Auxin Responsive Factor
ARE	Auxin Response Element
BAP	6-Benzylaminopurine
BLAST	Basic Local Alignment Search Tool
bp	Base Pairs
CA	Catecholamine
CB	Cytochrome *b*561 Electron Transport Domain
CID	Collision Induced Dissociation
DA	Dopamine
DoH	Dopamine-β-Hydroxylase
DPA	Dihydrophaseic Acid
DHZ	Dihydrozeatin
DHZR	Dihydrozeatin Riboside
dNTP	Deoxynucleoside Triphosphate
E	Epinephrine

ESI-MS/MS	Electrospray Ionization-Tandem Mass Spectrometry
GA	Gibberellic Acid
IAA	Indole-3-Acetic Acid
IAAsp	Indole-3-Aspartic Acid
IPA	Isopentenyladenosine
LM	Lateral Meristem
m/z	Mass to charge ratio
MRM	Multiple Reaction Monitoring
MS	Mass Spectrometry
PA	Phaseic Acid
PAT	Polar Auxin Transport
PE	Phenylethanolamine
PCR	Polymerase Chain Reaction
qRT-PCR	Real-Time Quantitative Reverse Transcriptase-Polymerase Chain Reaction
RT	Reverse Transcriptase
RAM	Root Apical Meristem
SAM	Shoot Apical Meristem
SDS	Sodium Dodecyl Sulfate
SSC	Sodium Chloride and Sodium Citrate
T_m	Melting Temperature of PCR Primers
TAE	Tris-Acetate-EDTA Buffer

Z	Zeatin
ZOG	Zeatin-*O*-Glucoside
ZR	Zeatin Riboside

1. INTRODUCTION

Brassica carinata, or Ethiopian mustard is an amphidiploid plant with the BB genome derived from *B. nigra* and the CC genome from *B. oleracea* (Snowdon et al., 1997). *B. carinata* has a number of traits that would make it useful as an oilseed crop for the Canadian prairies including resistance to *Leptosphaeria maculans*, the causative agent of blackleg disease, silique shattering resistance (Cohen and Knowles, 1983), high yield (Ferreres et al., 1983), and high protein content in the seed (Rakow and Getinet, 1998). *B. carinata* also has better tolerance to semi-arid conditions and drought stress compared to *B. napus* (Alemayehu and Becker, 2001). Despite these positive attributes, *B. carinata* is not appropriate for agricultural use at this time because of the high glucosinolate (Alemayehu and Becker, 2001) and high linolenic acid (Alonso et al., 1991) content of the seed and longer maturation time. Although, a *B. carinata* germplasm with low linolenic acid and zero erucic acid was recently generated (Velasco et al., 2004), it still takes 2-3 weeks longer to mature than *B. napus* resulting in underdeveloped seeds at the time of harvest (Getinet et al., 1996). Therefore, transferring the genes involved in the defense response of *B. carinata* to *B. napus* through marker-assisted breeding may be a more viable approach for the generation of canola cultivars with greater disease resistance (Marcroft et al., 2002).

The elucidation of the stress response pathways of *B. carinata* was the goal of a previous project that led to the discovery of *CIL1* (*COPPER CHLORIDE INDUCED* in *LEAVES*) (Uchacz, 2000; Zheng et al., 2001). As the name implies, the cDNA representing *CIL1* was isolated from a library of clones derived from mRNA of copper chloride treated *B. carinata* leaves. BLAST analysis of the *CIL1* cDNA did not reveal

any similarity to genes of known function. To gain some insight into the function of *CIL1*, a construct to express the gene in the antisense orientation was used to transform *B. carinata* plants to reduce expression of the gene (Z. Zheng and T. Uchacz, unpublished). Transformed plants displayed increased axillary branching during reproductive growth. This observation led to the hypothesis that *CIL1* influences hormone content, specifically the auxin:cytokinin ratio in *B. carinata*. This study was undertaken to further characterize *CIL1* and compare the hormone content of homozygous antisense transgenic plants to non-transformed plants.

2. LITERATURE REVIEW

2.1 General Overview

Organisms in the Kingdom Planta are ubiquitous throughout almost every region of the planet, colonizing areas ranging from mountains to grasslands. Despite the incredible diversity found in plants, they have a multitude of aspects common to their growth and development. In dicotyledonous plants, after germination has occurred, growth proceeds from the shoot apical meristem (SAM). In the SAM, new cells are constantly being produced that subsequently differentiate to fulfill specific functions.

Generally, leaves are produced from the shoot apical meristem of plants (Figure 2.1). The number of leaves produced at a lateral meristem, in addition to the number of nodes produced on a plant, is governed by both genetic and environmental controls. A number of genes have been isolated that act as transcriptional regulators of lateral meristem growth including *LATERAL SUPPRESSOR* (*LS*) (Williams, 1960) and *BLIND* (*BL*) (Schmitz et al., 2002) from tomato, and *REVOLUTA* (*REV*) (Otsuga et al., 2001) from *Arabidopsis thaliana*. A regulator of lateral organ size, *ARGOS* has also been discovered (Hu et al., 2003). Additionally, a mutation, designated as *supershoot* (*sps),* in a structural gene involved in cytokinin biosynthesis greatly enhanced the growth of axillary branches during the reproductive stage of the life cycle of *A. thaliana* (Tantikanjana et al., 2001).

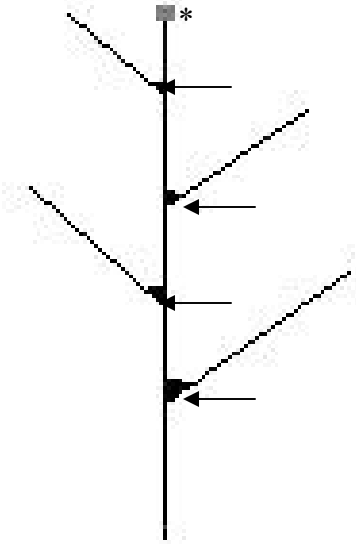

Figure 2.1 Diagram of the morphology of a dicotyledonous plant, showing the main stem, branches, lateral meristems (half circles), and shoot apex. The lateral meristems are indicated by arrows, while the shoot apex is indicated by an asterisk.

There are two prevalent hypotheses regarding the origin of lateral meristems. The first proposes that initiation can occur from cells derived from the shoot apical meristem that retain their meristematic identity (Garrison, 1955; Sussex, 1955). The second hypothesizes that cells in the leaf axil initiate meristematic cells *de novo* (Snow and Snow, 1942). After initiation, the *B. carinata* lateral meristem produces one leaf then the lateral meristem activity is inhibited unless some of the antagonists of lateral meristem growth are removed, or until the plant enters the reproductive stage of growth.

2.2 Plant Development and Phytohormones

Lateral meristem activity is regulated by phytohormones. Phytohormones are natural compounds that, at very low concentrations, (Romanov, 2002; Gaspar et al., 2003) act as signaling molecules to activate physiological processes. Phytohormones are

set apart from their mammalian counterparts for a number of reasons. Phytohormones can be synthesized in any living cell in the plant, though there are generally specific organs that synthesize the majority of a phytohormone (Gaspar et al., 2003), and phytohormone activity can occur in the cell they are synthesized in, or after transport to a target cell. Mammalian hormones, on the other hand, are synthesized in a specific organ, usually endocrine glands, and travel through the blood to the target cell, which responds to the hormone (Campbell et al., 1997).

Phytohormones are responsible for a wide range of phenomena that occur during the growth, development, and reproduction of a vascular plant. Historically, there were five classes of phytohormones: auxins, cytokinins, gibberellins, abscisic acid, and ethylene (Taiz and Zeiger, 1998). Recent advances have lead to the identification of several other signaling molecules present at low concentrations throughout the plant, such as brassinosteroids, jasmonic acid, and salicylic acid (Taiz and Zeiger, 1998).

Lateral meristem activity can be both promoted and inhibited in the presence of different phytohormones. Auxins inhibit the activity of the lateral meristem, however, the inhibition decreases the farther a lateral meristem is from the shoot apex (Cline, 1996; Leyser, 2002). Cytokinins, on the other hand, promote the growth of lateral meristems (Taiz and Zeiger, 1998), and thus auxins and cytokinins act as antagonists during lateral meristem development. Research has demonstrated that auxin does not directly affect the growth of lateral meristems, and may act through a second messenger, possibly cytokinin (Chatfield et al., 2000). However, this theory is tenuous, as cytokinin appears to independently regulate lateral meristem growth (Chatfield et al., 2000). Genes likely involved with perception or transduction of a secondary messenger have been isolated,

though the identity of the secondary messenger remains elusive (Beveridge, 2000; Stirnberg et al., 2002). The *rms* and *max* mutant in pea and *A. thaliana*, respectively, showed increased branching, as well as a decreased response to apically applied auxin, after decapitation (Beveridge, 2000; Beveridge et al., 2000; Stirnberg et al., 2002; Turnbull et al., 2002; Sorefan et al., 2003). The *RMS* and *MAX* genes were found to be orthologous and encode auxin-inducible polyene dioxygenases that function downstream of auxin in the production of a lateral meristem-inhibiting signal.

Additional small molecules that affect plant growth are the catecholamines (CA) which are mammalian neurotransmitters that have also been found in plants. These compounds were shown to exhibit cytokinin (Christou and Barton, 1989; Kuklin and Conger, 1995) and indole-3-acetic acid oxidase antagonist (Protacio et al., 1992) activities. The biosynthesis of catecholamines is stimulated by abscisic acid (Sweidrych et al., 2004). To date, the role of catecholamines in plant systems is unknown, though there is some evidence that suggests they are involved in the response to wounding (Swiedrych et al., 2004). The relevance of these compounds to CIL1 function will be discussed in detail later.

2.2.1 Auxin

Auxin, derived from the Greek term *auxein*, to increase, was the first of the five classic phytohormones to be discovered. The action of auxin was described first by Darwin (1880), when he observed that the apex of an oat coleoptile would bend toward a unidirectional source of light. Furthermore, when the apex was excised the coleoptile would grow vertically in one direction, regardless of the direction of the light source.

This coleoptile technique for detecting and observing curvature was perfected and refined by other researchers, who demonstrated that the apex was responsible for sending a chemical signal that directed growth, and that the signal would direct growth even in complete darkness (Boysen-Jensen, 1913; Paal, 1919; Went, 1926).

The phytohormones auxin and cytokinin are different from the other phytohormones in that they are an absolute requirement for viability (Taiz and Zeiger, 1998). To date, no mutants completely lacking either of these phytohormones have been isolated.

The most recognizable role of auxin is the phenomenon of apical dominance. Auxin synthesized in the apex of the plant is transported basipetally and acts on lateral buds to inhibit their growth. It was demonstrated that when the SAM is removed, plants begin to branch extensively. Auxin is also required for cell elongation, and has differing effects depending on the organ in which it is present; it stimulates elongation in the shoot, but inhibits it in the root (Taiz and Zeiger, 1998; Crozier et al., 2000). In addition to cell elongation, auxin is also involved in photo- and gravitropism, the processes whereby a plant grows toward light and gravity, respectively. Darwin demonstrated phototropism in 1880, while gravitropism was demonstrated later by Went (1926). Auxin also affects the differentiation of vascular tissue and vascular patterning in leaves (Naderi et al., 1997; Taiz and Zeiger, 1998). Recent research further suggests that auxin may be integral in regulating embryogenesis and plant totipotency (Ribnicky et al., 2002).

The most abundant naturally occurring auxin in plants is indole-3-acetic acid (IAA) (Bartel, 2001). IAA is synthesized by two main methods, tryptophan (Trp)-dependent, which uses the amino acid as a precursor or Trp-independent biosynthesis,

which uses indole-3-glycerol phosphate as a precursor in an as yet unknown pathway to IAA (Bartel, 2001; Coruzzi and Last, 2000; Crozier et al., 2000). The preferred method of IAA biosynthesis in plants was found to depend on the ambient temperature. In *Lemna gibba* at a temperature of 15 ^{o}C Trp-dependent IAA biosynthesis was favored, while at a temperature of 30 ^{o}C Trp-independent biosynthesis was favored (Rapparini et al., 2002). Further, Trp-dependent IAA biosynthesis occurs during periods of high auxin demand such as seed germination, embryo growth, or the wounding response. A sustained low amount of IAA is synthesized via the Trp-independent pathway during vegetative growth (Normanly and Bartel, 1999; Bartel et al., 2001). Biosynthesis of IAA in *A. thaliana* varies with the age of the plant, with the youngest organs having the highest IAA synthetic capacity and the older organs that have ceased cell division having the lowest capacity (Ljung et al., 2001). Although all parts of a young *A. thaliana* plant can contribute to the auxin pool, the leaves that are less than 0.5 mm in length have the highest synthetic capacity (Ljung et al., 2001).

After IAA is synthesized, it is transported throughout the plant by two methods: polar auxin transport (PAT), and phloem transport (Friml and Palme, 2002). Phloem transport is fast and non-directional. It is used to transport inactive auxin conjugates in addition to physiologically active auxins (Nowacki and Bandurski, 1980). Conversely, PAT is unidirectional, occurring in a cell-to-cell manner and is specific for active free auxins moving in a basipetal or lateral direction from the auxin source (Friml and Palme, 2002; Friml, 2003). Auxin transport is important for flower development and proper patterning of the vascular system in leaves (Naderi et al, 1997; Oka et al., 1999; Dengler and Kang, 2001). Impeding PAT results in a wide range of phenotypic abnormalities.

These abnormalities range from flower aberrations, including petal fusion and reduction, to whole plant effects, such as irregular shaped leaves with abaxial fusions to the adaxial side, and development of additional cotyledons (Naderi et al., 1997; Oka et al., 1999; Friml and Palme, 2002).

Metabolism of IAA occurs through catabolism or conjugation. Conjugated IAA is a source of readily accessible IAA that can be used when required (Bialek and Cohen, 1989). In *Lycopersicon esculentum,* IAA is conjugated through the addition of a glucose residue to the carboxyl group of the IAA side chain to form I-*O*- (indole-3-acetyl)-*B*-glucose (Crozier et al., 2000; Tam et al., 2000). The glucose side chain can be removed through the action of a β-glucosidase. Catabolism, which occurs through amino acid intermediates, irreversibly inactivates IAA and as a result, decreases the total IAA pool (Crozier et al., 2000). The rate of IAA turnover can be calculated through comparison of the amount of IAA catabolites relative to IAA.

Despite its importance to plant growth and development, the mechanisms of auxin response are only recently becoming elucidated through examination of the perception, action, and outcome of auxin application. The full manner in which auxin is perceived is still in question. However, both a membrane bound auxin binding protein (ABP1) and an intracellular auxin uptake carrier (AUX1) have been discovered (Hertel et al., 1972; Bennett et al., 1996). At this point, the purpose of multiple perception sites is not clear, but the versatility and redundancy is advantageous should a mutation occur.

Auxin response factors (ARF) are transcription factors that bind to the auxin response elements (ARE) present in the promoters of auxin-inducible genes (Ulmasov et al., 1997a). Conversely, promoter binding is inhibited by ARF interaction with dimers of

the AUX/IAA protein (Ulmasov et al., 1997b; Guilfoyle et al., 1998; Liscum and Reed, 2002; Dharmasiri and Estelle, 2002). After auxin treatment or during periods of auxin-induction, the ARF-AUX/IAA interaction is most likely disrupted through phosphorylation of AUX/IAA (Dharmasiri and Estelle, 2002). Data suggest that auxin regulates the degradation of AUX/IAA by AXR1 after dissociation from ARF (Leyser et al., 1993; Zenser et al., 2001). *AXR1* encodes a protein with similarity to an ubiquitin-activating enzyme and multiple *AXR* genes are required for normal auxin function (Berleth et al., 2004).

The molecular mechanisms for PAT are intricate and remain elusive. Carrier proteins located in the plasma membrane facilitate the influx and efflux of auxin (Morris, 2000). A putative auxin influx carrier, AUX1, has been identified in *A. thaliana*. It has similarity to a family of plant and fungal amino acid permeases, suggesting a transport function (Bennett et al., 1996). The *aux1* mutant was isolated in a screen for *A. thaliana* plants with diminished root elongation (Maher and Martindale, 1980). The *aux1* mutants displayed a delayed response to inhibitory amounts of exogenously applied IAA suggesting that uptake was affected (Evans et al., 1994). To examine this phenomenon in greater detail, root growth in the mutants was measured after treatment with IAA, 2,4-dichlorophenoxyacetic acid (2,4-D), and α-napthaleneacetic acid (α-NAA) (Yamamoto and Yamamoto, 1998). Treatment with α-NAA rescued the agravitropic root growth of *aux1* plants because it, unlike IAA and the other auxin analogues, diffuses through the plasma membrane (Marchant et al., 1999; Morris, 2000). Further examination of the *aux1* mutant revealed that it accumulated less than half the amount of 2,4-D as wild type plants as opposed to accumulating the same amount of α-NAA (Marchant et al., 1999).

Since AUX1 is confined to the roots (Marchant et al., 1999; Swarup et al., 2001), other auxin influx carriers must exist in the other parts of the plant, though none have been isolated to date.

The auxin efflux carriers are much better understood than the influx carriers. Auxin efflux research was facilitated by the discovery of auxin efflux inhibitors (Morris, 2000). Auxin efflux carriers are believed to be multi-component systems, consisting of transport, catalytic, and regulatory domains (Morris, 2000). The first identified auxin efflux carrier gene was *AtPIN1* (*A. thaliana PIN-FORMED*) (Galweiler et al., 1998). In *pin1* mutants, PAT is perturbed in the inflorescences whose pinnate apices develop into only a few, if any flowers. PIN1 was localized to the basipetal region of apical cells, transporting auxin from leaves into the vascular bundle. Two other *PIN* genes were found that function in different organs in *A. thaliana*. PIN2 was localized to meristematic and elongating regions (Muller et al., 1998) while PIN3 was localized to the columella initial cells of the root tip and on lateral membranes of endodermal cells in young stems (Friml et al., 2002). Recent research showed that PIN protein location determines auxin transport routes and that they are necessary for maintenance of the meristem zone in the root (Blilou et al., 2005).

Recent discoveries are shedding light on how PIN proteins and PAT are regulated in *A. thaliana*. It was found that *PLT* (*PLETHORA*) genes regulate the distribution of *PIN* mRNA while PIN proteins inhibit the expression of *PLT,* thus demonstrating the complexity of the interactions necessary for normal vascular patterning to occur. Depending on the concentration of PID (PINOID), a protein kinase, the localization of PIN switches at the intracellular level from basal to apical (Friml et al., 2004). Sub-

threshold amounts of PID result in basal localization of PIN while above-threshold amounts result in apical deposition of PIN. This switching directs auxin transport from cotyledons to either emerging primordia in the meristem or to the root for growth of the root apical meristem (RAM) (Kaplinsky and Barton, 2004). The switching also directs auxin from young leaves to emerging primordia or to the root, similar the cotyledons. In the root, TINY ROOT HAIR 1 (TRH1) is a putative potassium carrier required for auxin transport to root hairs (Vicente-Agullo et al., 2004). Plants with reduced TRH1 are impaired in auxin efflux from the stele, resulting in an agravitropic phenotype (Vicente-Agullo et al., 2004).

2.2.2 Cytokinins

A cytokinin, by definition, is a compound that induces cell division in plant tissue cultures in the presence of optimal auxin concentration. The first compound isolated that induced plant cytokinesis was derived from autoclaved herring sperm (Miller et al., 1955). The compound was identified as 6-(furfuryl)aminopurine and named kinetin. Kinetin promotes tobacco pith parenchyma differentiation in culture and stimulates totipotent plant cell growth (Sieberer et al., 2003). However, kinetin is not found in plant tissue and is likely the result of a rearrangement in heated DNA. The first naturally occurring cytokinin, zeatin (Z), was isolated from coconut liquid endosperm. Zeatin supports indefinite cell division in culture (Caplin and Steward, 1948). The first synthetic cytokinin found to effect plant growth in a similar manner was 6-benzylaminopurine (BAP), it is commonly used as a cytokinin in many studies

(http://www.chemicalland21.com/lifescience/agro/6-BENZYLAMINOPURINE.htm, first accessed July 2005; Walker and Leonard, 1974; Rulcova and Pospilova, 2001).

Cytokinins, like auxins are essential for many plant developmental processes (Taiz and Zeiger, 1998). These compounds enhance branching (Wang and Below, 1996), delay senescence (Richmond, 1957), and promote chlorophyll biosynthesis (Kato et al., 2002). To examine the effect of cytokinins on leaf senescence Richmond (1957) incubated *Xanthium pennsylvanicum* leaves in a kinetin solution for 10 days and compared their senescence to leaves incubated in water. He found that the kinetin-incubated leaves remained green while the water-incubated leaves senesced. Further, Gan and Amasino (1995) were able to delay senescence by transforming tobacco with a senescence associated gene promoter (SAG12)::*ISOPENTENYL TRANSFERASE* construct. The prolonged senescence was attributed to cytokinin biosynthesis occurring after the induction of the SAG12 promoter by the senescence-signaling pathway. It was shown that the cytokinin, zeatin-*O*-glucoside (ZOG), thought to be a storage form of Z, promotes chlorophyll biosynthesis in the shoot of young *Cucurbita maxima* up to 100 times more effectively than either Z or zeatin riboside (ZR), (Kato et al., 2002). Cytokinins also contribute to the growth and development of meristematic organs and enhance shoot formation (Johnston and Jeffcoat, 1977; Wang and Below, 1996). In the shoot, cytokinins act as positive regulators of SAM cell proliferation while acting as negative regulators in the root apical meristem (Werner et al., 2003).

Cytokinins are synthesized *de novo* or via the tRNA pathway (Brzobohaty et al., 1994; Crozier et al., 2000). The primary site of cytokinin biosynthesis is the root and the majority of cytokinins are synthesized *de novo* using isoprene (dimethylallyl

diphosphate) and adenosine-5'-monophosphate as precursors (Taya et al., 1978; Chen and Melitz, 1979; Crozier et al., 2000). The most physiologically active form of cytokinin is zeatin. Zeatin riboside (ZR) is also physiologically active and is the form of cytokinin that is transported from the roots to other regions of the plant (Taiz and Zeiger, 1998; Crozier et al., 2000). The intermediate forms of Z and ZR, isopentenyladenine (2iP) and isopentenyladenosine (IPA), respectively, have limited cytokinin activity. The two remaining naturally occurring cytokinins are dihydrozeatin (DHZ), and dihydrozeatin riboside (DHZR). Both these compounds are less physiologically active than the other cytokinins in most plants, except in some legumes, and are more difficult to metabolize (Crozier et al., 2000).

Cytokinins are transported from the roots to the destination organs through the xylem in the form of ZR (Nooden and Letham, 1993). At the destination organ, hydrolysis of ZR yields Z that subsequently may be glycosylated to form zeatin-O-glucoside (ZOG), a reversible form of Z (Taiz and Zeiger, 1998) that was thought to be inactive.

Unlike auxin transport, very little is known about the mechanisms of cytokinin transport. However, Burkle et al. (2003) discovered a family of purine transporters that act as carriers of both adenine and cytokinins.

Similar to cytokinin transport our knowledge of the mechanisms of cytokinin perception was, until recently, very limited. The situation began to change with the discovery of the histidine kinase homolog *CKI1* (*CYTOKININ INDEPENDENT*) in *A. thaliana* (Kakimoto, 1996). Overexpression of *CKI1* in *A. thaliana* induced cytokinin responses, implying an interaction between CKI1 and cytokinins. CKI1 was proposed to

be a member of a two-component regulator. Two-component signal transduction pathways sense a signal through a histidine kinase and react through a response regulator (Hwang and Sheen, 2001). These two-component systems are present in both prokaryotes and plants (Heyl and Schmulling, 2003). Subsequent attempts at detecting cytokinin receptor activity from CKI1 were unsuccessful, so its role in cytokinin perception remains unknown (Higuchi et al., 2004).

The first identified gene for a cytokinin receptor in *A. thaliana* was *CRE1* (*CYTOKININ RESPONSE 1)*, encoding a histidine kinase (Inoue et al., 2001). The *cre1* mutants generated were insensitive to exogenously applied kinetin (Inoue et al., 2001). Other groups also isolated this gene and designated it *WOL* (*WOODEN LEG*) and *AHK4* (*A. THALIANA HISTIDINE KINASE 4*) (Mahonen et al., 2000; Ueguchi et al., 2001). However, the function was not assessed until Inoue et al. (2001) discovered it as *CRE1*. Two other histidine kinases, AHK2 and AHK3, have similarity to CRE1 (Inoue et al., 2001; Higuchi et al., 2004). AHK2 and AHK3 function as cytokinin receptors in different regions of the plant (Higuchi et al., 2004). Further, all three receptors have overlapping roles in the regulation of shoot and root growth in *A. thaliana* (Nishimura et al., 2004). A study examining the expression of *CRE1*, *AHK2*, and *AHK3* in *A. thaliana* revealed that *CRE1* was highly expressed in the root, with lower expression in rosette leaves, while *AHK3* showed the opposite pattern (Higuchi et al., 2004). *AHK2*, however, was expressed in both the roots and the rosette leaves at similar concentrations to *AHK3* and *CRE1*, in the rosette leaves and roots, respectively. To assess the roles of the receptors Higuchi et al. (2004) generated double and triple mutants. Callus cultures of single mutants in *ahk2* or *ahk3* respond to exogenous cytokinin similar to wild type. The

cre1 callus cultures are smaller and have a reduced response to cytokinin compared to wild type (Inoue et al., 2001; Ueguchi et al., 2001). Double and triple mutants of *cre1*, *ahk2*, *ahk3* showed further reduced responses, demonstrating the redundancy of the cytokinin receptor genes (Higuchi et al., 2004). The triple mutants also displayed altered root growth, suggesting that AHK3 and CRE1 are key regulators of adventitious root growth in *A. thaliana*.

Soon after the discovery of the *CRE1* gene in *A. thaliana*, additional components of the cytokinin response pathway were found. Initial research by Brandstatter and Kieber (1998) indicated that some *ARR* (*A. THALIANA RESPONSE REGULATOR*) genes responded to cytokinin treatment. Later Sakai et al. (2000, 2001) discovered that ARR1 and ARR2 act as transcriptional activators after cytokinin-receptor binding.

The model for cytokinin action begins with binding of the compound to a receptor on the plasma membrane. This binding triggers phosphorylation of the receiver domain of the receptor. Subsequently, histidine phosphotransfer proteins phosphorylate the receiver domains of B-type ARR proteins and these transcription factors activate other *ARR* gene expression (Heyl and Schmulling, 2003). The response is dependent on the plant organ and developmental stage. For years, the pathway of cytokinin action was unknown then the molecular mechanisms of cytokinin signaling went from being poorly understood to one of the best-elucidated pathways in a very short time.

2.2.3 Abscisic Acid

Two groups simultaneously discovered the compound now known as abscisic acid (ABA) in 1963. One group named the molecule “abscisin II” (Ohkuma et al., 1963) for

its putative role in leaf abscission, later disproved, and the other group named the molecule "dormin" (Eagles et al., 1964) for its role in bud dormancy. Subsequently, the name "abscisic acid" was given to this phytohormone, despite the fact that ABA has no role in leaf abscission (Addicott et al., 1968). ABA has roles in dormancy, freezing tolerance, drought tolerance, and water flux in the roots. Unlike auxins and cytokinins, abscisic acid is not an absolute requirement for plant growth and development (Koornneef et al., 1998). However, the loss of ABA sensitivity results in phenotypic aberrations.

One of the most well characterised roles of ABA is negative regulation of stomatal opening during periods of low water potential. Water flux in plants is perceived in the roots (Mantyla et al., 1995; Taiz and Zeiger, 1998). Specifically, the interruption in water uptake is sensed in lateral roots and root hairs and induces ABA transport through the xylem to the photosynthetically active leaves (Hetherington, 2001; Schroeder et al., 2001). The ABA concentration in the xylem sap increases from approximately 1-15 nM to 3 μM (Schurr et al., 1992) in *Helianthus annulus* plants when water uptake is interrupted. In leaves, ABA enters the guard cells and triggers a series of signal cascades that lead to loss of turgor pressure and stomata closure (Schroeder et al., 2001).

Seed dormancy and desiccation tolerance are also influenced by ABA. Determination of the ABA content in seeds from a dormant ecotype of *A. thaliana*, Cape Verde Islands, demonstrated that ABA content was highest in dormant seeds and subsequently decreased under seed-breaking conditions finally reaching a concentration similar to non-dormant seeds (Ali-Rachedi et al., 2004).

2.2.4 Ethylene

Neljubow (1901) discovered that ethylene was the active ingredient of coal gas that caused defoliation of plants. Later, Cousins (1910) found that plants themselves produced ethylene. Ethylene has roles in fruit ripening, anaerobic stress response, leaf and flower abscission, flower senescence, and the breaking of seed dormancy in cereals (Doubt, 1917; Chang et al., 1993; Taiz and Zeiger, 1998 Vogel et al., 1998).

Ethylene, unlike all other plant hormones, is a gas under physiological conditions (Chang et al., 1993; Rodrigues-Pousada et al., 1999) and has a simple structure. Plants grown in darkness or in the presence of ethylene and light combined exhibit the "triple response". The triple response consists of diageotropism, inhibition of epicotyl elongation, and lateral enlargement of the epicotyl (Vogel et al., 1998; Bleecker, 1999; Crozier et al., 2000; Johri and Mitra, 2001). The triple response is a classical way of examining the sensitivity of plants to ethylene. The more attenuated the response, the less sensitive a plant is to ethylene. Complete attenuation of the triple response results in seedlings that resemble light grown seedlings, as is seen in the *etr1-1* (*ethylene-resistant 1*) mutant of *A. thaliana* (Chang et al., 1993). The gene was later found to encode an ethylene receptor functioning at the very onset of ethylene signaling (Chang et al., 1993; Bleecker, 1999).

Ethylene is synthesized from *S*-adenosyl-L-methionine through the intermediate 1-aminocylopropane-1-carboxylic acid (ACC). The initial reaction is catalyzed by ACC synthase with subsequent conversion to ethylene through the action of ACC oxidase (Crozier et al., 2000). Transgenic tomato plants expressing an antisense ACC oxidase construct produced fruit that made only 5% of the amount of ethylene made by fruit from

non-transformed plants. As a result, the fruit ripened but did not over ripen demonstrating the impact of ethylene (Crozier et al., 2000). Ethylene-insensitive plants, on the other hand, produce fruit that never ripen because the ethylene sensing mechanism is impaired.

2.2.5 Gibberellic Acid

Gibberellic acid (GA) was initially isolated from a culture of the fungal pathogen of rice *Gibberella fujikoroi* (Yabuta and Sumiki, 1938). The first publications on isolation of GA-like compounds from higher plants did not appear until the 1950's (Mitchell et al., 1951; Radley, 1956). Rice plants infected with *G. fujikoroi* grow very tall suggesting that GAs stimulate plant growth. Thus the most notable action of GA on plant growth and development is in stem elongation, however, GAs also influence a variety of other developmental processes such as seed germination, floral initiation and sex determination (Langridge, 1957; Taiz and Zeiger, 1997; Richards et al., 2001).

Gibberellins differ from other phytohormones in that there are over 100 identified forms, although only a few are biologically active (Richards et al., 2001). The biosynthesis of GA is very complex, involving a large number of intermediate forms leading to the most commonly found biologically active form, GA_3 (Phillips, 1998).

The role of GA in plant development has been investigated in a number of plants including barley, rice, pea, and *A. thaliana* (Richards et al., 2001). In *A. thaliana*, a long-day plant, it was found that two gibberellin mutants, *gai* (*gibberellic acid insensitive*), and *ga1-3*, showed altered reproductive development (Koornneef and van der Veen, 1980; Wilson et al., 1992). The *ga1-3* mutant never flowered under short-day conditions,

while the *gai* mutant flowered 20 days later than wild type *A. thaliana* Landsberg *erecta*. Although the *ga1-3* mutants never flowered in short-day conditions, with continual light they flowered 11 days later than wild type *A. thaliana*. After treatment with GAs, in continual light the *ga1-3* mutants flowered at a time comparable to the wild type *A. thaliana*, demonstrating that GA is required for the transition from vegetative to reproductive growth in long-day plants. This result suggested that an additional mechanism is involved in the transition from vegetative to reproductive growth.

2.3 Phytohormone Cross-Talk

Normal plant growth and development requires phytohormones to interact to regulate the various processes. This interaction is termed "cross-talk".

2.3.1 Auxin and Cytokinin

Skoog and Miller (1957) were the first to discover cross-talk when they observed that the ratio of auxin:cytokinin influenced organogenesis in plant tissue culture. An equal amount of auxin and cytokinin induced callus growth, while a higher auxin:cytokinin ratio induced root growth, and a lower auxin:cytokinin ratio stimulated shoot growth. Another plant response governed by the interaction of auxin and cytokinin is gravitropism. Prior to a graviresponse, cytokinins accumulate within stratocytes, resulting in decreased root elongation, while auxins, transported to the lateral roots by PIN3, stimulate root elongation (Friml et al., 2002; Aloni et al., 2004). The antagonism of the auxins and cytokinins in the roots results in differential growth. This differential growth rate produces root curvature. These data indicated that auxins and cytokinins

were antagonists. Further evidence of auxin to cytokinin antagonism is seen in leaf primordia in *A. thaliana*. Auxin-induced repression of *KNOX* (*KNOTTED1-LIKE HOMEOBOX*) expression in leaf primordia is necessary for correct leaf initial growth (Scanlon, 2003). The KNOX proteins may induce cytokinin biosynthesis (Ori et al., 1999; Hay et al., 2004).

Auxin to cytokinin antagonism includes each hormone's effects on the concentration of the other (Palni et al., 1988; Nordstrom et al., 2004). Although Palni et al. (1988) found that treating plants with α-NAA increased oxidative metabolism of ZR, it was eventually shown that cytokinins and auxins regulate each other by decreasing the rate of biosynthesis and transport rather than catabolism (Bangerth, 1994; Eklof et al., 1997). However, conversion of the active cytokinins, zeatin (Z) and zeatin riboside (ZR) in most plants to the inactive *N*-glycosylated forms is increased in the presence of auxin (Blagoeva et al., 2004).

The relationship between auxin content and cytokinin biosynthesis was examined in greater detail in *A. thaliana* plants treated with α-NAA. In a dose dependant manner, the treatment caused a decrease in the amount of both ZR and its precursor by acting on the isopentenyladenosine-5'-monophosphate independent pathway (Nordstrom et al., 2004). Auxin perception by the *AXR* gene family mediates this effect on cytokinin biosynthesis.

Unlike the fast reduction in cytokinin amounts seen after auxin treatment (Bangerth, 1994), cytokinin repression of auxin occurs over a much longer period, requiring up to 48 h (Nordstrom et al., 2004). These authors concluded that cytokinins indirectly influence auxin content. Bangerth (1994) proposed that auxin to cytokinin

cross-talk was a two-sided feedback loop involving auxin transport from the SAM and cytokinin transport from the root. Subsequent research by Bangerth (2000) and others (Eklof et al. 1997; Haver et al., 2003) indicated that feedback inhibition of auxin and cytokinin biosynthesis in the presence of high concentrations of the antagonist phytohormone was due to a decrease of IAA biosynthesis in the shoot apex and cytokinin biosynthesis in the root.

Auxin and cytokinin do not always act as antagonists. In very young organs, they are thought to interact synergistically to control progression of the cell cycle. One of the earliest studies on the roles of auxin and cytokinin in the cell cycle examined the effect of the hormones on $p34^{cdc2}$-like proteins; protein kinases activated when a cell is committed to division (Choi et al., 1991). In tobacco pith, auxin induces biosynthesis of a $p34^{cdc2}$-like protein and cytokinin is required for activation of the protein (John et al., 1993). In alfalfa leaf protoplast-derived cells, the absence of cytokinin completely abolished cdc2MsA/B activity, preventing cell cycle progression from the G_0-G_1 phase to S phase and from the G2 phase to mitosis. Further, in the absence of auxin, cyclin dependent kinases could not be isolated from the cells (Pasternak et al., 2000). Sieberer et al. (2003) obtained additional evidence for the interaction of auxin and cytokinin in cell cycle control. The *prz1*-1 (*proporz*) mutant was isolated from a screen for seedlings showing defective growth on auxin and cytokinin from a T-DNA-mutagenized population of *A. thaliana*. When *prz1-1* plants were grown in the presence of auxin and cytokinin uncontrolled cell proliferation increased dramatically. *PRZ1* appears to be a gene involved in the switch from cell proliferation to cell differentiation. It is a putative

transcriptional adaptor protein involved in the transcription of a cell cycle control protein (Sieberer et al., 2003).

Auxin and cytokinin also act synergistically to regulate cell differentiation. The highest concentrations of auxin and cytokinins are seen in young leaves (Nordstrom et al., 2004). The SAM was also found to contain high amounts of auxins and cytokinins, both of which were necessary for SAM cell division (Werner et al., 2001). Cytokinin rapidly induces expression of the *A. thaliana* response regulator *ARR4* (Yamada et al., 1998). In turn, ARR4 interacts with AtDBP1, a DNA binding protein (Alliotte et al., 1988). The interaction between ARR4 and AtDBP1 is induced by exogenous auxin, as part of an indirect, long-term auxin response (Yamada et al., 1998). This auxin- and cytokinin-inducible interaction and activation is required for phosphorelay activity in the cytokinin-responsive signaling pathway.

2.3.2 Auxin and Abscisic Acid

Cross-talk between auxin and ABA has not been studied as extensively as auxin and cytokinin cross-talk. In 1990, Wilson et al. discovered that *A. thaliana axr2* mutant plants were resistant to auxin, ethylene and ABA, thus indicating an interaction among these phytohormones. Additionally, drought induced rhizogenesis, the formation of lateral roots that are short, tuberous, and lacking root hairs (Vartanian, 1981), was decreased in both ABA insensitive mutants and in the auxin mutant *axr1-3* (Vartanian et al., 1994). A recent study examining the effect of drought on cross-talk between auxin and ABA in two auxin mutants, *axr1-3* and *axr2-1*, found that both of the mutants

displayed decreased ABA signaling (Bianchi et al., 2002). All these results suggest an overlap in auxin and ABA signal perception.

The molecular mechanisms that mediate auxin and ABA signaling remain largely unknown. Research at the molecular level has shown that abscisic acid and auxin have antagonistic interactions. Auxin was shown to enhance the telomerase activity in synchronized tobacco cells (Tamura et al., 1999). ABA treatment, however, abolished the positive effect on telomerase activity induced by auxin and inhibited telomerase activity in untreated cells (Yang et al., 2002). Further, ABA was shown to increase transcription of *ICK1* (*INHIBITORs/INTERACTORs OF CDK*), a cyclin-dependent protein kinase inhibitor, suggesting that ABA can inhibit cell cycle progression (Wang et al., 1997; Wang et al., 1998).

2.4 Catecholamines

Catecholamines (CAs) are a group of compounds characterized by a 3,4-dihydroxysubstituted phenyl ring (Szopa et al., 2001). In mammalian systems, the CAs dopamine (DA), epinephrine (E), and norepinephrine (NE) function as neurotransmitters (Kuklin and Conger, 1995). These compounds plus their precursor tyramine are also present in 44 plant families, including some plants grown commonly for human consumption, such as potato, bean, and tobacco (Smith, 1977). Little is known about the function of CAs in plants. They were found to induce an oxidative burst with a subsequent increase in cytosolic Ca^{2+} as is commonly seen in the biotic and abiotic stress response (Kawano et al., 2000). Addition of CAs to cell cultures produces varied responses giving rise to speculation that they are involved with the regulation of

phytohormone activity (Christou and Barton, 1989), the biosynthesis of certain phytohormones (Elstner et al., 1976), or the regulation of phytohormone catabolism (Protacio et al., 1992).

2.4.1 Catecholamines and Auxins

Auxin, in the form of 2,4-D, was found to stimulate the biosynthesis of DA in cell suspension cultures. The addition of 2,4-D to cultures also suppressed cell growth and the accumulation of 3,4-dihydroxyphenyl-L-alanine (L-DOPA), a catecholic amino acid (Wichers et al., 1993). It was hypothesized that the L-DOPA is decarboxylated to dopamine after the addition of 2,4-D at high concentrations and that these catecholic compounds are incorporated into tetrahydroisoquinolines by various plant species to be used as insect or herbivore deterrents.

Protacio et al. (1992) discovered that DA inhibited IAA oxidase activity. Further, DA inhibition of IAA oxidase activity required the presence of IAA, no effect was seen when 2,4-D was used. However, the structure of the CA required for this effect is apparently not as restrictive as the auxin. Lee et al. (1982) observed 99% inhibition of IAA oxidase activity in the presence of a diphenol similar in structure to DA. Additionally, synthetic dihydroxyphenols inhibited IAA oxidase and peroxidase activities (Beffa et al., 1990). These studies provide the first evidence of a specific function for CAs in plants and support the idea that IAA and CAs interact synergistically.

2.4.2 Catecholamines and Cytokinins

In much the same manner as auxin and CK are antagonists so are CAs and CKs. Cytokinin activity was repressed in the presence of the CA phenylethylamine (PE) (Christou and Barton, 1989). Repression of CK activity was also observed within min of callus exposure to octopamine, a precursor to E, NE, and PE (Christou and Barton, 1989).

2.4.3 Catecholamine and Ethylene, Gibberellins, and Abscisic Acid

Little published information is available regarding the effect of CA on ethylene, GAs, and ABA. DA, NE, and E all stimulated ethylene biosynthesis in potato cell suspension cultures (Dai et al., 1993). Additionally, endogenous 1-aminocyclopropane-1-carboxylic acid (ACC) biosynthesis was increased suggesting that ACC synthase activity was stimulated by addition of CA. DA application was also shown to stimulate the production of superoxide, which is thought to be a precursor to ethylene (Elstner et al., 1976).

ABA activates the initial steps of CA biosynthesis in potato tubers (Swiedrych et al., 2004) through the increase in activity of three CA biosynthetic enzymes. The authors propose that CA and ABA may be involved in biotic and abiotic stress responses and regulation of starch-sucrose conversion in plants.

As for GA and CA interaction, CA enhanced the GA effect on hypocotyl elongation in lettuce seedlings. The CA effect resembled that of the similarly structured dihydroconiferyl alcohol, acting as a synergist in GA-induced hypocotyl elongation (Kamisaka et al., 1979).

2.4.4 Catecholamines and Flower Development

In addition to its influence on phytohormone activity, data suggests that CAs are also involved in the induction of flowering in plants. Catecholamines likely have a role in controlling cyclic AMP (cAMP) amount in long-day duckweed, *Lemna gibba* G3 (Oota, 1974). Oota (1974) concluded that flowering in *L. gibba* G3 was dependent on the amount of cAMP and hypothesized that, similar to the mammalian system, CA regulated cAMP (Oota and Kondo, 1974). Further research conducted on *Lemna paucicostata* demonstrated that treatment with CA prior to flowering resulted in a greater number, longer-lived and faster developing flowers (Khurana et al., 1987). Further, a flower-inducing factor (FIF) was recently discovered in *L. paucicostata* that strongly induced flowering when combined with NE or DA (Yamaguchi et al., 2001). Similar to the FIF/CA system observed in *L. paucicostata*, FIF was identified in the short-day violet, *Pharbitis nil*. When CA was applied to the cotyledons under a short-day photoperiod, an increase in FIF production was detected in the cotyledons, but not in other organs (Suzuki et al., 2003). The regulation of flowering by CA was also examined using CA inhibitors in *P. nil*. Application of CA biosynthesis inhibitors suppressed flowering if application commenced prior to or during a period of darkness, but had no effect if applied after a dark period (Ueno and Shinozaki, 1999). Previous studies showed that E and NE are only accumulated in the dark (Endress et al., 1984), implying that dark treatment combined with catecholamines have a role in the regulation of flowering.

3. MATERIALS AND METHODS

3.1 Plant Material and Growth

The *B. carinata* breeding cultivar C90-1163 from Agriculture and Agri-Food Canada Research Station (Saskatoon, Saskatchewan, Canada) was used as the non-transformed and transformation recipient plant material. Z. Zheng (PBI/NRC) and T. Uchacz (University of Saskatchewan) produced the antisense *CIL1* transgenic plants. Antisense expression was driven by the cauliflower mosaic virus duplicated-enhancer 35S-promoter (Kay et al., 1987) and leader sequence from alfalfa mosaic virus RNA4 (Datla et al., 1993). This construct was cloned into the plant binary vector RD400 (Datla, et al., 1992) and was used to transform *B. carinata*, according to Babic et al. (1988). Transgenic antisense lines 2, 3, 5, 6, 10, and 13 were used for experiments involving transgenic plants. "Non-transformed" refers to a wild type *Brassica carinata* control for the experiments involving the transgenic plants. The *B. oleracea* CrGc 3-1 rapid cycling wild type cultivar from the Transgenic Plant Centre of the National Research Council (Saskatoon, Saskatchewan, Canada), and *B. nigra* wild type cultivar from Agriculture and Agri-Food Canada Research Station (Saskatoon, Saskatchewan, Canada) were also utilized in this study.

Seeds were sown at a density of approximately 2 seeds/cm^2 in Terra-Lite Redi-Earth fortified with Nutricote 14-14-14 fertiliser (Chisso-Asahi, Nagasaki, Japan) and grown in a Conviron PGV36 growth chamber with 50 % relative humidity. The temperature and photoperiod in day/night were 21/17 ^oC and 16/8 h, respectively with a light intensity of 216 μmol m^{-2} s^{-1} provided by Sylvania 40 W extended service incandescent bulbs and Sylvania 215 W cool white fluorescent bulbs.

For experiments involving *A. thaliana*, three lines were used in this study: wild-type Columbia, and the *supershoot* mutant (obtained from Dr. Sundaresan, Institute of Molecular Agrobiology, The National University of Singapore, Singapore). For all lines, seeds were sown at a density of 3 seeds/cm^2 in Terra-Lite Redi-Earth and grown in a Conviron C1010 growth chamber with a 16 h photoperiod, a light intensity of 102 μmol m^{-2} s^{-1} and a constant temperature of 21°C. After germination, plants were thinned to 4 plants per pot, and grown until the plants senesced.

Prior to plating on selection media, transgenic *B. carinata* seeds were surface sterilized in 10% (v/v) bleach for 30 min, and washed twice in deionized water for 5 min each. After surface sterilization, transgenic seeds were imbibed in a solution of ½ Murashige & Skoog medium (MS, Gibco, Carlsbad, CA, USA), 1% (w/v) sucrose, containing 50 mg/L kanamycin for 9 h, then transferred to plates containing ½ MS (Gibco, Carlsbad, CA, USA), 1% (w/v) sucrose, 0.7% (w/v) Phytagar (Gibco, Carlsbad, CA, USA) with 75 mg/L kanamycin. The plates were sealed with parafilm and placed in a Conviron C1114 growth chamber, with a photoperiod of 16/8 h of day/night at a constant temperature of 24 °C and a light intensity of 120 μmol m^{-2} s^{-1} during the day. After approximately two weeks of growth, the first true leaf of the seedling emerged, and the seedlings were transferred to soil in 15.3 cm diameter pots at approximately 4 seedlings per pot.

Seeds used to propagate transgenic lines by self-fertilisation were sown in 15.3 cm diameter pots at a density of approximately 1 seed/cm^2. The plants were thinned to 2-4 plants/pot prior to bolting, and after bolting had occurred, the plants were transferred to 21 cm diameter pots. Prior to floret opening, 22.8 x 76.2 cm bags were placed on each

individual plant to prevent cross-pollination with other plants. Seeds were harvested after the plants senesced. Plants used for organ samples and time course experiments were generally sown at approximately 2 seeds/cm^2 in 15.3 cm diameter pots.

3.2 DNA and RNA Isolation

3.2.1 Small Scale DNA Preparations

Genomic DNA was isolated according to Dellaporta (1983) with slight modifications. Approximately 200 mg fresh weight of leaf tissue was frozen in liquid N_2 in a 1.5 mL microcentrifuge tube and ground with a pestle to a fine powder. The powder was then homogenized in 500 μL extraction buffer (100 mM Tris-HCl pH 8.5, 50 mM EDTA, 500 mM NaCl, 10 mM β-mercaptoethanol). Subsequently, 35 μL of 20 % (w/v) SDS was added, the tube was inverted four times and incubated at 65 ^oC for 5 min, 160 μL of 5 M potassium acetate was added and the sample was mixed by inverting. The sample was incubated on ice for 10 min, followed by centrifugation at 4 ^oC in a microcentrifuge at 13,000 rpm. After centrifugation, the supernatant was transferred to a clean 1.5 mL microcentrifuge tube and 100 μL of 3 M sodium acetate was added. The DNA was precipitated with isopropyl alcohol, recovered by centrifugation and then dissolved in TNE buffer (50 mM Tris-HCL pH 7.5, 140 mM NaCl, 5 mM EDTA). The samples were treated with 15 μg RNAse A at 37 ^oC for 10 min. The reactions were extracted with phenol/chloroform, pH 8.0, and the DNA was precipitated with isopropyl alcohol. The DNA was recovered by centrifugation and washed once with 70% (v/v) ethanol. After drying, the DNA was dissolved in sterile deionized H_2O and stored at –20 ^oC.

3.2.2 RNA Sample Preparations

RNA isolation was done using Trizol (Invitrogen, Carlsbad, CA, USA) following the manufacturer's directions. The extractions were performed on 200 mg fresh weight of plant material. The material was frozen in liquid N_2 and ground with a pestle to a fine powder before extraction. The RNA was dissolved in DEPC-treated H_2O and stored at $-80\ ^{o}C$.

3.2.3 Quantification of DNA and RNA

Quantification of RNA and DNA was achieved using a GeneQuant RNA/DNA Calculator spectrophotometric unit (Pfizer Inc., New York, NY, USA). Absorbances were measured at 320, 280, 260 and 230 nm wavelengths.

3.3 Recombinant DNA Preparation

Primers used for polymerase chain reaction (PCR), semi-quantitative reverse transcriptase polymerase chain reaction (RT-PCR), and real time quantitative reverse transcriptase polymerase chain reaction (qRT-PCR) were designed using Primer Design version 1.0 software (Scientific and Educational Software, 1990). The criteria for primer design in the software was set to examine the *CIL1* sequence for primers between 17 and 20 bp in length with a GC content between 40 and 50 %. The primers were also specified to have a T_m between 50 and 65 ^{o}C. Primers containing runs of bases, secondary structure, or primer interactions involving the 3' end were discarded. Primer sequences were checked using NetPrimer

(http://www.premierbiosoft.com/netprimer/netprlaunch/netprlaunch.html, first accessed October, 2002). Prior to ordering, primer sequences were checked by BLASTN queries to determine if there were any similarities to other plant genes. The DNA Technologies unit at the National Research Council Plant Biotechnology Institute, Saskatoon, Saskatchewan, Canada synthesized all the primers. The primers used for PCR are given in Table 3.1.

3.3.1 PCR Amplification

The reactions for amplification of *CIL1* products contained 5 pmol each forward and reverse primer, 2 mM $MgCl_2$, 1 X FastStart High Fidelity Reaction Buffer (Roche Diagnostics Canada, Laval, Quebec, Canada) 0.20 mM each deoxyribonucelotide, 2.5 U of Expand High Fidelity Enzyme Mix (Roche Diagnostics Canada, Laval, Quebec, Canada), containing a mixture of *Taq* polymerase and *Tgo* polymerase which possesses 3'-5' exonuclease activity, and 250 ng of genomic DNA. The reaction conditions consisted of an initial denaturation at 94˚ C for 30 s, subsequently 35 cycles of 94˚ C for 30 s, 61˚ C for 1 min and 72˚ C for 2 min were performed. A final extension of 72˚ C for 1 min was followed by an indefinite hold at 4˚ C. The resultant fragment was approximately 1030 bp in size, confirmed by sequencing.

Table 3.1 Primers used for PCR, semi-quantitative RT-PCR, and real-time quantitative RT-PCR amplification of samples.

Name	Primer Sequence	Use	Source	Annealing Temperature (^{o}C) at 2 mM $MgCl_2$
BcActR	5′-GAGCACAATGTTACCGT-3′	Semi- and Real-time Quantitative RT-PCR	Uchacz, 2000	58
BcActL	5′-ACTACGAGCAGGAGATG-3′	Semi- and Real-time Quantitative RT-PCR	Uchacz, 2000	57
CIL1770F	5′-TTGGTTATGTTGGCTTCAGT-3′	Semi- and Real-time Quantitative RT-PCR	This Study	66
CIL1770R	5′-GAGAGATAGAGATAGGTGGA-3′	Semi- and Real-time Quantitative RT-PCR	This Study	58
CIL1F	5′-CAGAACTCAACTCAGCCATG-3′	Amplifying Genomic Clone	This Study	66
CIL1F2	5′-AACAGGATCGTGATCTACAC-3′	Sequencing Genomic Clone	This Study	62
CIL1R	5′-ATAGGTGGAAACACAAAACG-3′	Amplifying Genomic Clone	This Study	66
M13RP	5′-CAGGAAACAGCTATGAC-3′	Sequencing of Plasmids	DNA Technologies Unit (NRC-PBI)	55
M13UP	5′-TGTAAAACGACGGCCAGT-3′	Sequencing of Plasmids	DNA Technologies Unit (NRC-PBI)	67
NPT-JH1	5′-ATCTCCTGTCATCTCACC-3′	Confirming Presence of *NPTII*	Joe Hammerlindl (NRC-PBI)	58
NPT-JH2	5′-AAGAAGGCGATAGAAGGC-3′	Confirming Presence of *NPTII*	Joe Hammerlindl (NRC-PBI)	65
pRD400F	5′-CAGCTATGACCATGATTACG-3′	Confirmation of the Presence of Antisense Construct	This Study	64

The reactions for PCR amplification of neomycin phosphotranferase (*NPTII*) consisted of 5 pmol each forward (JH1) and reverse (JH2) primers, 4 mM $MgCl_2$, 1 X PCR buffer (Invitrogen, Mississauga, ON, list components), 0.20 mM each deoxyribonucleotide, 1.0 U *Taq* polymerase and 250 ng genomic DNA. The reaction conditions consisted of an initial denaturation at 94˚ C for 30 s, subsequently 30 cycles were performed of 94˚ C for 30 s, 62.9˚ C for 1 min and 72˚ C for 30 s. A final extension of 72˚ C for 1 min was followed by an indefinite hold at 4˚ C for a resultant PCR fragment of approximately 400 bp.

The PCR amplifications were carried out in either a PTC-200 thermal cycler (MJ Research, Waltham, MA, USA) or in a GeneAmp PCR system 2400 (Perkin Elmer, Boston, MA). Aliquots of the PCR amplifications were analyzed on 0.7% (w/v) agarose, 1 X TAE, ethidium bromide gel (Sambrook and Russell, 2001).

3.3.2 Cloning of PCR Products

Cloning of PCR products was accomplished using the Topo TA cloning system (Invitrogen, Carlsbad, CA, USA) following the manual's directions. Either chemically competent or electrocompetent *Escherichia coli* TOP10 strain with genotype - F^- *mcr*AΔ(*mrr-hsd*RMS-*mcr*BC) Φ80*lac*ZDM15 Δ*lac*X74 *rec*A1 *ara*D139Δ (*ara-lea*)7679 *gal*U *gal*K *rps*L (Str^R) *end*A1 *nup*G were used for transformation. For electroporation, the Gene Pulser (Bio-Rad, Hercules, CA, USA) was set at 25 μFarad capacitance, 200 ohms resistance, and delivered a 12.50 kV/cm pulse. For chemical transformation, the directions from the manufacturer were followed (Invitrogen, Carlsbad, CA, USA). Plasmid DNA was recovered from clones using the QIAprep miniprep kit (Qiagen,

Hilden, Germany) according to manufacturer's instructions. Restriction enzyme analysis and DNA sequencing were used to verify the identity of the PCR products. The DNA was submitted for sequencing to the DNA Technologies Unit (NRC-PBI), sequenced with universal primer, and reverse primer using an ABI Prism 377 DNA Sequencer (Applied Biosystems, Foster City, CA, USA). Sequences were analysed using the Editseq program (DNASTAR Inc., Madison, WI, USA).

3.4 Southern Blot Analysis

Southern blot analysis was used to estimate the copy number of the *CIL1* gene in three *Brassica* species: *B. carinata*, *B. nigra*, and *B. oleracea*. DNA was extracted from first leaves of 3-week old plants using the method previously described. To confirm the concentration of the genomic DNA determined by A_{260}, 4 μL of each sample was loaded alongside 4 μL of High DNA Mass Ladder (1 – 10 kb fragments, 20 – 200 ng DNA) (Invitrogen, Carlsbad, CA, USA). Approximately 10 μg of genomic DNA was digested with either 60 U of *Bam*HI, 60 U of *Eco*RI or 100 U of *Hind*III (New England Biolabs, Beverly, MA). The digested DNA was separated on a 0.7% (w/v) agarose, 1 X TAE, ethidium bromide gel and the results photographed. The DNA was transferred to Hybond-N+ nylon membrane (Amersham, Little Chalfont, Buckinghamshire, UK) by capillary action (Sambrook and Russell, 2001).

Southern blots were also used to analyse the copy number of the antisense cassette in transgenic plants. In this case, genomic DNA was extracted from first leaves of 3-week old transgenic *B. carinata* lines 2, 3, 5, 6, 10, and 13. Five micrograms of genomic DNA from each transgenic line was digested with 25 U of *Nhe*I and *Pac*I to excise the

antisense cassette and electrophoresed alongside amounts of the plasmid clone of antisense *CIL1*/*NPTII* cassette equivalent to 1, 5, 10 and 20 copies. The gel electrophoresis and Southern blot were carried out as described above.

Probes for Southern blot hybridization were prepared as follows: 1) plasmid DNA was restriction enzyme digested to release the insert, 2) the fragment corresponding to the insert was excised and purified from the gel using the QIAEX II (Qiagen, Strasse 1, Hilden, Germany) system following the instructions in the manual and, 3) the DNA fragment was labeled with ^{32}P-dCTP (3000 Ci/mmole) utilizing the Random Primers DNA Labeling System (Invitrogen, Carlsbad, CA, USA) following the manufacturer's directions.

Hybridization was done using QuikHyb hybridization solution (Stratagene, La Jolla, CA, USA) according to manufacturer's directions. Membranes were prehybridized in roller bottles at 65 ^{o}C for 30 min then hybridized with the probe for 1 h. Following hybridization, the membrane was removed, and washed twice for 15 min at room temperature with 2 X SSC buffer and 0.1% (w/v) SDS wash solution. After the second wash, membranes were scanned using a Geiger counter. If the counts were too high to discern regions containing genomic DNA from background, an additional wash for 30 min at 60 ^{o}C with a 0.1 X SSC buffer and 0.1% (w/v) SDS wash solution was performed (Sambrook and Russell, 2001). Hybridized membranes were exposed to Kodak X-OMAT AR film at –80 ^{o}C.

3.5 Phytohormone Treatments and Expression Analysis

Plants were grown as previously described and the time of sampling for both phytohormone and gene expression analysis were standardized to avoid discrepancies in the data caused by fluctuations of transcript and phytohormone amounts over the course of the photoperiod.

Samples used for expression analysis included the 3rd lateral meristem (counted apically from the most basal lateral meristem), the shoot apical meristem, the 1st leaf, the stem (from the epicotyl apically to, but not including, the shoot apical meristem), and the entire root. First leaves were collected once the second leaf began to expand. All other samples were taken once plants had reached the fourth leaf stage, after approximately 4 weeks of growth. All gene expression analysis experiments were conducted in triplicate. Samples were collected at 0, 1, 2, 4, 6, 8, 12, 16, 24 h after the start of the time course and *CIL1* expression was analysed using RT-PCR and the CIL1770F/R primer set.

For *CIL1* expression analysis after phytohormone treatment, the 3rd lateral meristems were treated with 200 μL of hormone solution containing 0.1% (v/v) Triton X-100. Each sample was collected from a separate plant. The concentrations of hormone solutions used were 50 μM α-napthaleneacetic acid (α-NAA) (Sigma-Aldrich, Oakville, Ontario, Canada) (Neuteboom et al., 1999), 5 μM 6-benzylaminopurine (BAP) (Caisson Laboratories Inc, Rexburg, Idaho, USA) (Crosby et al., 1981; Fei and Vessey, 2004), or 10 μM +/- abscisic acid (ABA) (Sigma-Aldrich, Oakville, Ontario, Canada) (Zheng et al., 2001). To minimize variability, the time course analyses all began at the same time of day after the same stage of growth had been reached.

In the case of real-time quantitative RT-PCR, the samples were collected at the same time of day in all cases. After plants had reached the 4th-leaf stage of growth, samples were collected from the basally 3rd lateral meristem, the shoot apical meristem, the basally 3rd leaf, the stem, and the entire root.

3.6 Semi-Quantitative RT-PCR Analysis

Semi-quantitative RT-PCR was used to analyse the expression of *CIL1* in treated and untreated *B. carinata* organs. The RT-PCR protocol presented was found to produce the optimal results. Prior to the RT reaction, 200 ng RNA was treated with 1 U of RNase-free DNase I (Amersham, Little Chalfont, Buckinghamshire, UK) and 40 U of RNase OUT (Invitrogen, Carlsbad, CA, USA) in the presence of 10 µl of 5X first-strand buffer (Invitrogen, Carlsbad, CA, USA) at 37 ^{o}C for 15 min. Reverse transcription was carried out using Superscript II (Invitrogen, Carlsbad, CA, USA) according to supplier's directions. Subsequently, 500 nL of the RT reaction was added to the corresponding PCR amplification. The PCR amplifications contained: 2 pmol each of the actin primers, 5 pmol each of the *CIL1* primers, 2 mM $MgCl_2$, 1X PCR buffer (Invitrogen, Carlsbad, CA, USA), 0.20 mM dNTP, and 1.0 U of *Taq* polymerase (Invitrogen, Carlsbad, CA, USA). The samples were electrophoresed on a 2% (w/v) agarose 1 X TAE gel and a photograph of the gel was taken using a Bio-Rad Gel Doc 2000 with the Quantity One software (Bio-Rad, Hercules, CA, USA).

3.6.1 Quantitation of Semi-Quantitative RT-PCR

Photographs of gels were analysed using the Gel-Pro Analyser software (Media Cybernetics, San Diego, CA, USA). To analyse the gel photo, the lane size was defined manually, both automatic and manual designation was used for fragment location. On the lane profile graph, created for each individual lane, the region of the band to be analysed was specified, and the optical densities were re-calculated. The maximum optical density (OD) value was recorded, and calculations were carried out to obtain a semi-quantitative value for *CIL1* expression at the time point examined. To obtain the expression value or, "relative intensity" at each time point, the maximum OD of the *CIL1* PCR fragment was divided by the value for the BcAct PCR fragment. An example of the results used for calculation is presented in Figure 3.1, the BcAct OD value was 65.21 while the CIL1770 OD value was 73.45 for the 0 hour time point in an untreated lateral meristem time course. Using the calculation outlined above, 73.45/65.21 yields a relative intensity of 1.13. Using this method, the BcAct value normalizes the values for the time course. The mean, standard deviation and standard error were calculated for the corrected intensity values of the replicates. The results of the time courses were graphed using Microsoft Excel, in histogram format.

3.6.2 Real Time Quantitative RT-PCR Analysis

Samples were collected from both transgenic and non-transformed *B. carinata* from the basally 3rd lateral meristem; shoot apical meristem, basally 3rd leaf, stem, and whole root. Samples were collected from homozygous antisense transgenic lines 2, 3, 5,

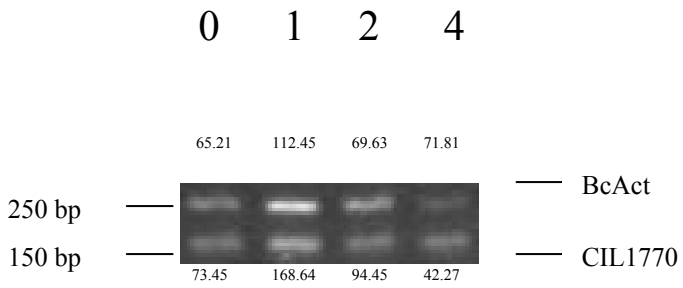

Figure 3.1. Semi-Quantitative RT-PCR analysis of *CIL1* expression in lateral meristems. Optical densities were determined using Gel-Pro Analyser software (Media Cybernetics). Each time point's corrected intensity was calculated by dividing the PCR fragment optical density for *CIL1* by the fragment optical density for actin. The top numbers represent the time of sampling in h while the numbers directly below them represent the OD of the BcAct PCR product for the corresponding time point. The numbers below the photo represent the OD of the CIL1770 samples for the corresponding time point. An example calculation involving the 1 h time point would result in: 168.44/112.45 = 1.49. All samples were calculated using this method.

6, 10, and 13. All samples were collected at the same time of day, and were collected after the plants had reached the 4th-leaf stage of growth.

Quantitative RT-PCR analysis was performed using the QuantiTect SYBR Green RT-PCR kit (Qiagen, Strasse 1, Hilden, Germany) according to the instructions in the handbook with the following modifications. Prior to the RT-PCR reactions, 1.25 μg of RNA was digested with 2 U of RNase free DNase I (Amersham, Little Chalfont, Buckinghamshire, UK) for 10 min at 37 ^{o}C in 1 X first strand buffer (Invitrogen, Carlsbad, CA, USA). Subsequently, each reaction was made up to contain 1X SYBR Green Master Mix, 0.5 μM each CIL1770F and R or 0.5 μM BcActL and R, 0.5 μL QuantiTect RT Mix, 1X fluorescein, and RNase-free water to 48 μL per sample. The RT reaction was carried out at 50 ^{o}C for 30 min. After the RT reaction was completed, the samples were transferred to a 96-well plate designed for use with the iCycler (Bio-Rad, Hercules, CA, USA). The cycling conditions used for the PCR amplification step were as follows, an initial PCR denaturation step at 95 ^{o}C for 15 min followed by 40 cycles of 15 s at 94 ^{o}C, 30 s at 58 ^{o}C, and 30 s at 72 ^{o}C. After the 40 cycles were completed, a melt curve was generated by holding the samples at 58 ^{o}C for 30 s and increasing the temperature by 0.5 ^{o}C every cycle for 74 times, with a final measurement at 92 ^{o}C.

3.6.3 Real Time Quantitative RT-PCR Data Analysis

The results of the real-time RT-PCR were analysed using a Microsoft Excel macro that calculates data using the $\Delta\Delta C_T$ formula, where "C_T" is the threshold cycle when the sample being amplified by PCR enters the log stage of replication (Pfaffl, 2001; Livak and Schmittgen, 2001). Using the $\Delta\Delta C_T$ method, the gene of interest can be

compared with a constitutively expressed gene, under the conditions of this experiment, such as actin to calculate relative expression. The $\Delta\Delta C_T$ method utilizes two genes to calculate relative quantitative expression, and the genes must amplify with a similar efficiency. In that case, an efficiency of "2" can be assigned to them, and this number is used in the equation: Amount of target = $2^{-(S\Delta C_T - C\Delta C_T)}$. The amount of target is normalized to an endogenous reference, in this case the *B. carinata* actin gene, with the *CIL1* transcript amount in non-transformed *B. carinata* plants as the control to which everything is normalized. The efficiency of the primers can be tested by RT-PCR amplifying a series of dilutions of an aliquot of RNA with both primer sets, analysing them using the $\Delta\Delta C_T$ calculation, and then graphing them. If the primers amplify with a similar efficiency, the slope of the line will be close to zero. This experiment was completed prior to analysing any samples for the gene expression study. An example of the data used for the $\Delta\Delta C_T$ calculation is presented in Table 3.2. The standard error calculation was performed according to Vandesompele et al. (2002). In some cases, outlier biological replicates were removed from the sample set because their values were vastly different from the other two values. The data were graphed using Microsoft Excel, in histogram format.

Table 3.2 Real-Time Quantitative RT-PCR Data Analysis

Sample		CIL1 C_T	Mean CIL1 C_T	BcAct C_T	Mean BcAct C_T	ΔC_T	$S\Delta C_T$-$C\Delta C_T$	Relative Expression
Non-transformed	1	23.0		21.9*		$C\Delta C_T^{\psi}$		
	2	23.6		16.2				
	3	23.2	23.26	16.7	16.45	6.8	0	1.00
Line 2	1	23.2		16.8		$S\Delta C_T$		
	2	22.8		16.2				
	3	23.2	23.06	16.2	16.40	6.6	-0.15	1.11
Line 6	1	25.1		15.9				
	2	25.0		16.1				
	3	25.8	25.30	16.0	16.0	9.3	2.48	0.18

C_T = Cycle threshold of the PCR amplification
ΔC_T = Mean CIL1 C_T – Mean BcAct C_T
$S\Delta C_T$-$C\Delta C_T$ = Sample ΔC_T-control ΔC_T
Relative Expression = 2-($S\Delta C_T$-$C\Delta C_T$)
* = Outlier value ignored
ψ = For calculation of the relative expression of the non-transformed line, it is both the sample and the control.

3.7 Senescence Bioassay

Plants were grown to the 4th-leaf stage, at which point 0.6 cm diameter discs were cut from the distal regions of young leaves, generally the 3rd and 4th leaves. Chlorophyll was extracted according to Burkhanova et al. (2001) with modifications. Approximately 15 leaf discs were collected per replicate, with 3 biological replicates per line. The leaf discs were placed on filter paper pre-wetted with deionized water in Petri plates, sealed, and placed in the dark at 23 ^{o}C for 72 h. The discs were then homogenized in 80% (v/v) acetone using a mortar and pestle, centrifuged in a microcentrifuge at 13,000 rpm for 10 min, and the supernatant was transferred to a cuvette. The absorbance was measured at 645 and 663 nm, to determine the content of chlorophyll A and B. Chlorophyll content is expressed as mg/L = 20.2 * A_{645} + 8.02 * A_{663} (Jeffrey and Humphrey, 1975).

3.8 Phenotypic Characterization

Two studies were conducted to compare the plant height and leaf surface area of non-transformed and antisense T_4 *CIL1* transgenic plants. The first study compared transgenic lines 2, 3, 5, 10, and 13 to the non-transformed line; transgenic line 6 was included in the second study. Measurements were taken from eight plants for each transgenic line and from four non-transformed plants and the means were determined. Measurements were taken every 4 days after the appearance of two true leaves and continued until the plants bolted. Leaf location was recorded and the length was measured from the petiole to the most distal region of the leaf blade while width was measured at the approximate centre of the leaf. Plant height was measured from the cotyledonary node to the shoot apical meristem.

3.9 Phytohormone Profiling

The 1st leaves were collected when the plants had reached the 2nd-leaf stage of growth. The basally 3rd lateral meristem, the shoot apical meristem, the stem, and the entire root were collected when the plants reached the 4th-leaf stage. All samples were collected at the same time of day to minimize any variation due to environment. The samples were frozen in liquid nitrogen and held at –80 ^{o}C until they were freeze-dried in a Labconco Freezone 4.5 (Labconco Corp., Kansas City, MI, USA) for 3 days.

The phytohormone analysis was carried out, with modifications, as described by Chiwocha et al. (2003). The plant organs were divided into three 50 mg samples in skirted 2 mL tubes with an o-ring closure. A 6.35 mm ceramic bead was added, and the tube was placed in a FastPrep FP120 (Bio101 Savant, Irvine CA, USA). The samples were homogenized in the FastPrep for 15 seconds at speed setting 5. If the sample was not completely homogenized after the initial 15 seconds, the samples were shaken for an additional 10 seconds at speed 5. The samples were transferred to 15 mL conical bottom centrifuge tubes containing 3 mL of the extraction solution (80% v/v isopropyl alcohol, 1% v/v glacial acetic acid). Twenty nanograms of each deuterated internal standard was added to each of the sample tubes. Master mixes were made, containing non-deuterated analytes and deuterated internal standards at concentrations of 1 ng/μL. Deuterated internal standards included in the samples, quality control (QC; contained non-deuterated and deuterated standards), and internal standard mixture (IS; contained deuterated standards) were: d_2 GA_1 and GA_4; d_3 DPA, PA, neo-PA, DHZ, and DHZR; d_4 7'OH-ABA and ABA; d_5 ABA-GE, ZOG, and IAA, and d_6 2iP and IPA. The QC also included non-deuterated standards 2iP, 7'OH-ABA, ABA, ABA-GE, DHZ, DHZR, DPA, GA_1,

GA_3, GA_4, GA_7, IAA, IAAsp, IPA, neo-PA, Z, ZOG, and ZR. All chemicals, both deuterated and non-deuterated were obtained from Dr. Sheila Chiwocha at the NRC Plant Biotechnology Institute (Saskatoon, Saskatchewan, Canada).

Samples were extracted in the dark at 4 ^{o}C in an orbital shaker at 300 rpm for 24 h, centrifuged at 290 x g for 10 min, the supernatant was transferred to a new tube. The remaining pellets were re-suspended in 500 µL extraction solution, centrifuged for 10 more min and the supernatants were combined. Extracts were evaporated to dryness in a Speed-Vac (Bio101 Savant, Irvine CA, USA), then re-suspended in 1 mL of 99:1 isopropyl alcohol:glacial acetic acid, vortexed vigorously for 10 min, sonicated in a Branson 2210 Ultrasonic Cleaner (Branson, Danbury, CT, USA) for 10 min and finally, centrifuged at 13,000 rpm for 10 min in a microcentrifuge. Supernatant were transferred to a new tube and evaporated to dryness in a Speed-Vac. Extracts were reconstituted in 50 µL 99:1 methanol:glacial acetic acid using vortexing and sonication for 10 min. Following the reconstitution, 500 µL of a 1% (v/v) glacial acetic acid aqueous solution was added to each sample, and mixed by vortexing. One millilitre of n-hexanes was added to each sample, vortexed vigorously for 2 min until an emulsion was formed and incubated at room temperature for 30 min to allow phase separation. The samples were centrifuged at 13,000 rpm for 2 min in a microcentrifuge, and the upper solvent phases were removed. A second hexane extraction was performed. Aqueous phases were then evaporated to dryness in a Speed-Vac, and each extract was reconstituted with 1 mL of methanol:water:glacial acetic acid (80:19:1). The extracts were applied to C18 Sep-Pak (Waters, Milford, MA, USA) columns and eluted with 500 µL methanol:water:glacial acetic acid (80:19:1). Twenty nanogram of d_6-ABA was added as a recovery standard to

each sample extract, quality control (QC), and internal standard (IS). Extracts, evaporated to dryness in a Speed-Vac were reconstituted with 80 μL 99:1 methanol:glacial acetic acid, and mixed by vortexing. After the residue was dissolved, 120 μL 1% (v/v) glacial acetic acid was added, the samples were vortexed for 30 seconds, sonicated for 10 min, and centrifuged at 13,000 rpm for 10 min. The extracts were transferred to low volume HPLC tubes and capped.

3.9.1 High-performance liquid chromatography

High-performance liquid chromatography (HPLC) was used to separate phytohormones in the plant extracts. The Alliance 2695 separation module (Waters, Milford, MA, USA) was outfitted with a 100 mm x 2.1 mm, 4-μm Genesis C18 HPLC column (model FK10960EJ, Jones Chromatography, Hengoed, UK). A solvent system composed of acetonitrile (A), de-ionized water (B), 5% v/v glacial acetic acid in de-ionized water (C), and 100% methanol (D) was used for the chromatography. A 1.0 mm Opti-Guard C18 HPLC column, violet (Optimize Technologies Inc # 10-02-00007, ChromSpec distribution # M100200007, OR, USA) was used to remove particulate matter in the sample to ensure optimal performance of the Genesis C18 column. The chromatography was performed using a gradient of increasing acetonitrile concentration and a constant glacial acetic acid concentration of 7 mM (pH 3.4) with an initial flow rate of 0.200 mL min^{-1}. The gradient was linearly increased from 2.0% (v/v) A, 94.2% (v/v) B, 0.8% (v/v) C, 3.0% (v/v) D to 60.0% (v/v) A, 0.0% (v/v) B, 0.8% (v/v) C, 39.2% (v/v) D over 46 min and held for 3 min with an increased flow rate of 0.350 mL min^{-1}. After 1 min of holding, the initial conditions of the chromatography were restored, and the

column was equilibrated for 8 min, yielding a gradient program with a 57-minute duration and a sample turnaround of 60 min in total (Table 9.2).

3.9.2 Mass Spectrometry

The determination of precursor-to-product ion fragmentation was required prior to mass spectrometric analysis of phytohormone samples. For the selection of the ion transitions, 10 mM standards for the deuterated and non-deuterated analytes were infused individually using ESI-MS/MS with a Harvard Apparatus Pump II at a flow rate of 20 μL min^{-1} into a quadrupole tandem mass spectrometer (Quattro Ultima, Micromass, Manchester, UK) outfitted with an electrospray ion source. The electrospray and cone voltages were adjusted to optimal conditions for the production of the precursor ions in negative or positive ionization mode. IAA, IAAsp, ABA, 7'-OH-ABA, neo-PA, PA, DPA, ABA-GE, GA_1, GA_3, GA_4, GA_7, and their respective internal standards were analysed in negative ion mode, while the cytokinins Z, ZR, 2iP, and IPA and their respective internal standards were analysed in positive ion mode. The transition parent to daughter ion is shown in Table 3.3. Argon gas was used in the collision cell to cause collision-induced dissociation (CID) of the precursor ions. Once the precursor-to-product transition had been determined, a mixture containing all the deuterated and non-deuterated analytes, the QC, a mixture containing the deuterated analytes, the IS, the samples, prepared as outlined above, and the solvent blanks, were separated by reversed-phase HPLC and analysed by tandem mass spectrometry with multiple reaction monitoring (MRM). Analysis of variance (ANOVA) was performed on all organs for all treatments. ANOVA results were considered significant if $\rho \leq 0.05$.

Table 3.3 Reverse phase high performance liquid chromatography retention times and mass spectrometric precursor-to-product transitions of analysed phytohormones.

Analyte	Transition (*m/z*)	Retention Time (min)	Internal Standard	Transition (*m/z*)	Retention Time (min)
2iP	204 > 136	22.47	d_2-GA_1	349 > 275	21.63
7'-OH-ABA	279 > 151	26.08	d_2-GA_4	333 > 215	43.28
ABA	263 > 153	30.46	d_3-DPA	284 > 174	18.64
ABA-GE	425 > 263	23.05	d_3-PA	282 > 142	22.84
DHZ	222 > 136	13.01	d_3-neo PA	282 > 208	26.88
DHZR	354 > 222	18.86	d_3-DHZ	225 > 136	13.19
DPA	281 > 171	19.15	d_3-DHZR	357 > 225	18.41
GA_1	347 > 273	22.31	d_4-7'-OH-ABA	430 > 268	25.21
GA_3	345 > 221	21.92	d_4-ABA	267 > 156	29.39
GA_4	331 > 213	44.67	d_5-ABA-GE	430 > 268	22.41
GA_7	329 > 253	43.53	d_5-ZOG	387 > 225	12.18
IAA	174 > 130	25.01	d_5-IAA	179 > 135	23.98
IAAsp	289 > 132	19.43	d_5-IAAsp	294 > 132	18.48
iPA	336 > 204	26.58	d_6-2iP	210 > 137	21.89
neo-PA	279 > 205	27.85	d_6-iPA	342 > 210	25.75
PA	279 > 139	23.50			
Z	220 > 136	12.26			
ZR	352 > 220	18.59			
ZOG	387 > 225	11.89			

The ZR data were transformed logarithmically to stabilize the variance, and analysed by ANOVA.

4. RESULTS

4.1 Sequence Analysis of *CIL1*

The *CIL1* cDNA was selected from a clone library derived from mRNA isolated from leaves of *B. carinata* 12 h after they were sprayed with 5 mM $CuCl_2$ (Uchacz, 2000). The full-length 1030 bp cDNA was obtained using the GeneRacer kit (Invitrogen, Carlsbad, USA) and encoded an open reading frame of 810 bp. The cDNA and derived amino acid sequence are shown in Figure 4.1. The amino acid sequence consists of 269 residues with an estimated molecular weight of 27,331 Daltons and pI of 7.14. No introns were detected in the PCR product of *B. carinata* genomic DNA after amplification with a high fidelity polymerase and primers derived from the cDNA sequence. No significant similarities to the *CIL1* nucleotide sequence other than *AIR12* were found in the nucleotide BLAST database. However, BLAST searching with the derived amino acid sequence did reveal several other similar sequences. The most similar (59% identity) sequence was the *A. thaliana* AIR12, which is encoded by a gene that is expressed during auxin-induced lateral root formation. Analysis of AIR12 and CIL1 sequences suggests they are attached to the plasma membrane by glycosylphosphatidylinositol (GPI) anchors.

```
   1 - CCAGAACTCAACTCAGCCATGGCTTCAAACGCTTCTCTCACTCTTGTCCTAGCCGTTGCT
                           M  A  S  N  A  S  L  T  L  V  L  A  V  A
  61 - TGCTTCGTCTCTCTTATCTCACCGGCGATTTCACAGACGTGCTCTACGCAGAACGTCACC
         C  F  V  S  L  I  S  P  A  I  S  Q  T  C  S  T  Q  N  V  T
 121 - GGCGACTTCAAGAATTGCATGGACCTCCCCGTACTCGATTCCTTCCTCCACTACACATAC
         G  D  F  K  N  C  M  D  L  P  V  L  D  S  F  L  H  Y  T  Y
 181 - GACGCAGCCAACTCATCCCTCTCCGTCGCTTTCGTCGCTACTCCGCCTCGTTCCGGCGAC
         D  A  A  N  S  S  L  S  V  A  F  V  A  T  P  P  R  S  G  D
 241 - TGGGTCGCTTGGGGTATCAACCCCACGGGGACTAAAATGATCGGCTCTCAGGCGTTCGTC
         W  V  A  W  G  I  N  P  T  G  T  K  M  I  G  S  Q  A  F  V
 301 - GCCTACAGTCCTCGAGCCGGTGCGCGTCCCGAGGTGAACACGTACAACATCAGCAGCTAC
         A  Y  S  P  R  A  G  A  R  P  E  V  N  T  Y  N  I  S  S  Y
 361 - AGCCTCAGCGCAGGAAGGCTCACCTTCGACTTCTGGAACCTACGCGCTGAATCCATGGCC
         S  L  S  A  G  R  L  T  F  D  F  W  N  L  R  A  E  S  M  A
 421 - GGTAACAGGATCGTGATCTACACGTCGGTTAAGGTTCCGGCGGGAGCTGACAGCGTGAAC
         G  N  R  I  V  I  Y  T  S  V  K  V  P  A  G  A  D  S  V  N
 481 - CAGGTGTGGCAGATCGGCGGGAATGTGACTGGCGGTCGTCCGGGACCGCATCCTATGACT
         Q  V  W  Q  I  G  G  N  V  T  G  G  R  P  G  P  H  P  M  T
 541 - CCGGCGAACTTGGCCTCTACGAGGATGTTGAGATTGACTGGCTCCGACGCTCCGAGCTCT
         P  A  N  L  A  S  T  R  M  L  R  L  T  G  S  D  A  P  S  S
 601 - GCTCCAGGCTCCGCTCCGAGCTCTGGTCCGGGGTCTGCTCCAAGCTCTGGTCCGGGGTCT
         A  P  G  S  A  P  S  S  G  P  G  S  A  P  S  S  G  P  G  S
 661 - GCTCCAGGGTCTGTTCCAGGGTCTGCTGAGGGGCCGACCACTCCTGATGCCTCGACCACT
         A  P  G  S  V  P  G  S  A  E  G  P  T  T  P  D  A  S  T  T
 721 - CCTGGACAGGCGGGTAGTCCAGGGAACGCGGGTTCGATGACGACTAGCGTAAATTTCGGG
         P  G  Q  A  G  S  P  G  N  A  G  S  M  T  T  S  V  N  F  G
 781 - GTCAATTTTGGAATTTTGGTTATGTTGGCTTCAGTTTTCATATTCTGAGTATGATTTCAT
         V  N  F  G  I  L  V  M  L  A  S  V  F  I  F  *
 841 - CTTCTTCACATTCCTTTTTTGGTGTTGCATAATAATGGAGTTACATACTGTTTGTTTTAT
 901 - CGTTTTAGTACTAGTCTTTAGAGTCATTTACTCGTTTTGTGTTTCCACCTATCTCTATCT
 961 - CTCTCTCCACATTATTCTGAGTTATTAATATTGGATTGTATGGACCACTAAAAAAAAAAA
1021 - AAAAAAAAAA - 1030
```

Figure 4.1 cDNA and derived amino acid sequence of *Brassica carinata CIL1*

4.1.1 Catecholamine (CA) Binding Domain

A search of the Conserved Domain Database (Marchler-Bauer et al., 2003) was conducted with CIL1 and a high similarity to a possible CA-binding domain was found (Figure 4.2). It is a predominantly beta-sheet domain present as a regulatory N-terminal domain in dopamine beta-hydroxylase, mono-oxygenase X and SDR2. Its function remains unknown at present. The conserved domain length is 148 residues, 98.6% of the catecholamine-binding domain aligned with the CIL1 amino acid sequence. The similarity score for CIL1 is 78.2 and the probability that this degree of similarity could occur by chance is $9e^{-16}$. The domain model also has relationships to two other conserved domains: pfam03351, a DOMON domain (dopamine β-monooxygenase N-terminal) thought to mediate extracellular interactions. The second relationship is to a family of uncharacterized plant proteins, DUF568.

4.1.2 Dopamine-β-Hydroxylase Homologies

Vereslt and Asard (2004) performed alignments of the regulatory N-terminal domain of dopamine beta-hydroxylase (DoH) and related proteins, such as AIR12, with and without an associated cytochrome *b*561 electron transport domain (CB), from a variety of monocot and dicot plants. To investigate the relationship between CIL1 and the proteins reported by Vereslt and Asard (2004), an alignment was performed using ClustalW (Figure 9.1). The amino acid sequences used originated from four different plants: The CIL1 amino acid sequence from *B. carinata*, the CAC37356 amino acid sequence from *Solanum tuberosum*, the BAC01247 amino acid sequence from *Oryza sativa*, and the AAC62613 (AIR12), BAB09428, AAL57706, NP_199564, AAM64730,

```
CIL1            -----MASNASLTLVLAVACFVSLISPAIS-QTCSTQNVT--GDFKNCMDLPVLDSFLHY 52
AIR12           EQNSAMASSSSSLLILAVACFVSLISPAISQQACKSQNLNSAGPFDSCEDLPVLNSYLHY 60
DoH             ----------------------------------------------------CDYFLSW 7
                                                                     : :* :

CIL1            TYDAANSSLSVAFVATPPRS-GDWVAWGINPTGTKMIGSQAFVAYSPRAGARPEVNTYNI 111
AIR12           TYNSSNSSLSVAFVATPSQANGGWVAWAINPTGTKMAGSQAFLAYRSGGGAAPVVKTYNI 120
DoH             TVDGEE---TIAFELSGPTSTNGWVAIGFSDDG-QMAGADVVVAWVDNNG-RVTVKDYYT 62
                * :. :   ::**  : . : ..*** .:.  * :* *::..:*:    *    *: *

CIL1            SSYS-LSAGRLTFDFWNLRAESMAGNRIVIYT-SVKVPAGAD------SVNQVWQIGGNV 163
AIR12           SSYSSLVEGKLAFDFWNLRAESLSGGRIAIFNRTVKVPAGRD------SVNQVWQIGGNV 174
DoH             SGYSPPVPDLQQDVTDLFRATYENGVLTIRFRRKLSTNDPDDKSLLDGTVHVLWAKGPLS 122
                *.**    .        :**    *     :  .:..    *      :*: :*  *

CIL1            TGGRPGPHPMTPANLASTRMLRLTGSDAPSSAPGSAPSSGPGSAPSSGPGSAPGSVPGSA 223
AIR12           TNGRPGVHPFGPDNLGSHRVLSFT----EDAAPGSAPS--PGSAPS--PGSAP--APGTS 224
DoH             PNGGLGYHDFSPKSTKKVCLLSCT---------------------------------- 146
                ..*  * * : * .  .  :*  *

CIL1            EGPTTPDASTTPG-QAGSPGNAGSMTTSVNFGVNFGILVMLASVFIF 269
AIR12           G-------STTPGTAAGGPGNAGSLTRNVNFGVNLGILVLLGSIFIF 264
DoH             --------------------------------------------
```

Figure 4.2 BLASTP alignment of *Brassica carinata* CIL1 with possible catecholamine binding domain and the AIR12 amino acid sequence. |CDD|15053, smart 00664, DoH, Possible catecholamine-binding domain present in a variety of eukaryotic proteins.
"-" Regions of an amino acid sequence that did not align to the consensus.
"*" Residues are identical in all sequences in the column.
":" Conserved amino acid substitutions observed in the column.
"." Semi-conserved substitutions observed in the column.

AAM65781, NP_566763, NP_191466, AAM61181, NP_191734, and NP_566313 amino acid sequences from *A. thaliana*. Of the *A. thaliana* amino acid sequences used, AAC62613 and BAB09428 are similar to DoH proteins, while all other *A. thaliana* amino acid sequences are similar to DoH-CB proteins. A phylogenetic tree was constructed using the GeneBee Graphical Phylogenetic Tree software (http://www.genebee.msu.su/clustal/basic.html, first accessed December, 2004) with the default settings, tree output set to "phylogenetic" and bootstrap values enabled (Figures 4.3 and 9.1). The phylogram indicates that the AIR12, CIL1, and BAB09428 proteins are more closely related to each other than to the other *A. thaliana* amino acid sequences, the *Solanum tuberosum* amino acid sequence, or the *Oryza sativa* amino acid sequence used in the alignment. The existence of genes such as *CIL1* with similarity to only the N terminal domain of DoH suggests that the enzyme arose as the product of a fusion between genes encoding a dopamine-binding domain and a cytochrome b561 electron transport domain.

4.2 *CIL1* Copy Number

Southern blot analysis was used to estimate the copy number of *CIL1* in three *Brassica* species, *B. carinata*, *B. oleracea*, and *B. nigra*. *B. carinata* is an amphidiploid with the BBCC genome, n=34. Therefore, its most closely related diploid relatives are *B. nigra* (BB) and *B. oleracea* (CC). Genomic DNA from the three species was digested singly with the restriction enzymes *Bam*HI, *Eco*RI or *Hind*III, the fragments were separated by gel electrophoresis and the Southern blot was hybridized to a radioactively labeled *CIL1* probe (Figure 4.4). The hybridization patterns for the *Bam* HI digests of *B.*

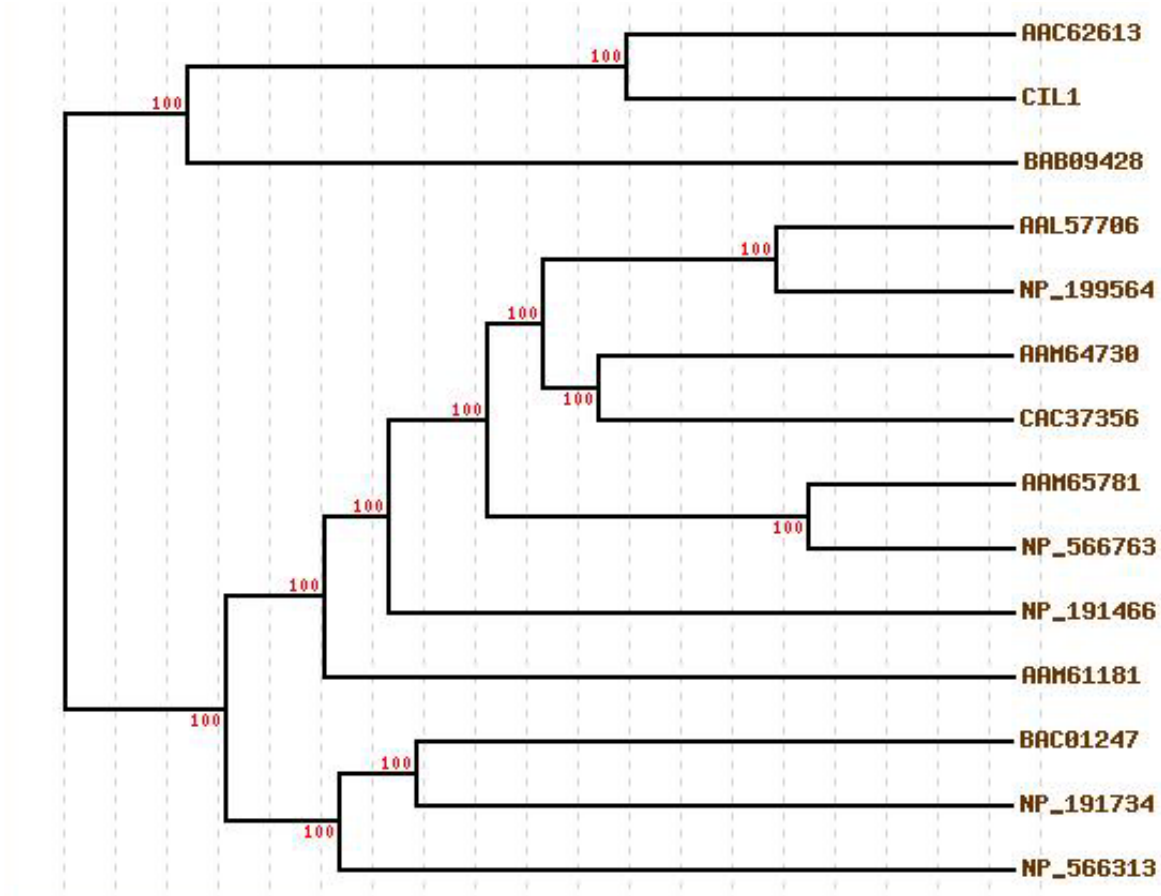

Figure 4.3. Phylogram generated using ClustalW version 1.87 software at http://www.genebee.msu.su/clustal/basic.html. AIR12 accession number AAC62613. *Arabidopsis thaliana* proteins – NP_191734, NP_566313, AAL57706, NP_199564, AAM64730, AAM65781, NP_566763, NP191466, AAM61181, BAB09428; *Solanum tuberosum* protein CAC37356, *Oryza sativa* protein BAC01247, and *Brassica carinata* CIL1 protein were included in the phylogram, and bootstrap values were calculated. Bootstrap values indicating support for the arrangement of amino acid sequences appear to the left of their respective group.

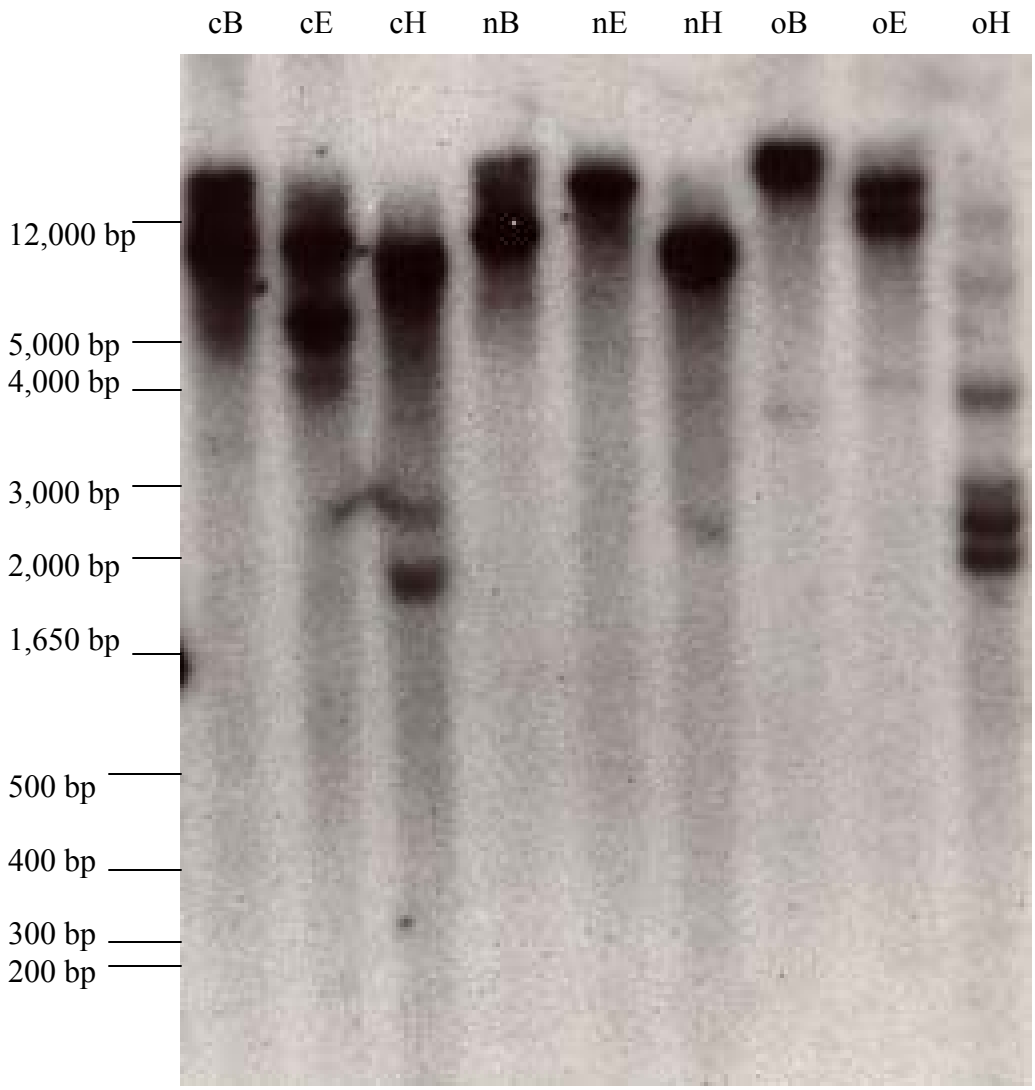

Figure 4.4 Southern blot analysis of *CIL1* gene arrangement in three *Brassica* species: *B. carinata*, *B. oleracea*, and *B. nigra*. Five micrograms of genomic DNA were used for restriction enzyme digests in each sample. The first letter in each lane represents the *Brassica* species that was examined while the second letter in each lane represents the restriction enzyme used to digest the sample: c= *B. carinata*; n = *B. nigra*; o = *B. oleracea*; B = *Bam*HI; E = *Eco*RI; H = *Hind*III.

carinata and *B. nigra* suggested incomplete digestion, however, subsequent digests with greater amounts of enzyme did not alter the results. These DNA samples may have contained enzyme activity inhibitors. In the *Bam*HI digest of *B. oleracea* DNA, the *CIL1* hybridization was seen in an apparent single fragment of greater than 12,000 bp. In the *Eco*RI digest of *B. carinata* genomic DNA the strongest hybridization signals were from fragments of approximately 12,000 bp and 7,000 bp with a fainter hybridization to a 4,000 bp fragment. In *B. nigra*, a single *Eco*RI fragment of greater than 12,000 bp hybridized to *CIL1* while in *B. oleracea* two fragments greater than 12,000 bp showed hybridization. The *Hind*III digested DNA of *B. carinata* displayed the strongest hybridization to fragments of ~10,000 and 1800 bp with weaker hybridization to a 2700 bp fragment. In *B. nigra*, the strongest hybridization was present on a ~10,000 bp *Hind*III fragment and possibly some hybridization to a 2200 bp fragment. The most complex pattern of *CIL1* hybridization was observed in the *Hind*III digest of *B. oleracea*. Here, the most intensely hybridizing DNA fragments were 2200 and 2000 bp while moderate hybridization was seen at 3700 and 3000 bp and weak hybridization at 12,000 and 9,000 bp. Overall, the data indicate that there are multiple copies of *CIL1* in *B. carinata* and that there is a similarity in the *CIL1* genome arrangement between *B. carinata* and *B. nigra*.

4.3 Organ Specificity of *CIL1* Expression

The expression of *CIL1* in various organs over a 24 h period was examined using semi-quantitative RT-PCR (Figure 4.5). The plants were sampled at the fourth-leaf stage of growth. The optical density of the ethidium bromide stained *CIL1* RT-PCR product

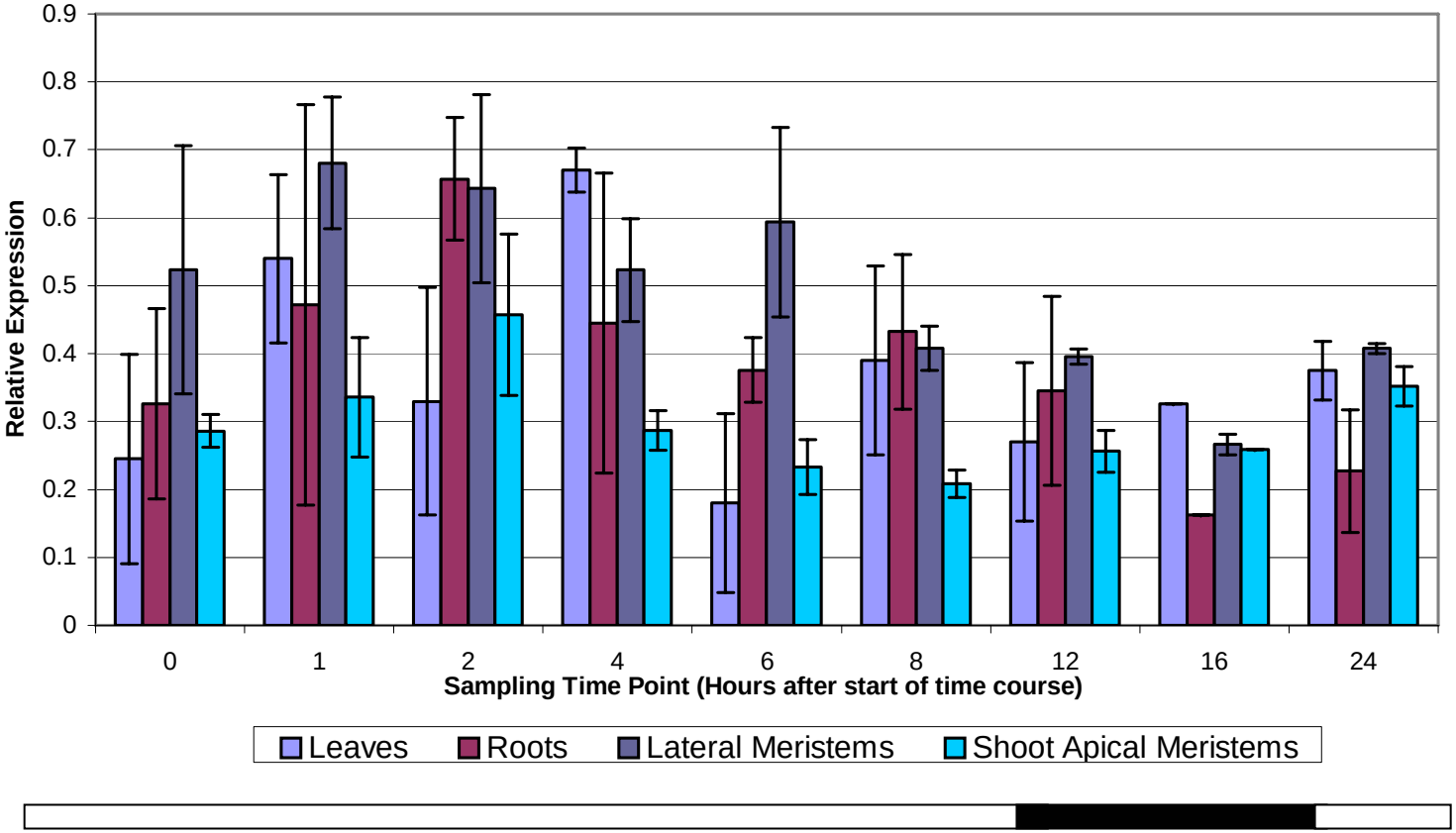

Figure 4.5 Expression of *CIL1* in third leaves, whole roots, lateral meristems and shoot apical meristems of *Brassica carinata*. The RNA was extracted from plants at the fourth leaf growth stage at 1 h time intervals for 24 h and used for semi-quantitative RT-PCR. The relative expression of *CIL1* was determined through comparison of the optical density of ethidium bromide stained PCR products of *CIL1* with actin. The bar below the graph represents periods of light and darkness. Each organ at each time point was analysed in triplicate. Error bars represent the standard error of the mean.

was compared to that of actin to determine relative expression. The *CIL1* transcript was found in third leaves, whole roots, lateral meristems and apical meristems. Variation in the transcript amounts over the 24 h period was evident in each organ. The leaves displayed the highest degree of variation over the entire time course with a 3.5 fold difference in relative expression between the maximum at 4 h and the minimum at 6 h. Root expression also varied, though not to the same degree as in the leaves. By the 2-hour time point, 2.5 times the amount of *CIL1* transcript was present in the root compared to the 0-hour point, with expression decreasing thereafter. The amount of transcript in lateral meristems also varied by 2.5 fold with a maximum at 1 h and minimum at 16 h after sampling commenced. The apical meristem showed slightly less variation in *CIL1* transcript amount over the time course with a 2.2 fold difference between the maximum at 2 h and minimum at 8 h. Overall, the lateral meristems showed high expression and maintained fairly consistent amounts of *CIL1* mRNA throughout the time course compared to the other organs examined.

4.4 Effects of Phytohormone Treatment on *CIL1* Expression

The lateral meristems were chosen for the study of the effects of phytohormone treatment on *CIL1* expression since they displayed the most prominent antisense phenotype and highest, most consistent amount of *CIL1* mRNA. Adherence of the phytohormone solutions to these meristems required the incorporation of 1% (v/v) Triton X-100. To evaluate the effect of Triton X-100, if any, on *CIL1* expression the third lateral meristems of wild type plants were treated with Triton X-100 solution at the fourth leaf stage of growth (Figure 4.6). The relative expression of *CIL1* in the lateral

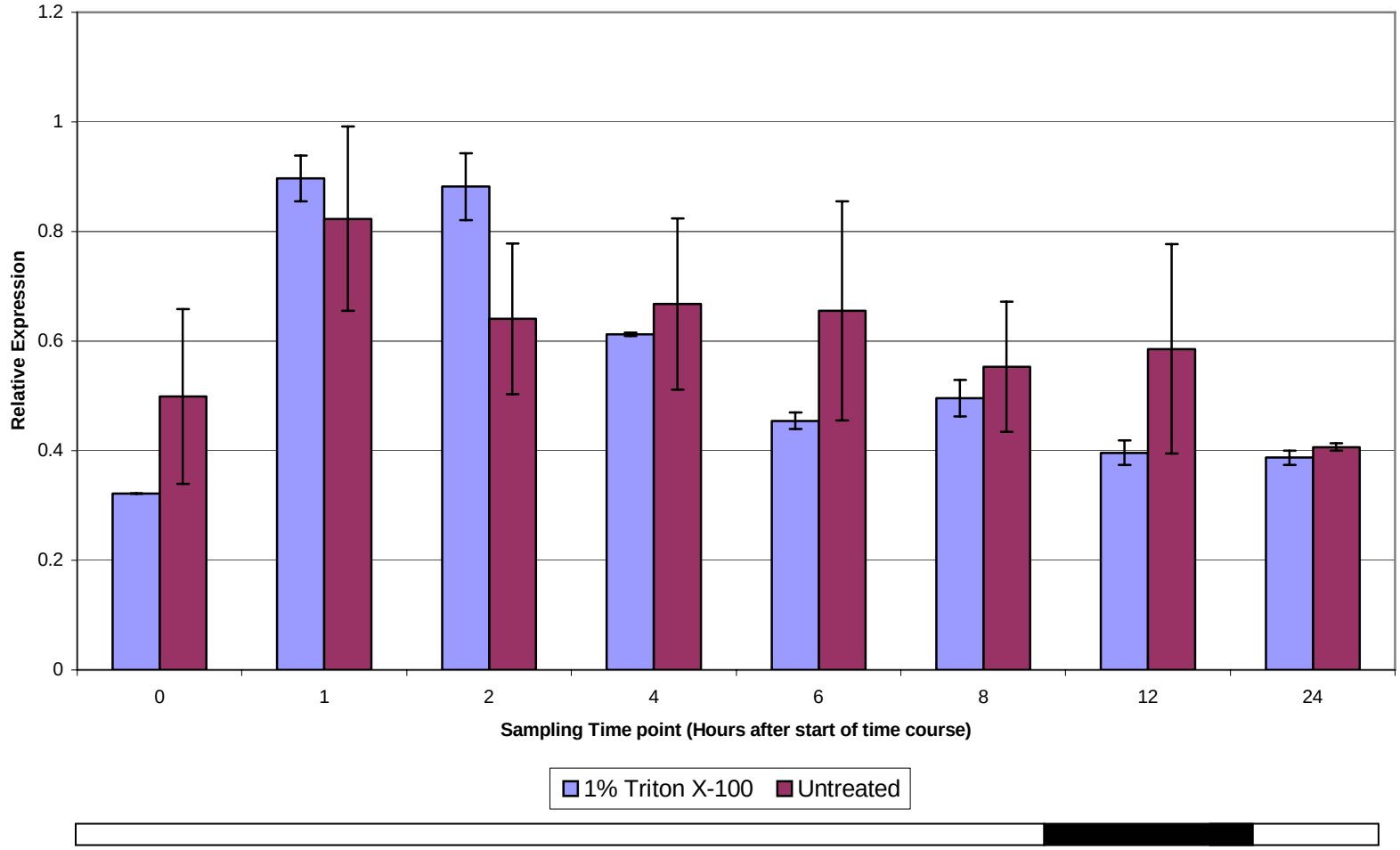

Figure 4.6 Semi-quantitative RT-PCR analysis of *CIL1* expression after treatment with 1% Triton X-100. The third lateral meristems of non-transformed *Brassica carinata* plants were treated at the fourth leaf stage of growth. RNA was extracted at the time intervals indicated after spraying. The relative expression of *CIL1* was determined through comparison of the optical density of ethidium bromide stained PCR products of *CIL1* with actin. The bar below the graph represents periods of light and darkness. Three samples per time point were collected for both treatments. Error bars represent standard error of the mean.

meristems did not vary greatly from untreated plants after the Triton treatment. The selection of BAP and α-NAA concentrations was based on previous studies (Crosby et al., 1981; Neuteboom et al., 1999; Fei and Vessey, 2004). However, the optimal treatment concentration for +/- ABA was determined empirically (Figure 4.7). Differences in *CIL1* expression correlating to the different +/- ABA concentrations used to treat the organs were observed one hour after +/- ABA application. At that time point, the 10 μM concentration showed the largest effect and, therefore, that concentration was used in the subsequent time course study.

The 3rd lateral meristems of non-transformed *B. carinata* plants were treated with either 5 μM BAP, 50 μM α-NAA, or 10 μM +/- ABA and the *CIL1* expression was analysed using semi-quantitative RT-PCR (Figure 4.8). Expression of *CIL1* increased nearly three-fold one hour after BAP treatment; thereafter it decreased but remained largely above untreated amounts. At six hours of darkness, the amount of *CIL1* mRNA had dropped to 0 h amounts, but increased again by 24 h after treatment. These results indicate that BAP treatment induces either directly or indirectly, a rapid and sustained increase in *CIL1* expression. The decreased *CIL1* expression noted at 6 h of darkness suggests that the effect of BAP is modulated by the photoperiod.

The amount of *CIL1* transcript increased significantly by one hour after the α-NAA treatment, thereafter returning to 0 h amounts. However, similar to BAP, there appeared to be a further decrease of expression coinciding with 6 h of darkness, and the effect was reversed with light. The data show that auxin induces a rapid but very transient increase in *CIL1* expression.

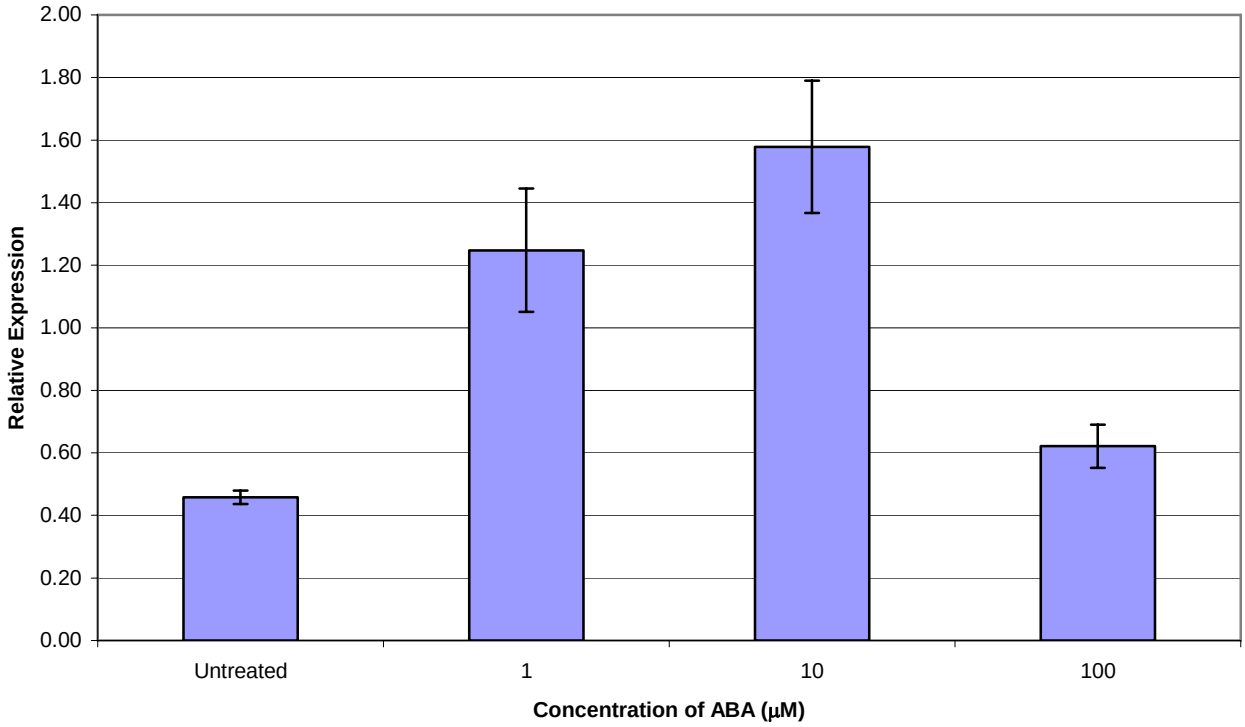

Figure 4.7 Analysis of *CIL1* expression in *Brassica carinata* after treatment with abscisic acid. Non-transformed plants were treated once they had reached the fourth leaf stage of growth. The third lateral meristems of the plants were treated with 100 μL of racemic abscisic acid solutions at the stated concentrations. The meristems were collected one hour after treatment and RNA extracted. Two hundred nanogram of RNA was used in semi-quantitative RT-PCR amplifications. The relative expression of *CIL1* was determined through comparison of the optical density of ethidium bromide stained PCR products of *CIL1* with actin. Three replicates were conducted per treatment. Error bars represent the standard error of the mean.

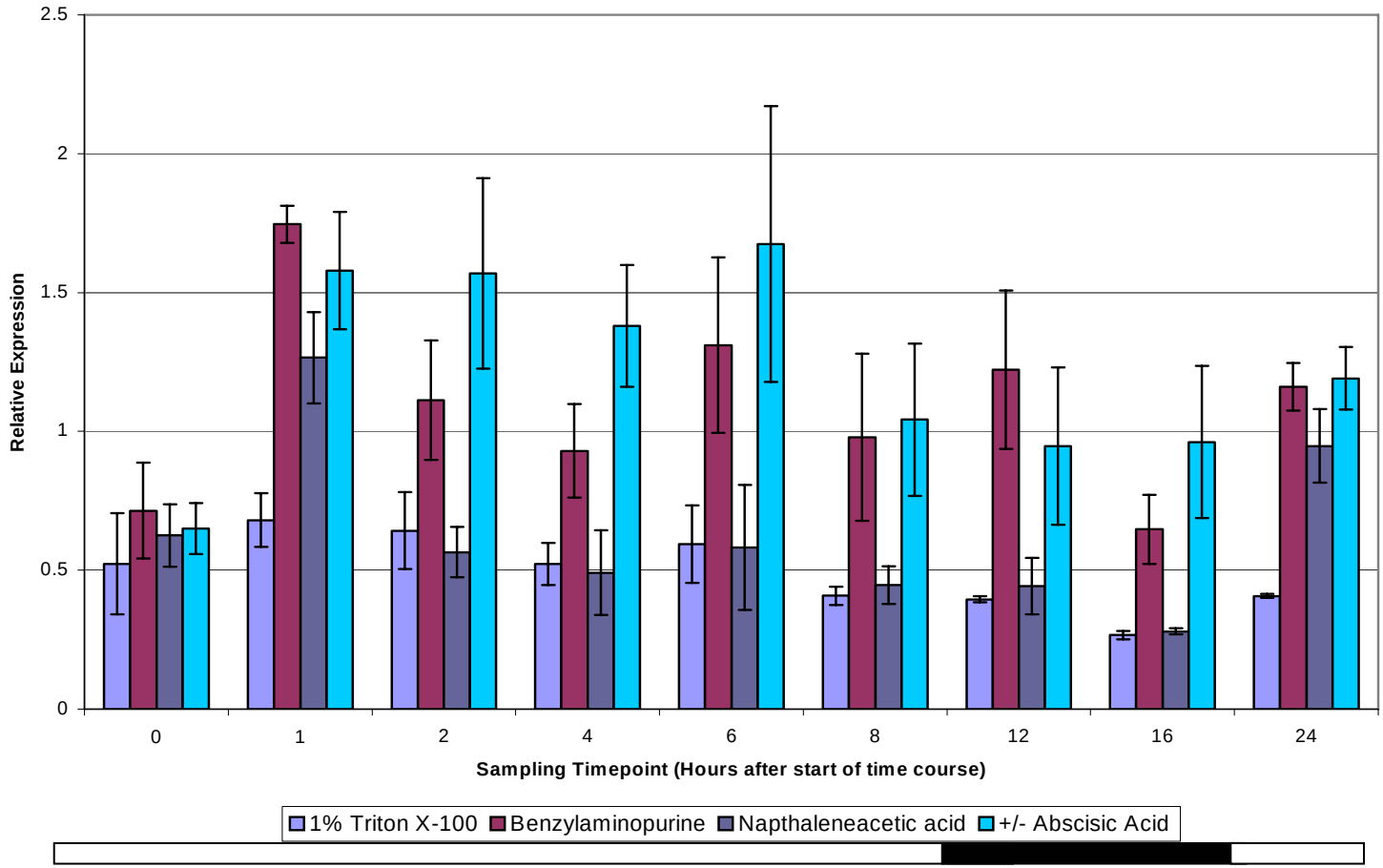

Figure 4.8 Analysis of the effects of various phytohormone treatments on *CIL1* expression. The third lateral meristems of non-transformed *Brassica carinata* plants at the fourth leaf stage of growth were treated with 100 µL solutions of either 5 µM 6-benzylaminopurine, 50 µM α-napthaleneacetic acid, or 10 µM +/- abscisic acid. Two hundred nanogram of total RNA was used for semi-quantitative RT-PCR. The relative expression of *CIL1* was determined through comparison of the optical density of ethidium bromide stained PCR products of *CIL1* with actin. The bar below the graph represents periods of light and darkness. Three replicates were collected at each time point from separate plants for each treatment. Error bars represent the standard error of the mean.

Similar to BAP and α-NAA, treatment with +/- ABA induced a rapid increase in *CIL1* expression. The transcript amounts remained above 0 h amounts throughout the 24-hour period examined. Unlike the BAP and α-NAA treatments, there was no significant decrease in *CIL1* expression during darkness. These data revealed that treatment with any of these three phytohormones induced a rapid increase in *CIL1* expression. However, the response to α-NAA was transient, whereas the responses elicited by BAP and ABA were more sustained.

4.5 Copy Number Analysis of Selfed Antisense *CIL1* Transgenic *B. carinata* Plants

Southern blot analysis was used to determine the copy number of the insertion of the *CIL1* antisense construct in the T_3 and T_4 generations of the transformed plants. Genomic DNA from the transgenic plants was digested with *Nhe*I and *Pac*I, electrophoresed and the resulting fragments were transferred to a nylon membrane. The Southern blot was hybridized with a probe to the neomycin phosphotransferase (*NPT II*) gene that had been used as the transformation selection marker (Figure 4.9A). The hybridization signal of the DNA from the transgenic lines 2, 3, 6, 10, and 13 displayed a similar intensity to the single copy *NPT II* hybridization signal. The intensity of the hybridization signal from line 5 suggests that it could contain up to five copies of the cassette and line 11 likely contains between 5-7 copies of the cassette. The location of the hybridization signal in the transgenic plant samples on the blot appears to be slightly different than the plasmid controls. This is likely due to the much larger amount of DNA that was loaded in these lanes and/or impurities in the samples. However, although the hybridization signal for transgenic line 10 is weak, it appears to be located at a much

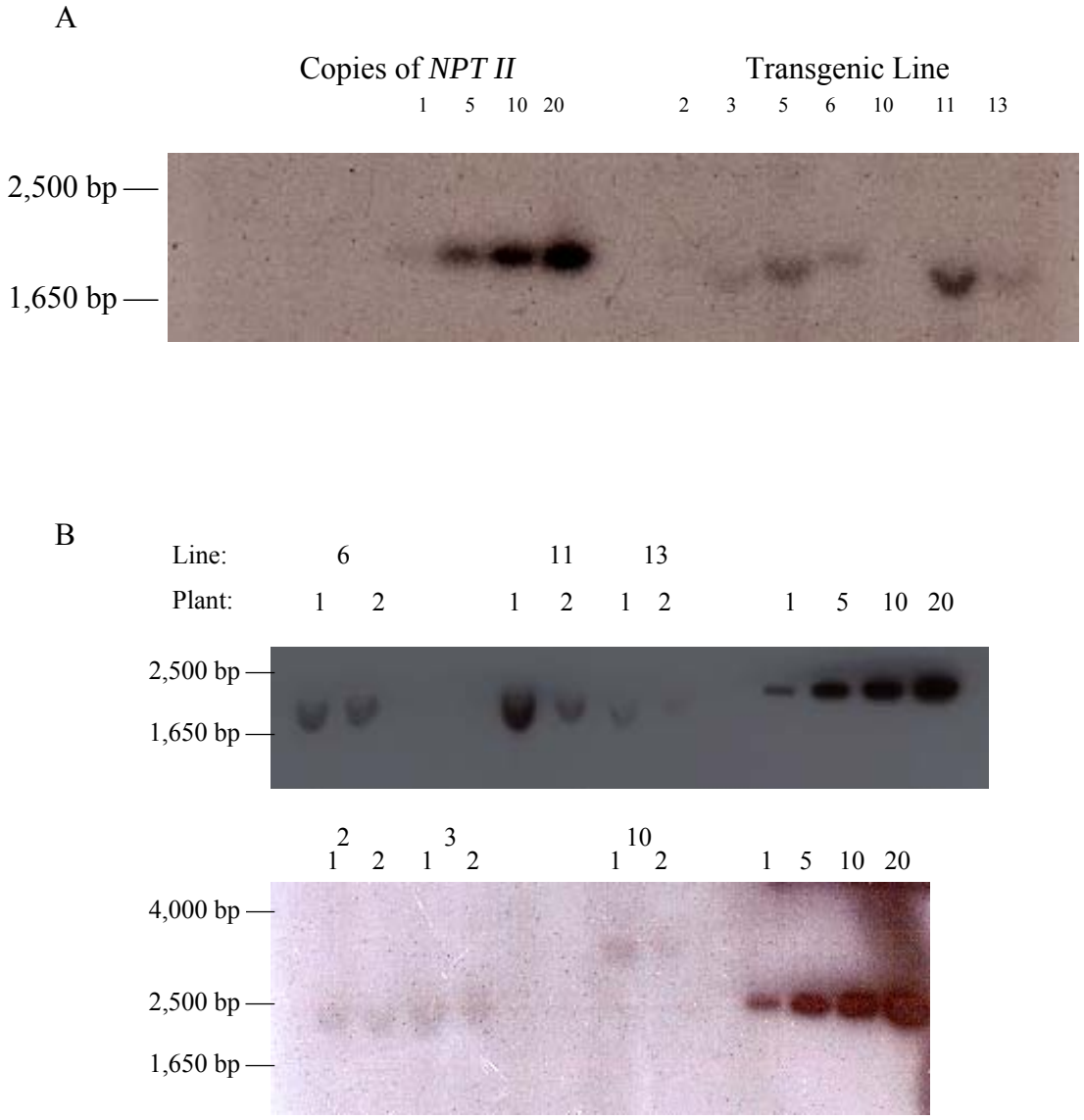

Figure 4.9 Southern blot analysis of T_3 (A) and T_4 (B) antisense *CIL1* transgenic *Brassica carinata* plants. Five micrograms of genomic DNA from each transgenic line was digested with *Nhe*I and *Pac*I. The transformation vector was loaded in amounts equivalent to 1, 5, 10, and 20 copies. The blot was hybridized to a radioactively labeled PCR product of the neomycin phosphotransferase gene (*NPT II*).

higher molecular size than the control or the other transgenic lines. This result suggests that a rearrangement of the insert has occurred in this line.

These data indicate that lines 2, 3, 6, 10, and 13 are possibly homozygous for the *CIL1* antisense cassette in the T_3 generation. To confirm that no segregation of the antisense cassette occurred in the progeny of the T_3 plants, another Southern blot was conducted on DNA isolated from two T_4 plants. The data from this Southern blot (Figure 4.9B) qualitatively confirmed that transgenic lines 2, 3, 6, 10 and 13 were homozygous for single copy insertion events. The higher molecular size of the DNA fragment hybridizing to the probe in transgenic line 10 is more evident in this blot than the previous. It appears that transgenic line 11 was still segregating, showing one plant that contained approximately 5 copies of the cassette and the other plant having 1-3 copies. Therefore, the homozygous single-insert transgenic lines 2, 3, 6, 10 and 13 were used for all further analyses.

4.6 Analysis of Senescence in Antisense *CIL1* Transgenic *B. carinata*

Initial visual observations suggested that the antisense *CIL1* plants were slower to senesce than the non-transformed plants. To examine this phenomenon in greater detail, a senescence bioassay was conducted to measure the chlorophyll content of leaf discs after a period of darkness (Figure 4.10). The bioassay was conducted twice, with three biological replicates per line analysed each time. With the exception of transgenic line 3, little difference in the chlorophyll breakdown was observed among the non-transformed and the antisense *CIL1* transformed lines. Slightly elevated chlorophyll decay was

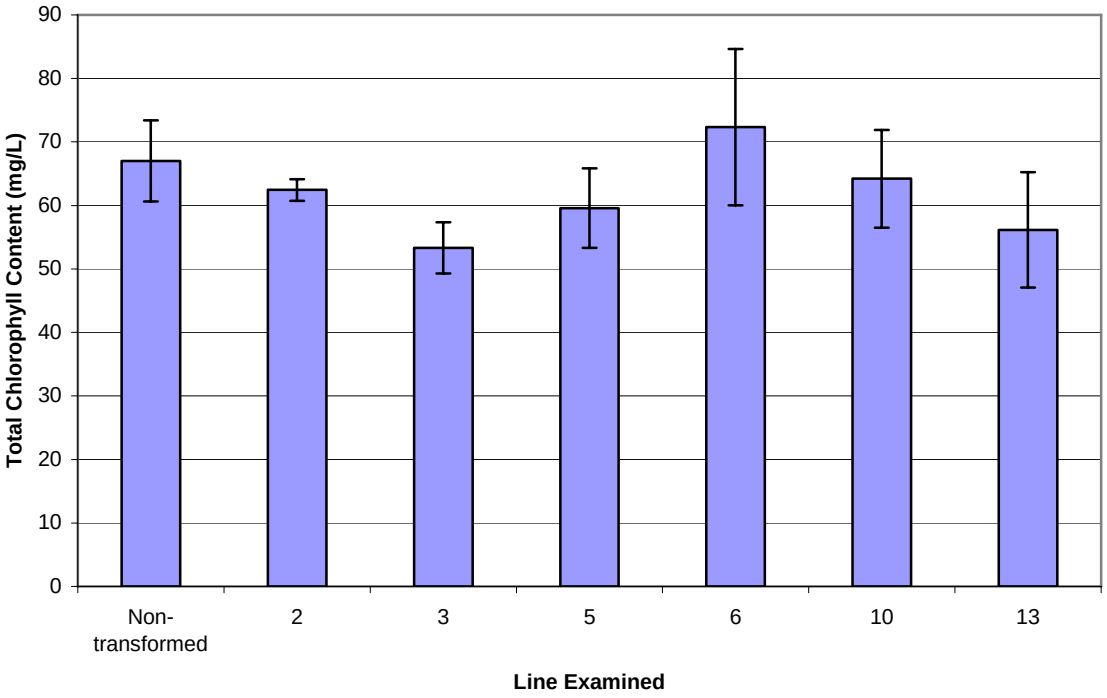

Figure 4.10 Chlorophyll content in leaf discs of *Brassica carinata* non-transformed and antisense *CIL1* transgenic plants. Leaf discs were incubated at room temperature in the dark for 72 h prior to extraction. Three biological replicates were collected from each line, and two experiments were conducted for a total of 6 measurements per line. Error bars represent the standard error of the mean.

observed in transgenic line 3. These results suggest that the observation of slower senescence was not due to higher chlorophyll content in leaves.

4.7 Phenotypic Characterization of Homozygous Antisense *CIL1* Transgenic Plants

Initial observations also suggested that transgenic plants had larger leaves than the non-transformed plants over the entire vegetative life cycle. To examine this phenomenon in greater deal, the phenotype was characterized by measuring the surface area of the leaves at various stages during the life cycle of the plants. Two experiments were conducted and eight biological replicates were taken during the first experiment, and four during the second (Figure 4.11). In the first experiment (Figure 4.11 A) at 5 days after germination the leaves of the antisense transgenic line 2 showed little surface area difference compared to the non-transformed. In contrast, leaf surface area of transgenic lines 3, 5, 10, and 13 were smaller than the non-transformed. Five days later the trend was unchanged for lines 2, 3, 5 and 10. The mean leaf surface area of lines 2 and 13 was similar to non-transformed and remained so for the remainder of the experiment. The mean leaf surface area of transgenic line 5 remained smaller than that of the non-transformed line throughout the experiment. Transgenic lines 3 and 10 mean leaf surface areas were less than the non-transformed line at all measurements except the final one, 20 days after germination, where they were comparable to non-transformed mean leaf surface area. In the second experiment (Figure 4.11 B), the mean leaf surface area of the transgenic lines was less than the non-transformed at 12 days after germination but

4.11 A

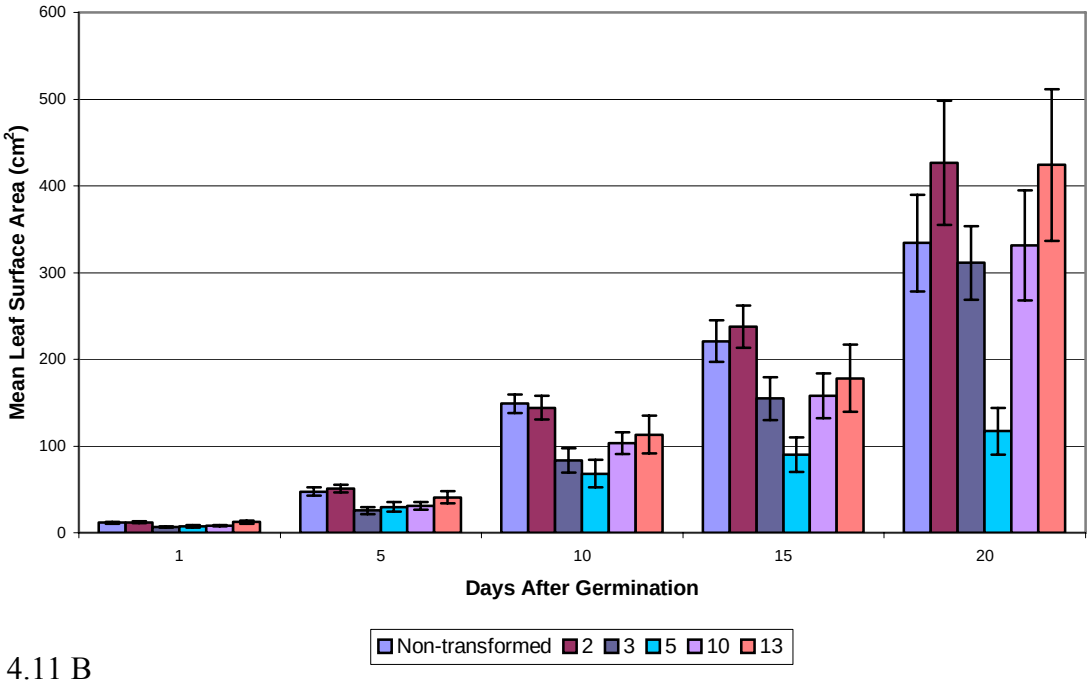

4.11 B

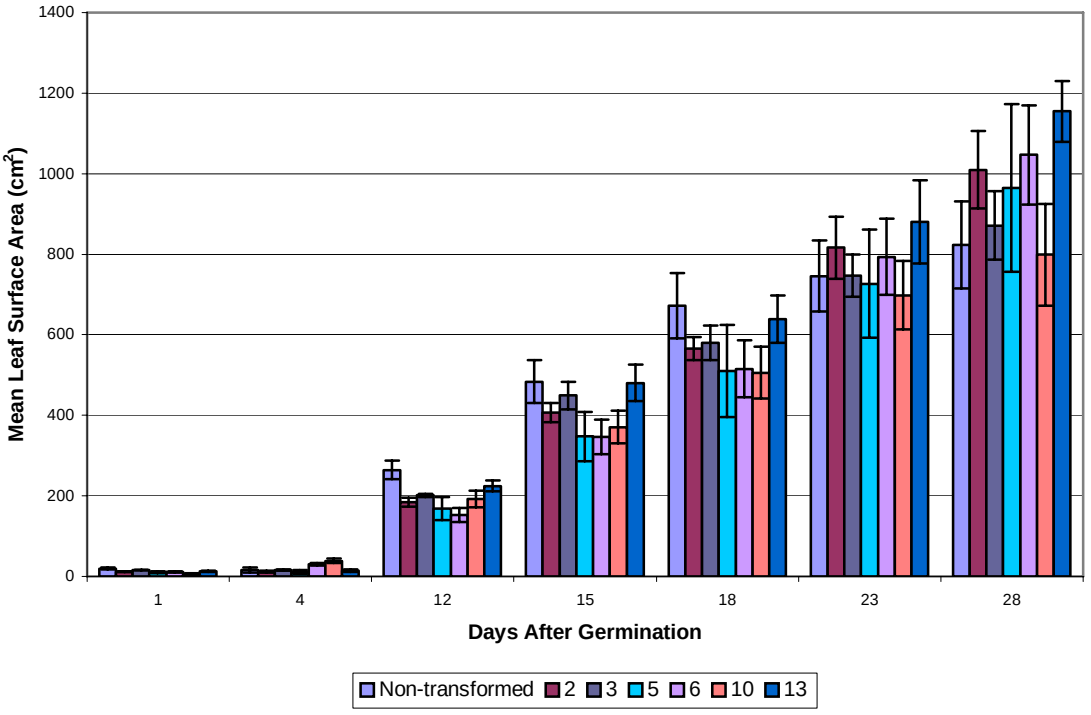

Figure 4.11 Analysis of leaf surface area of non-transformed and transgenic antisense *CIL1 Brassica carinata* plants. Leaf surface area was measured for each leaf for each plant, the results were summed, and a mean for the replicates was calculated. A. First experiment examining leaf size, with 8 biological replicates per line. B. Second experiment examining leaf size, with 4 biological replicates per line. Error bars represent the standard error of the mean.

was nearly comparable 3 days later and remained so for another 8 days. At that time transgenic lines 2, 6 and 13 started to show slightly greater mean leaf surface area than the leaves of the non-transformed and continued so throughout the rest of the experiment.

A large degree of variation of leaf mean surface area was observed over the two experiments (Figure 4.11 A, B), despite using the same growth conditions, soil, and seed for each experiment. The cause of the initial observation of significantly greater leaf surface area for the transgenic lines is unknown, however, it may be attributable to planting density. The transgenic plants produced larger leaves and exhibited a pronounced release of apical dominance with a plant density less than 3 seeds/cm^2, while the non-transformed plants were unaffected by plant density.

Additional phenotypic variations of antisense *CIL1* transgenic plants in comparison to non-transformed were observed; plants of all transgenic lines produced multiple leaves at one node demonstrating a release of apical dominance (Figure 4.12), formed true leaves at the cotyledon axils (Figure 4.13), and generated lateral florets at any node on the plant, down to the soil level (Figure 4.14). In contrast, the non-transformed *B. carinata* plants did not exhibit any of these phenotypes. All the homozygous transgenic lines exhibited these phenotypes to varying degrees, although line 6 produced these phenotypes at the greatest frequency and to the highest degree. While line 10 produced very elongated, ovate first leaves at 15 days after germination (Figure 4.15). Additional leaf production was observed to be dependent on plant density. Lateral meristem leaf growth, but not lateral inflorescence growth in transgenic plants was inhibited at a planting density of greater than 3 seeds/cm^2. The planting density of

Figure 4.12 Comparison of lateral meristem development of transgenic antisense *CIL1* line 6 (top photograph) and a non-transformed plant (bottom photograph). At the third node of the plant of transgenic line 6, five leaves are visible, numbered from oldest to youngest. A sixth leaf is developing in the lateral bud, denoted with an asterisk. Both photographs were taken 38 days after germination.

Figure 4.13 Photograph of a plant from transgenic antisense *CIL1* line 6 demonstrating a release of apical dominance, as well as the differentiation of true leaves at the cotyledon axils. The cotyledon axils are marked with asterisks while the additional leaf present is denoted with an arrow. A senescent cotyledon is visible just below the left true leaf at the cotyledon axil.

Figure 4.14 Comparison of branching of transgenic antisense *CIL1* line 2 (left photograph) and non-transformed *Brassica carinata* (right photograph). The arrow on the left panel marks the basal-most lateral inflorescence, while the arrow on the right panel shows the absence of any inflorescences at the same position on the non-transformed plant.

Figure 4.15 Comparison of leaf morphology and vasculature unique to transgenic antisense *CIL1* line 10 (left photograph) with a non-transformed plant (right photograph). The abnormal first leaves from line 10 are marked with asterisks, while the non-transformed first leaves are denoted with a "0". Photographs were taken 15 days after germination.

the non-transformed plants did not affect lateral meristem leaf growth, or lateral inflorescence growth. *Brassica carinata* produces leaves with an alternate phyllotaxy, and this phyllotaxy was maintained in the production of additional leaves by the antisense *CIL1* transgenic lines. Although *NPTII* hybridization was not observed in the T_4 plants of transgenic line 5 using Southern blot analysis, the line displayed the transgenic phenotype, and was positive for the presence of the *NPTII* and antisense *CIL1* genes as determined by PCR analyses.

A comparison was made between the phenotype of the antisense *CIL1* transformed *B. carinata* and the *A. thaliana* cytokinin mutant *supershoot.* The *supershoot* mutant displayed an increase in axillary leaf production during the vegetative stage and a vast increase in secondary inflorescence proliferation during the reproductive phase. However, in contrast to the antisense *CIL1* transformed *B. carinata*, the homozygous *supershoot* plants were small, infertile, and senesced much later than wild type Columbia *A. thaliana* (Personal Observation).

4.8 Real-Time Quantitative RT-PCR Analysis of Homozygous Antisense *CIL1* Transgenic Plants

Real-time quantitative RT-PCR (qRT-PCR) was used to analyse the expression of *CIL1* in homozygous antisense plants. Multiplex reactions could not be performed since only one dye was used to track the products of the qRT-PCR reactions. Therefore, the *CIL1* and actin (*BcAct*) primer sets were used in separate amplification reactions.

4.8.1 Test of Primer Efficiency

To calculate expression, the $\Delta\Delta C_T$ method was used. This method combines the data from two different data sets (*CIL1* and BcAct) and compares the change in the threshold cycle to a normalized threshold cycle (the non-transformed samples). One caveat of this method is that the primers must amplify with a similar efficiency (Livak and Schmittgen, 2001).

Primer efficiencies were tested with RNA from 31-day old non-transformed roots. As seen in Figure 4.16 the slope of the line was negative $1.4x10^{-3}$, indicating that the primers amplified with very similar efficiencies.

Based on the recommendation in the QuantiTect SYBR Green RT-PCR Kit (Qiagen, Hilden, Germany) 250 ng of RNA was used in all the reactions.

4.8.2 Analysis of Samples

The results of the qRT-PCR are presented in Figure 4.17. It is evident that not only does the effect of the antisense construct vary from one transgenic line to another but also from one plant organ to another. The leaves of 31-day old plants from transgenic lines 3 and 10 had 4-fold and nearly 1.8-fold more *CIL1* transcript, respectively, than the non-transformed plants. However, transgenic lines 6, 13 and possibly 5 had slightly less and line 2 nearly the same amount of *CIL1* mRNA as in leaves of the non-transformed plants. Greater expression of *CIL1* in comparison to non-transformed plants was also found in the lateral meristems of 29-day old plants of transgenic lines 2, 5, and 10. Similar to leaves, in the lateral meristems of lines 6 and 13 the expression of *CIL1* was less than in non-transformed plants. The greatest effect of the antisense construct on

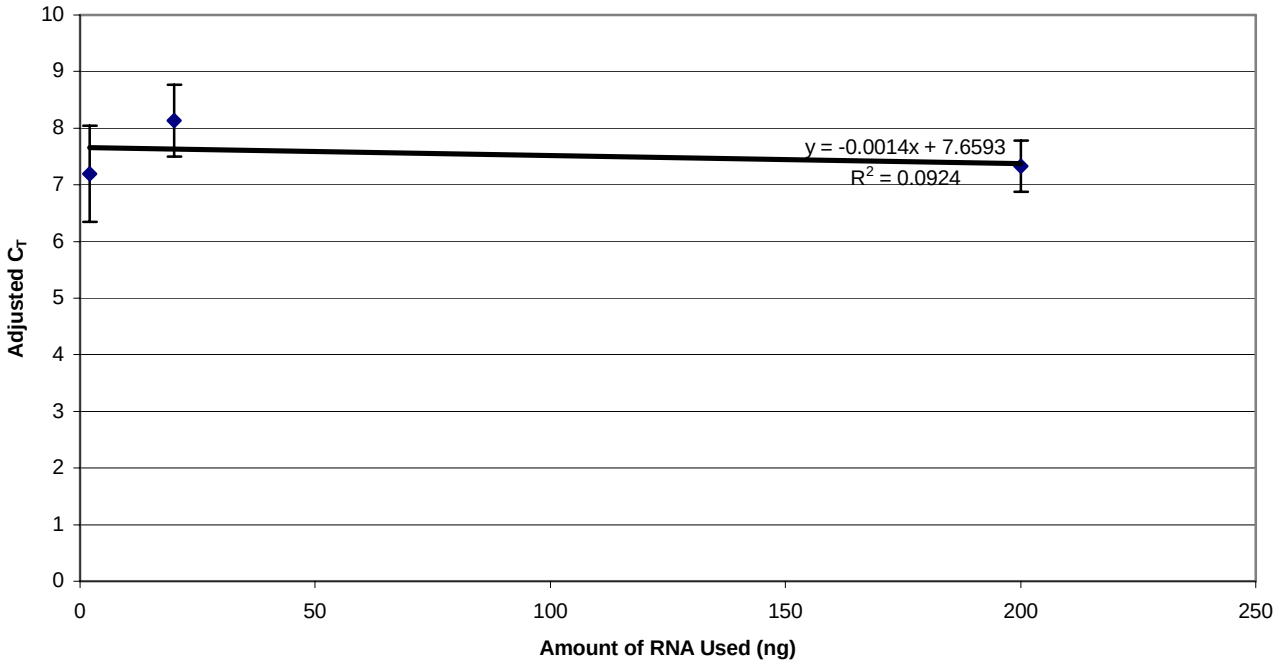

Figure 4.16 Primer efficiency test of the CIL1770 and BcAct primer sets using real-time quantitative RT-PCR. The expression was calculated using the $\Delta\Delta C_T$ method (Pfaffl, 2001; Vandesompele et al., 2002). The RNA was extracted from 31-day old non-transformed *Brassica carinata* roots. The amounts used were 200 ng, 20 ng, and 2 ng. Three biological replicates were amplified per sample. Error bars represent standard error of the mean. The slope of the line is -1.4×10^{-3} as calculated by Microsoft Excel.

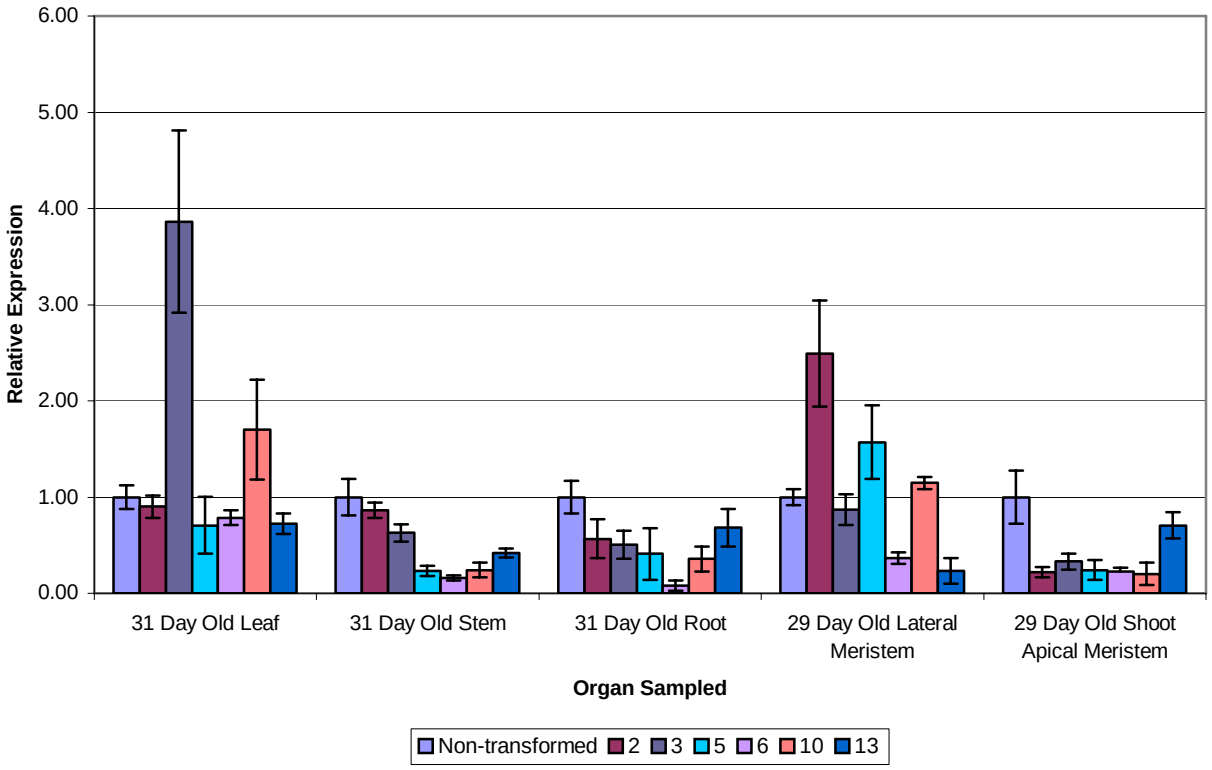

Figure 4.17. Real-time quantitative RT-PCR analysis of *CIL1* expression in antisense transgenic *CIL1* and non-transformed *Brassica carinata* plants. The analysis was performed on transgenic lines 2, 3, 5, 6, 10, 13 and non-transformed *B. carinata*. Two hundred and fifty nanogram of RNA was used in each reaction. The results were analysed using the $\Delta\Delta C_T$ formula (Pfaffl, 2001; Vandesompele et al., 2002) with actin used as a control for RNA amounts. Three biological replicates per sample per line were analysed. Error bars represent standard error of the mean.

transcript amount in transgenic lines was observed in the shoot apical meristem with approximately 5-fold reductions for all but line 13. Correlating with the degree of transgenic phenotype observed, the 29-day old lateral meristem from transgenic line 6 had the least amount of *CIL1* transcript. However, the greatest reduction in transcript in this line was seen in the root with 8% *CIL1* mRNA present compared to non-transformed plants. In the 31-day old stem, lines 3, 5, 6, 10, and 13 all had smaller amounts of *CIL1* mRNA compared to line 2 and the non-transformed line. In the shoot apical meristem, all the transgenic lines except for line 13 had a vast reduction in *CIL1* mRNA amount, while line 13 was slightly reduced in comparison to the non-transformed line.

4.9 Analysis of Phytohormones in Homozygous Antisense *CIL1* Transgenic Plants

Reversed phase HPLC with tandem MS coupled with electrospray ionisation was used to analyse the phytohormones present in non-transformed and antisense *CIL1* transgenic *B. carinata*. For these analyses, three biological replicates of the root, stem, first leaf, lateral meristem, and shoot apical meristem were analysed. Lateral meristem samples collected from transgenic plants were phenotypically equivalent to non-transformed plants and were collected prior to the development of the "multiple leaf" phenotype. The phytohormones examined over the course of this experiment were IAA, IAAsp, Z, ZR, 2iP, IPA, DHZ, DHZR, ZOG, 7'-OH-ABA, ABA-GE, PA, DPA, and neo-PA. For the plant material examined, only IAA (Figure 4.18), ZR (Figure 4.19), ABA (Figure 4.20), and DPA (Figure 4.21) were quantified with reproducible results. For the other phytohormones examined, either the amounts were below the limit of detection, or quantification, or they were very inconsistent among the replicates.

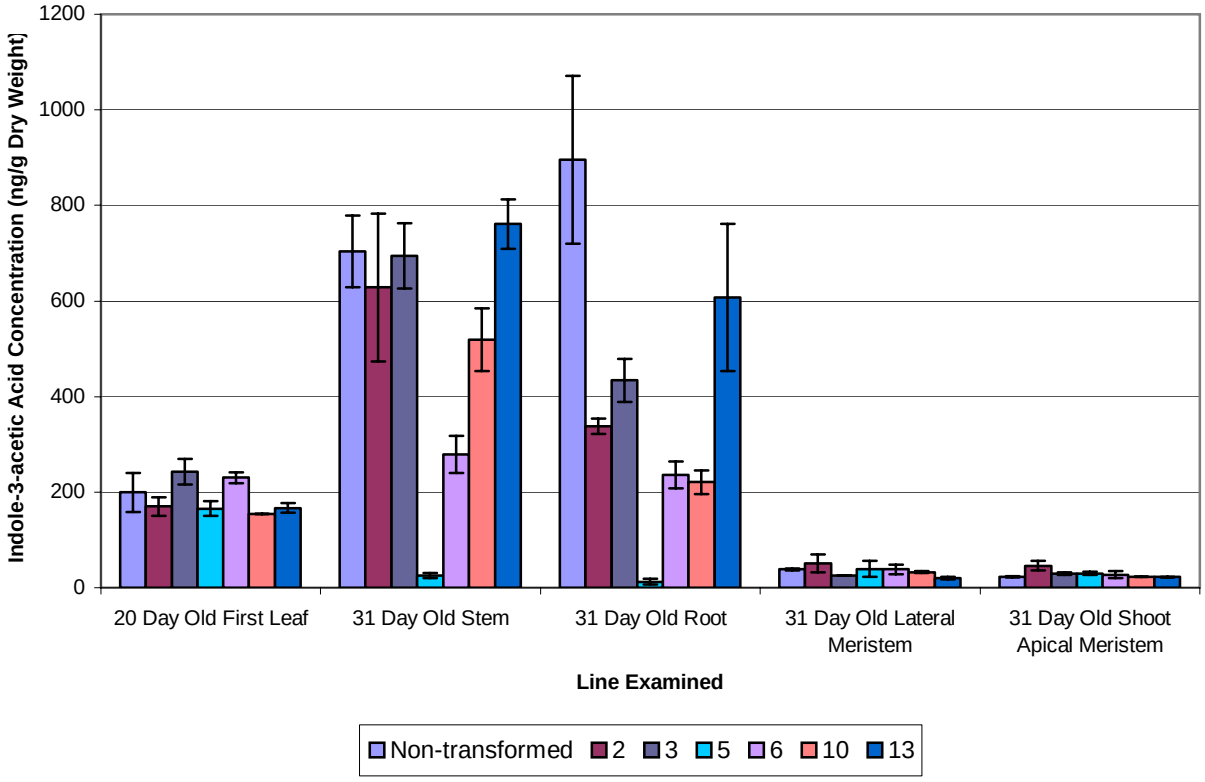

Figure 4.18 Indole-3-acetic acid present in organs of *CIL1* antisense transgenic and non-transformed *Brassica carinata*. First leaves, stems, roots, lateral meristems, and shoot apical meristems were examined. Samples were collected in triplicate from the lines indicated at 20 or 31 days after germination. The results for the 31-day old stem and root are significantly different at $\rho \leq 0.01$ while the results for 31-day old lateral meristem are significantly different at $\rho \leq 0.05$ by ANOVA. Error bars represent standard error of the mean.

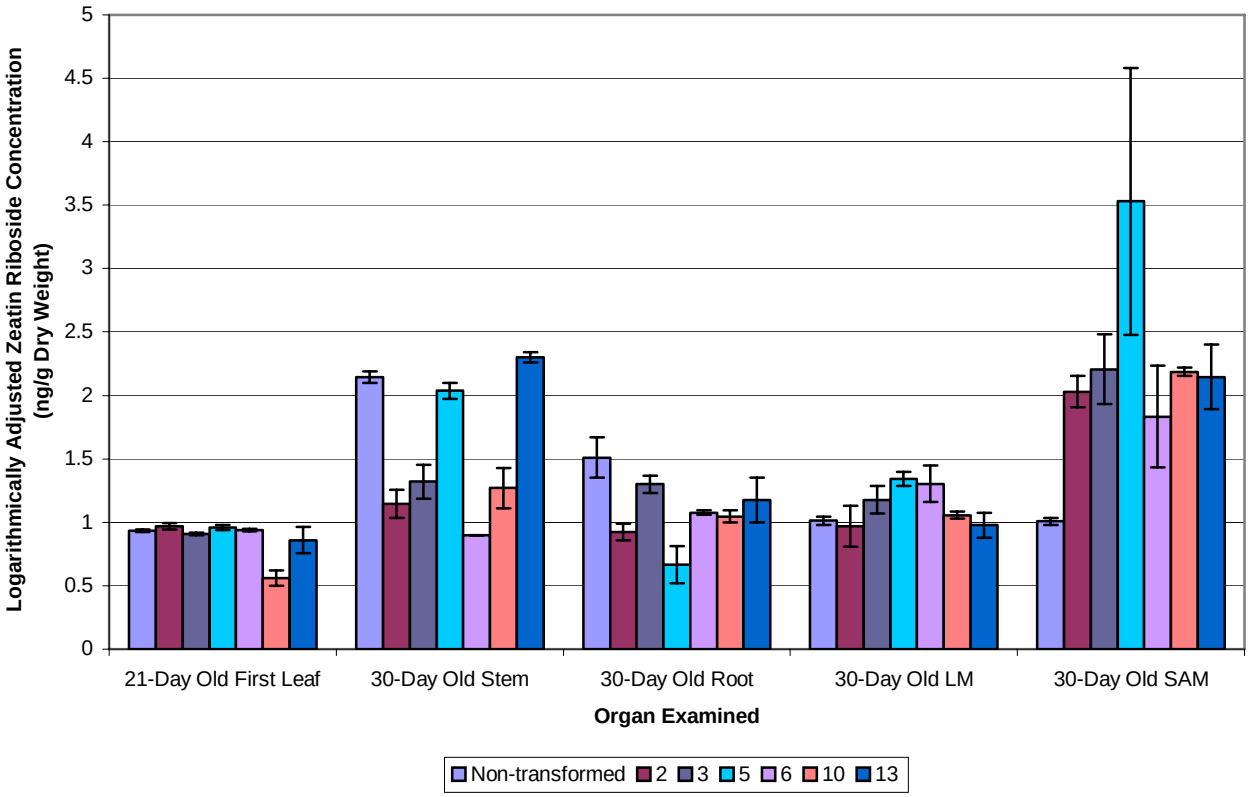

Figure 4.19. Zeatin riboside present in organs of transgenic antisense *CIL1* and non-transformed *Brassica carinata*. First leaves, stems, roots, lateral meristems, and shoot apical meristems were examined. Samples were collected in triplicate from the lines indicated at 20 or 31 days after germination. The data were logarithmically adjusted to stabilise the variance. The results for 20-day old first leaf, 31-day old stem, and 31-day old root are significantly different at $\rho \leq 0.01$ while the results for 31-day old shoot apical meristem are significantly different at $\rho \leq 0.05$ by ANOVA. The data for 31-day old lateral meristem were not significantly different among the samples using ANOVA. Error bars represent standard error of the mean.

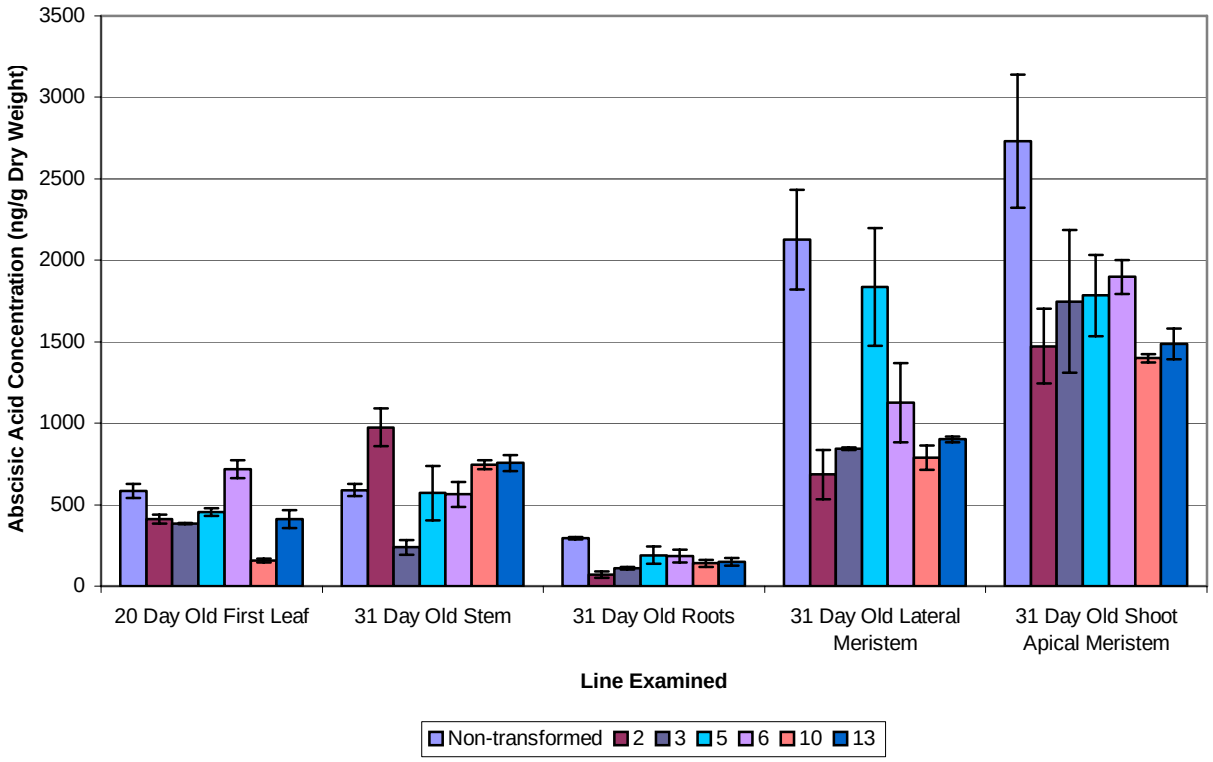

Figure 4.20 Abscisic acid present in organs of transgenic antisense *CIL1* and non-transformed *Brassica carinata*. First leaves, stems, roots, lateral meristems, and shoot apical meristems were examined. Samples were collected in triplicate from the lines indicated at 20 or 31 days after germination. Data from the 20-day old first leaf, 31-day old root and lateral meristem are significantly different at $\rho \leq 0.01$ while the stem data is significantly different at $\rho \leq 0.05$ by ANOVA. Error bars represent standard error of the mean.

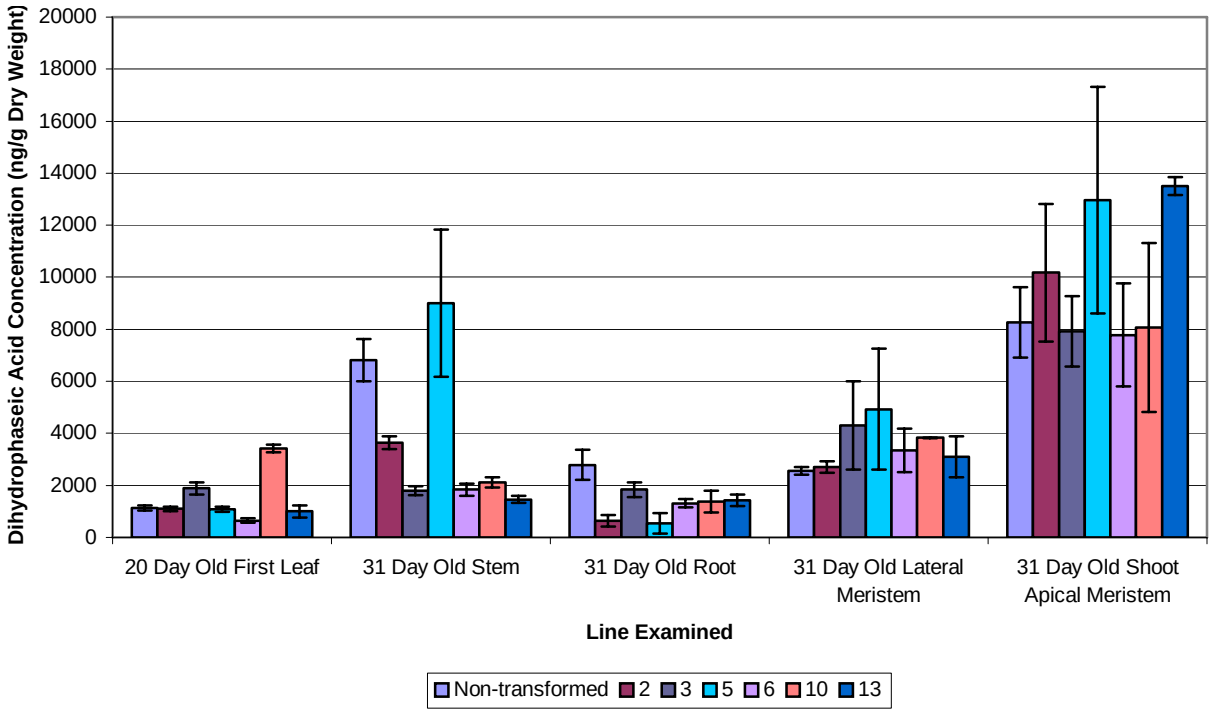

Figure 4.21 Dihydrophaseic acid present in organs of transgenic antisense *CIL1* and non-transformed *Brassica carinata*. First leaves, stems, roots, lateral meristems, and shoot apical meristems were examined. Samples were collected in triplicate from the lines indicated at 20 or 31 days after germination. Data from the 20-day old first leaves is significantly different at $\rho \leq 0.01$ while the 30-day old stem and root data is significantly different at $\rho \leq 0.05$ using ANOVA. Data from the 31-day old lateral meristem and shoot apical meristem samples were not significantly different among the samples using ANOVA. Error bars represent standard error of the mean.

Only small differences in IAA concentration that were not statistically significant as determined by ANOVA were observed in the first leaves among the non-transformed and the antisense transgenic lines (Figure 4.18). A significantly lesser concentration of IAA ($\rho \leq 0.01$) was present in the stem in transgenic lines 5, 6, and 10 compared to the non-transformed plants. These data are proportional to the *CIL1* expression data (Figure 4.17). The IAA concentration in roots was also significantly less ($\rho \leq 0.01$) in transgenic lines 2, 3, 5, 6, and 10 compared to non-transformed plants. Similar to the stem, these data directly correlated to *CIL1* expression observed in roots of transgenic versus non-transformed plants. In lateral meristems, transgenic lines 3 and 13 had significantly ($\rho \leq 0.05$) less IAA than the non-transformed plants. The IAA concentration in the shoot apical meristem appeared greater in transgenic lines 2, 3, and 5 compared to the non-transformed plants while it was slightly less in lines 10 and 13. These data did not correlate with the highly reduced *CIL1* expression observed in the shoot apical meristem in the transgenic plants (Figure 4.17).

There was a large degree of variation in the ZR data that interfered with the ANOVA. Therefore, the ZR data were transformed to logarithmic values and ANOVA was used to determine the significance within the data. The amount of ZR present in the first leaf did differ significantly (Figure 4.19) with ANOVA ($\rho \leq 0.01$). Transgenic lines 2, 5 and 6 had slightly greater amounts while lines 3, 10 and 13 had lesser amounts than the non-transformed plants. The amount of ZR in 31-day old stems was highly variable among the transgenic lines. In comparison to the non-transformed, the ZR concentration in transgenic lines 2, 3, 6 and 10 was significantly ($\rho \leq 0.01$) less, in line 5 it was slightly less and in line 13 it was slightly greater. In 31-day old roots, all the transgenic lines had

significantly less ZR ($\rho \leq 0.01$) compared to the non-transformed plants. In 31-day old lateral meristems, the observed differences in ZR concentration were not found to be significant by ANOVA. In the shoot apical meristem the ZR content was dramatically increased ($\rho \leq 0.05$) in all the transgenic lines compared to the non-transformed plants.

The ABA content in the first leaf, with the exception of transgenic line 6, was significantly less in the antisense *CIL1* lines compared to the non-transformed line. The results were more variable for the ABA content measured in 31-day old stems. Transgenic lines 5 and 6 had similar concentrations to the non-transformed line, line 3 had much less ABA, while lines 2, 10 and 13 had more ABA in the stems than the non-transformed line (Figure 4.20). These differences were statistically significant ($\rho \leq 0.05$). The pattern of ABA content was more consistent in the roots of the transgenic plants than was seen in the stems. Here the amount of ABA was significantly less ($\rho \leq 0.01$) in all the transgenic lines compared to the non-transformed plants. With the exception of transgenic line 5, the ABA content was also significantly less ($\rho \leq 0.01$) in the lateral meristems of the transgenic lines compared to the non-transformed. In the shoot apical meristem, the concentration of ABA was less in all transgenic lines compared to the non-transformed line, however, the differences were not statistically significant by ANOVA.

The amount of the ABA metabolite, dihydrophaseic acid (DPA), present in the first leaves of the antisense *CIL1* transgenic lines was not consistent (Figure 4.21). Transgenic line 6 had significantly less DPA while transgenic lines 3 and 10 had more ($\rho \leq 0.01$) and lines 2, 5 and 13 had approximately the same amount as the non-transformed plants. In the stem, with the exception of line 5, all the transgenic lines had significantly less ($\rho \leq 0.05$) DPA than the non-transformed. Considerably less DPA was

also found in the roots of all of the transgenic lines ($\rho \leq 0.05$) compared to the non-transformed. These results correlate well with the *CIL1* expression data. For the lateral meristems, only transgenic line 10 had a consistently higher amount of DPA compared to the non-transformed plants. Much the same results were seen for the shoot apical meristem, with only transgenic line 13 having a consistently greater amount of DPA than the non-transformed line. However, the differences observed in the lateral and shoot meristems were not statistically significant by ANOVA.

4.9.1 Effect of the Antisense Transformation on the IAA:ZR Ratio

To compare the change in auxin:cytokinin in the transgenic plants versus the non-transformed plants, the IAA:ZR concentration ratio was calculated in each organ (Table 4.1). In the first leaf, the transgenic lines 2, 5 and 13 had slightly reduced IAA:ZR ratios while lines 3, 6 and 10 had greater ratios than non-transformed plants. These results roughly correlate with *CIL1* expression observed in this organ (Figure 4.17). In the 31 day-old stem, transgenic lines 2, 6, and 10 had a ratio of IAA:ZR of 8, 7, and 5 times as large as the non-transformed ratio, respectively, while lines 3 and 13 were similar to the non-transformed in IAA:ZR ratio. Line 5, on the other hand, had a ratio 21 times smaller than the non-transformed IAA:ZR ratio. All the transgenic lines had reduced IAA:ZR ratios in the root compared to the non-transformed correlating well with the reduced *CIL1* expression observed there. In the lateral meristem, transgenic lines 3, 5, 6 and 13 had slightly reduced IAA:ZR ratios, line 10 was the same and line 2 was slightly greater than the non-transformed plants. Similar to the root, consistant reductions in the transgenic shoot apical meristem IAA:ZR ratio were also observed with reductions

Table 4.1 Ratio of IAA:ZR in non-transformed and transgenic antisense *CIL1* *Brassica carinata* plants.

IAA Concentration (ng/g Dry Weight)	First Leaf	Stem	Root	Lateral Meristem	Shoot Apical Meristem
Non-Transformed	199	703	895	38.2	23.3
Line 2	170	628	338	50.9	46.0
Line 3	243	694	434	24.9	29.5
Line 5	165	25.7	12.5	39.2	29.8
Line 6	230	278	236	38.5	27.0
Line 10	154	519	220	32.7	22.9
Line 13	166	761	607	20.6	22.3
ZR Concentration (ng/g Dry Weight)					
Non-Transformed	8.59	140	14.1	13.5	10.1
Line 2	9.35	15.1	8.50	10.8	118
Line 3	8.15	228	20.2	15.6	195
Line 5	9.16	111	5.00	22.3	347
Line 6	8.71	8.00	12.0	22.3	172
Line 10	4.00	20.0	11.2	11.5	154
Line 13	9.07	203	16.3	10.0	201
Ratio of IAA:ZR					
Non-Transformed	23:1	5:1	63:1	3:1	2:1
Line 2	18:1	41:1	40:1	5:1	0.4:1
Line 3	29:1	3:1	21:1	2:1	0.15:1
Line 5	18:1	0.23:1	3:1	2:1	0.08:1
Line 6	26:1	35:1	20:1	2:1	0.16:1
Line 10	38:1	26:1	20:1	3:1	0.15:1
Line 13	18:1	4:1	37:1	2:1	0.11:1

ranging from twice as small in line 2 to 25 times as small in line 5.

5. DISCUSSION

The cDNA representing *CIL1* of *B. carinata* was discovered in a screen for genes expression of which was induced by copper chloride. Copper chloride is an abiotic elicitor of the plant defense response. High concentrations of copper ions were shown to increase membrane permeability, lipid peroxidation and cause breakdown of chlorophyll and carotenoids (De Vos et al., 1992; De Vos et al., 1993; Luna et al., 1994). Copper ions were also found to catalyze the production of active oxygen species and increase the expression of antioxidant genes (De Vos et al., 1993; Luna et al., 1994; Baker and Orlandi, 1995). Therefore, *CIL1* may be involved with plant defense.

BLASTP analysis of the *CIL1* cDNA ORF did not reveal high similarity to any gene of known function. However, similarity to putative catecholamine binding domains was found. The potential significance of this similarity will be discussed later. Since similarity searching did not reveal a likely function for *CIL1*, an antisense construct was made and used to transform *B. carinata*. Here it was discovered that decreasing *CIL1* expression altered normal plant development. Specifically, some abnormal leaf morphology and multiple leaf development from lateral meristems were observed. The present study was undertaken to gain some understanding of the function of CIL1.

5.1 *CIL1* Expression Analysis

CIL1 was constitutively expressed in all organs examined. This observation suggests that the gene may have cellular maintenance as well as stress response functions.

Further, since the gene's expression is not limited to meristematic tissue, a function beyond shoot growth regulation is implied.

Although *CIL1* was expressed constitutively, increases in expression correlated with auxin, cytokinin and ABA treatment. Therefore, it may have a role in interconnecting hormone response pathways. However, the pattern of gene induction differed among the hormone treatments. The gene expression responded rapidly but transiently to auxin. This observation may indicate that *CIL1* must "reset" for frequent response to changes in auxin content. Alternatively, the protein turnover rate may be slow. The rapid and sustained induction of *CIL1* expression after cytokinin and ABA treatment indicates that the gene also has a role early in the response pathways of these hormones. However, either its role in these pathways is more sustained than in the auxin response pathway or the protein turnover rate may be faster under these circumstances.

5.2 Catecholamine Binding Domain and Putative CIL1 Function

The alignment conducted comparing the CIL1 amino acid sequence to DoH amino acid sequences showed that CIL1 has similarities to these proteins. The DoH domains are believed to bind or respond to CA. CAs are aromatic amines and among this group of compounds are the mammalian neurotransmitters dopamine, norepinephrine and epinephrine. These animal hormones are involved in the rapid response to stress. Therefore, the induction of CIL1 implies a similarity between plants and animals in the compounds that are involved in some stress responses.

Forty-four plant families are reported to contain CA (Smith, T.A. 1977). However, no essential metabolic functions for CAs in plants have been assigned.

Nonetheless, epinephrine and norepinephrine were found to promote flowering in duckweed (Khurana et al., 1987), increase root length in *Vigna unguiculata* (Kaur and Thurkral, 1990), and promote growth in tobacco thin cell layer cultures (Protacio et al., 1992). Additionally, epinephrine in micromolar concentrations was shown to stimulate somatic embryogenesis in orchardgrass (Schenk and Hildebrandt, 1972). These data provide precedent for the observation of altered plant development in antisense *CIL1* transgenic lines.

Simple protein modeling of AIR12 by Verelst and Asard (2004) indicated that it may consist of a single membrane spanning domain at the N-terminus, with a DoH domain on the outside of the plasma membrane at the C-terminal end. Further, AIR12 is anchored to the membrane by glycosylphosphatidylinositol (Borner et al., 2003). The similarity of CIL1 to AIR12 suggests that it has a similar structure. Structural determination of the bovine dopamine-β-hydroxylase found that the N- and C- termini exist close to one another and are extracellular while the active site is within two interior domains stabilized by disulfide bonds (Robertson et al., 1994). Since CIL1 is only 269 amino acids (aa) in length compared to the 603 aa of bovine DoH, it is doubtful that CIL1 has the same function. CIL1, AIR12, and BAB09428 all lack the CB, which enables the conversion of DA to E. The absence of the CB likely limits these proteins to interactions with CAs. However, although there is no precedent for CA binding and CB being separately encoded, it is possible.

It is clear that CIL1 has a role in determining plant architecture and that it affects hormone content. CIL1 may be a CA sensor located in the plasma membrane as part of a signal transduction pathway that ultimately connects to hormone pathways. Prior

research on the interactions between CAs and phytohormones has demonstrated that they can influence one another.

5.3 Possible Interactions of CIL1 with Hormones

Peroxidase assays that examined the effect of CAs on IAA activity showed that they inhibit IAA degradation by the enzyme IAA oxidase (Protacio et al., 1992). In the IAA profile of the antisense *CIL1* plants at least half of the transgenic lines had less IAA in the first leaf, stem, roots, and lateral meristems then the non-transformed plants. If reduced *CIL1* expression results in reduced CA perception than one consequence of this might be increased IAA oxidase activity. It would follow that IAA content would decrease as was seen in the transgenic lines. The transgenic line-to-line variation in IAA content seen in first leaf, stem, roots and to a lesser extent in lateral meristems roughly parallels *CIL1* expression data. The exception to this trend was the apical meristem where despite a drastic reduction in *CIL1* expression in the transgenic lines there was little difference in IAA content compared to non-transformed plants. These results suggest that the rate and control of IAA biosynthesis in the shoot apical meristem could be compensating for any increase in IAA oxidase activity. Alternatively, if the catecholamines are synthesized and retained in the cells of the meristem, no external sensor may be required. However, in that case what is the function of CIL1 in these cells? Alternatively, it may be that predominant control of the oxidase activity resides in proteins other than CIL1 in the apical meristem.

The interaction of CAs with cytokinins is less clearly defined. Christou and Barton (1989) found that octopamine was toxic to normal tobacco callus but had no effect

on crown gall tissues. The survival of the crown gall tissue was attributable to the presence of isopentenyl transferase, the enzyme that catalyzes the first step in cytokinin biosynthesis. In turn, addition of cytokinins to the callus before octopamine treatment prevented necrosis. The authors' conclusion was that cytokinins and CAs are antagonists. Therefore, if CA perception is decreased in antisense *CIL1* transgenic lines, the amount of cytokinin might increase. Unfortunately, in this study the only reliably detected cytokinin was ZR. Zeatin riboside is the main form of transported cytokinin through the stem (Taiz and Zeiger, 1998). In the SAM, there was a large increase in ZR content in all transgenic lines compared to non-transformed plants. This inverse relationship between *CIL1* expression and ZR content would support the hypothesis that CA and cytokinins are antagonists. A very slight suggestion of an inverse relationship between *CIL1* expression and ZR content was also found in the first leaf. *CIL1* expression in the leaves of transgenic lines 3 and 10 was greater than non-transformed while the ZR content in line 10 was significantly less and in line 3 it appeared to be slightly less. In turn, those transgenic lines with decreased *CIL1* expression appeared to have slightly more ZR content. In stems, only line 13 showed an inverse relationship of *CIL1* expression and ZR concentration while in the lateral meristems lines 3 and 6 displayed this inverse relationship. No suggestion of antagonism between CIL1 and ZR content was found in roots. The similarity in ZR content between non-transformed roots and transgenic lines 3, 6, 10, and 13 was not surprising given the lower IAA content also observed in this organ, which might be expected to result in increased or unchanged cytokinin content. Overall, the results do not strongly support a role for CIL1 in

mediating CA and cytokinin antagonism. However, the relationship between *CIL1* mRNA and protein amounts is unknown at this time.

There is little information available in the literature regarding interactions between ABA and CAs, though one study showed that treatment with ABA activated the initial steps of CA biosynthesis in potato tubers (Swiedrych et al., 2004). This result implies a synergistic relationship between CAs and ABA. If this were the case one would expect that decreased CA perception might correspond to decreased ABA content. In first leaf, all but one of the transgenic lines did show reduced ABA content compared to non-transformed. However, the qRT-PCR had indicated that *CIL1* expression in lines 3 and 10 was greater than in non-transformed plants at 31 days. Therefore, a conclusion that *CIL1* expression and ABA content are positively correlated in this organ cannot be made. A similar case was seen in the lateral meristem. In stems, no correlation of *CIL1* expression and ABA content was observed. In the roots of transgenic plants the reduction of *CIL1* expression correlated well with reduced ABA content, suggesting synergism. Alternatively, this result may have been due to the reduced IAA content also seen in this organ. The auxin *axr* mutant displays reduced ABA signaling (Bianchi et al., 2002). However, there was also a correlation of reduced *CIL1* expression and reduced ABA content observed in shoot apical meristem. Since the IAA content in this organ did not differ significantly from transgenic to non-transformed plants, the alteration in ABA cannot be attributed to it. Therefore, CAs and ABA may interact synergistically in some plant organs.

Abscisic acid undergoes two forms of metabolism (Hirai et al., 2003). One metabolic pathway involves a conjugation that can be either reversible or irreversible

(Kleczkowski and Schall, 1995). The other pathway for ABA metabolism involves an 8' hydroxylation followed by spontaneous rearrangement to form PA and subsequent reduction to DPA. This metabolism was assessed in the antisense *CIL1* transgenic plants. In first leaves, the DPA content was greater in transgenic lines 3 and 10 than in non-transformed plants. These are also lines that had greater expression of *CIL1* than non-transformed. The implication of these data is that increased CA perception stimulated ABA metabolism in this organ, suggesting CA and ABA antagonism. The DPA amounts in the first leaf of the transgenic lines 3, 6 and 10 were also inversely correlated to ABA amounts, which may infer that this was the predominant pathway for ABA metabolism in the leaf. With the exception of transgenic line 5, DPA content in stems and roots of transgenic lines was much reduced in comparison to non-transformed plants. Again the results parallel the *CIL1* expression data. No correlation of *CIL1* expression and DPA content was observed in lateral or apical meristems. Indeed, little variation from the DPA content in non-transformed plants was observed in these organs in transgenic plants. These inconsistencies preclude making any conclusion about an interaction of CIL1 and ABA metabolism.

An overall examination of the relationship between *CIL1* expression and ABA concentration favors a view that there is synergism between *CIL1* mRNA amount and ABA biosynthesis.

Assessing the results on an organ-to-organ basis a number of conclusions can be drawn. Firstly, the antisense construct was not effective in significantly decreasing *CIL1* expression in first leaf or lateral meristem. Therefore, it is not surprising that there is little change in hormone content in these organs from transgenic to non-transformed.

Then the question arises as to why the phenotype associated with antisense *CIL1* involves the lateral meristem. The apparent contradiction may be attributable to the plant material selected for analysis. To obtain equivalent material from transgenic and non-transformed plants, lateral meristems were excised before development of further leaves. Future analysis should involve a time course study of hormone content to observe changes in the material as secondary branching develops. The picture is equally confusing in the stem and apical meristem. In stems, the three transgenic lines with the greatest reduction in *CIL1* expression only consistently showed reduced IAA. These data link CIL1 closest to the auxin response pathway and suggest that a threshold exists above which increases in *CIL1* expression have little effect. The most logical conclusion is that CA perception affects only the cell-to-cell transport of auxin and not its transport through phloem. The most significant reduction in *CIL1* expression was observed in the shoot apical meristem. The roots also displayed a consistent reduction in *CIL1* expression, and this correlated with a reduction in IAA, ZR, ABA, and DPA. Interestingly, no readily observable phenotype accompanied this hormone reduction. Further, the ratio of IAA:ZR in various organs of the transgenic lines varied widely from the non-transformed yet, with the exception of the secondary branching and some cotyledon distortion, the plants were normal and fertile. These results run counter to the auxin:cytokinin ratio hypothesis of Skoog and Miller (1957) and support Eklöf et al.'s (1997) conclusion that individual hormones may induce developmental pathways if critical values are exceeded. However, since our hormone profiling experiments did not detect all the types of auxin and cytokinin molecules, we cannot conclusively state that the ratios of total auxins and cytokinins differed significantly.

5.4 Phytohormone Profiling Error Sources and Problems

Tandem mass spectrometry utilizes two mass analysers to examine a previously determined precursor ion that is mass-selected so that its ionization can be investigated without interference from other ions formed during the ionization (Polce and Wesdemiotis, 2002). This mass spectrometry utilizes three quadrupole mass analysers, each with different roles. The first quadrupole mass analyser detects the parent ion, examining a particular mass to charge ratio (*m/z*). Ions matching the predetermined *m/z* pass through to the second quadrupole, which acts as the collision cell. In the collision cell, the parent ions are subjected to CID by bombardment with the inert gas, argon. The bombardment fragments the parent ion into daughter ions that proceed to the third quadrupole mass analyser. In the third quadrupole the daughter ions matching the predetermined *m/z* pass through the quadrupole and are detected with a photomultiplier detector. Multiple reaction monitoring was utilized in this study. In this technique the transition from parent to daughter ion is observed, greatly increasing the accuracy and reproducibility of the equipment when impure samples are used (Waters, 2003).

The method of phytohormone profiling used in this study represents a powerful technique that is flexible enough to measure a wide range of metabolites while retaining specificity, accuracy, and precision (Chiwocha et al., 2003). Although this is a powerful technique, it is in its infancy, and is prone to several failings that affected the results in this study. The method was initially designed to optimize extraction of ABA and its metabolites in *A. thaliana* and *Lactuca sativa* seedlings. To facilitate the extraction and quantification of cytokinins and auxins, the aqueous content of the extraction solution and HPLC conditions were adjusted, however, only 1 out of the 7 possible forms of cytokinin

could be quantified consistently. Recovery standards for ABA were used to determine the accuracy and precision of detection of the phytohormones. The use of recovery standards in conjunction with the internal standards allowed for an accurate calculation of the extraction efficiency of samples. Unfortunately, as yet, recovery standards are not available for cytokinins, auxins, or gibberellins. Additionally, it was found that components in the *Brassica* extracts suppressed the MS signal from a number of the phytohormones. Some success in dealing with the interference was achieved when the chromatography time was increased from 40 min to 60 min resulting in an increase in chromatography resolution. Further, a higher aqueous concentration was used to increase the resolution of the polar cytokinins and a hexane-partitioning step was added to remove non-polar compounds. However, the hexane partitioning may have in itself decreased phytohormone recovery with losses in the interfacial layer. The extraction method needs to be modified further to optimize recovery of the auxins and cytokinins.

The lateral meristem and shoot apical meristem samples were analysed later than the first leaf, stem, and root. Equipment failure and scheduling problems led to a three-month delay in sample analysis. The long-term storage may have caused the loss of signal from the deuterated internal standards since only 1/20 of the originally added amount was detected. Consequently, a large degree of sensitivity was lost and in most cases, the signal was too small to generate reliable results. The only phytohormones that could be quantified with reliable results were IAA, ZR, ABA, and DPA. Through the use of calibration standards an estimate of the amounts of phytohormones in these organs was calculated. Thus, the results presented for the lateral and shoot apical meristems

represent an extrapolation of the data based on the calibration curve. More precise results will require the preparation of new samples.

5.5 Possible Modes of Action of CAs/ CIL1 in Plants

As discussed earlier, CAs inhibit IAA oxidase activity, therefore, CIL1 as a CA sensor could have a role in maintaining auxin content. Consequently, CIL1 would have a role in suppressing leaf development. Additionally, exogenous application of dopamine was found to stimulate ethylene biosynthesis (Elstner et al., 1976). Ethylene is proposed to have a role in inhibiting development of leaf primordia through reducing the expression of the KNAT2 transcription factor (Vandenbussche and Van Der Straeten, 2004). In higher planting densities the multiple leaf phenotype of the *CIL1* antisense transgenic lines was suppressed. Perhaps under these conditions an above threshold amount of ethylene was accumulated.

However, Kamisaka (1979) found that epinephrine acted synergistically with GA to stimulate hypocotyl elongation. The suggestion of these combined findings is that CAs are another component of the complex and finely-tuned network of pathways that control plant development.

There are several publications that provide evidence for the existence of CA receptors in plants. In 1987, Khurana et al. reported that the β-adrenergic blocking agent, propranolol, inhibited flowering in duckweed. The inhibition could be relieved with epinephrine. Later, Roshchina (1989, 1990) found that dopamine, epinephrine and norepinephrine regulated ion permeability and photophosphorylation of chloroplasts. Further, he demonstrated that the membrane-binding constants for CAs were similar to

known adrenoreceptors in mammals. In the mouse telencephalon, dopamine and its' receptors D_1 and D_2 have roles in controlling cell proliferation and differentiation. Dopamine apparently exerts this control through modulating the cell cycle (Ohtani et al., 2003). Interestingly, dependent on the receptor to which dopamine binds, the G_1 to S-phase transition is either inhibited (D_1) or stimulated (D_2). Therefore, it is the distribution of the two receptors that determines the response of the cell. Binding of dopamine to the D_1 receptor on cells in the ventricular zone decreases DNA synthesis and promotes neuronal differentiation, while binding to the D_2 receptor on cells in the subventricular zone increases DNA synthesis and stimulates glial precursor proliferation (Popolo et al., 2004). A similar model might be suggested for plants with CIL1 functioning in maintaining meristematic tissue. Analysis of the *A. thaliana* genome revealed two genes consisting only of putative CA-binding domains, *AIR12* and BAB09428 (Verelst and Asard, 2004). These proteins could be considered the equivalent of D_1 and D_2-type receptors. If this scenario is correct than CAs in plants have a direct role in determining plant architecture rather than simply mediating phytohormone responses, in which case they themselves should be considered to be phytohormones. However, organ sensitivity to CAs and endogenous concentrations at which they act must be established.

5.6 Comparison of Antisense *CIL1* Plants to Plant Architecture Mutants

The antisense *CIL1* transgenic plants have similarities to several auxin-deficient mutants. The *dad1-1* mutant of petunia has greatly increased secondary branching and like antisense *CIL1* plants develops branches at the cotyledon axil (Napoli, 1996). However, *dad1-1* mutants also display the additional mutant traits of delayed onset of

flowering, shortened internodes, propensity for adventitious root formation and mild leaf chlorosis. None of these traits were observed in the antisense *CIL1* transgenic plants. The IAA-deficient *bushy* mutant in pea has short, thin stems, very small leaves and increased branching (Symons et al., 2002). The phenotype of the antisense *CIL1* transgenic plants is similar to these auxin-deficient mutants but does not exactly match any of them.

Alternatively, overproduction of Z-type cytokinins also results in profuse secondary branching. The *supershoot* (*sps*) mutant, with a 3 to 9-fold increase in cytokinins, produces inflorescences at every leaf axil on the plant (Tantikanjana et al., 2001). Seeds from the *sps* line were grown to determine if there was any resemblance in phenotype to that of the transgenic antisense *CIL1* plants. Unlike wild type *A. thaliana*, *sps* plants produced a prolific amount of leaves from a large number of branches. Further, upon reaching the reproductive stage of development, the *sps* plants formed a great number of inflorescences that were generally smaller than the wild type inflorescences and were largely sterile. In comparison, the antisense *CIL1* transgenic plants had increased branching in both vegetative and reproductive growth phases and initiated leaves or inflorescences at any axil, depending on the phase of growth. The antisense *CIL1* plants were also comparable in size and fertility to non-transformed *B. carinata*.

Only a few genes with roles in regulating lateral meristem development have been isolated. The majority of these genes encode transcription factors such as the *LATERAL SUPPRESSOR* gene, a member of the GRAS family (Greb et al., 2003), and *REVOLUTA*, a member of the homeodomain leucine-zipper gene family (Otsuga et al., 2001). An

exception is the tomato arabinogalactan protein-1 (AGP-1), which, like CIL1, is a glycosylphosphatidylinositol-anchored protein (Sun et al., 2004). However, distinguishing it from CIL1, over-expression of *LeAGP-1* produced plants of shorter stature with more branches and more flower buds. Further, most of the flowers did not mature and seeds in the fruits that did develop were significantly smaller than normal seeds. Unlike *CIL1* whose expression is induced by auxin, cytokinin and ABA, *AGP-1* expression is induced by cytokinin but inhibited by auxin and ABA.

5.7 Modulations of *CIL1* Expression and Phytohormone Concentration in Transgenic Plants

The ratio of auxin:cytokinin has been shown to influence plant development in some cases, where in other cases, absolute amounts of phytohormones influence development (Eklof et al., 1997; Eklof et al., 2000). The transgenic plants showed wide variation in the degree of alteration of both IAA and ZR concentration (Figures 4.19 and 4.20). Noticeable differences also existed in the IAA:ZR ratio (Table 4.1). Least effected by the reduction of *CIL1* expression in the transgenic lines were the 20 day-old first leaf and 31-day old lateral meristem. The lateral meristem IAA:ZR ratio in the transgenic lines were nearly identical to the non-transformed line, while there were small increases and decreases in the IAA:ZR ratio in the 20 day-old first leaf over the transgenic lines compared to the non-transformed line. These data correlate well with the *CIL1* expression data (Figure 4.17), demonstrating that the development of the phenotype in the transgenic plants does not likely involve the first leaf. However, the same

conclusion cannot be made about the lateral meristem since the hormone content was analysed before development of the multiple leaf phenotype.

The shoot apical meristem displayed a consistant reduction in the IAA:ZR ratio compared to the non-transformed line. The large increase in ZR concentration coupled with the unchanged IAA concentration greatly altered the ratio. This result suggests that the loss of apical dominance might be attributable to the IAA:ZR ratio rather than the absolute amount of IAA.

Alternatively, the stems and roots of the transgenic lines had the largest alterations in IAA:ZR ratio. Increased IAA metabolism in the transgenic plants as a result of the interactions between CIL1, CA, and IAA oxidase may reduce the IAA available for transport. Thus the degree of apical dominance exerted at the lateral meristems would also be decreased in the transgenic plants.

6. CONCLUSIONS

Many questions about the function of CIL1 in plant development remain to be answered. However, the following conclusions are possible based on sequence comparison and the results of this study. *CIL1* does not have introns and is a member of a small gene family in *Brassica* species. Gene duplication of *CIL1* appears to have occurred in *B. oleracea* but not in *B. carinata* or *B. nigra*. The gene is expressed constitutively in leaf, root, stem, lateral and apical meristem. *CIL1* expression is induced by multiple signals including copper chloride, α-NAA, BAP and ABA. Translation of the *CIL1* ORF yielded a putative protein of 269 amino acids with an approximate molecular weight of 27,332 Daltons. The protein is predicted to have a N-terminal transmembrane domain and putative catecholamine-binding domain. Transformation of *B. carinata* with an antisense *CIL1* construct driven by the 35S promoter alters expression of the gene in leaf, root, stem, lateral and apical meristem. However, the effect of the antisense construct on *CIL1* expression varied widely from organ-to-organ, reducing gene expression to the greatest extent in apical meristem and to the least extent in first leaf. The reduction of *CIL1* expression was accompanied by the formation of multiple leaves from lateral meristems. Therefore, CIL1 has a role in determining plant architecture. That role likely involves interaction, either directly or indirectly, with several phytohormones. The largest and most consistent reduction of *CIL1* expression was observed in the shoot apical meristem. This expression data correlated with an increase in ZR concentration, a decrease in the IAA:ZR ratio and a decrease in ABA concentration. A fairly consistent reduction in *CIL1* expression was also observed in the root. Again, this was accompanied by a decrease in the IAA:ZR ratio. Therefore, it is

likely that CIL1 plays a role in controlling the auxin:cytokinin ratio in plants. However, the mechanism of this control remains to be elucidated. Hopefully, further characterization of *CIL1* will help define the role of catecholamines in plants.

7. FUTURE DIRECTIONS

This study comprised a thorough examination of the *CIL1* copy number and genomic location, the coding region composition, the gene's expression pattern, and response to hormone treatment. However, it represents only the initial stages of the functional characterization of CIL1. Much remains to be learned about the role of CIL1 in plant growth and development. Firstly, given the identification of a putative CA binding domain in CIL1, the CA content of the antisense transgenic plants should be compared to non-transformed *B. carinata*. Further, the hormone profiling of the lateral meristems and shoot apical meristem needs to be repeated encompassing additional developmental stages. Additional hormone profiling may also include a wider variety of organs, such as the inflorescence stem, flower buds, young and mature seeds, senescing material, cauline leaves, and leaves from plants in flower.

While the hormone profiling of the antisense transgenic plants should add much to our knowledge of the role of *CIL1* in plant development, biochemical analyses are also required. Those analyses will be aimed at elucidating the location of CIL1, ligand binding, post-translational processing and interactions with other proteins. Immunolocalization will determine if, as predicted, CIL1 is membrane bound. Protein crystallization followed by X-ray crystallography or 2D-NMR of CIL1 in the presence of CAs should determine ligand binding. Microscopic study of a fusion of the N-terminal end of CIL1 with green fluorescent protein can determine if, as predicted, the C-terminus is cleaved to release that end of the protein into the apoplast. Finally, employing yeast two-hybrid or immunoprecipitation to detect interacting proteins may reveal if CIL1 is

part of a signal transduction pathway. It would also be worthwhile to generate *CIL1* over-expressing lines to examine the effect on *B. carinata* growth and development.

8. REFERENCES

Addicott FT, Lyon JL, Ohkuma K, Thiessen WE, Carns HR, Smith OE, Cornforth JW, Milborrow BV, Ryback G, and Wareing PF, 1968. Abscisic acid: a new name for abscisin II (dormin). Science 159:1493.

Alemayehu N and Becker HC, 2001. Variation and inheritance of erucic acid content in *Brassica carinata* germplasm collections from Ethiopia. Plant Breeding 120:331-335.

Ali-Rachedi S, Bouinot D, Wagner M, Bonnet M, Sotta B, Grappin P, and Jullien M, 2004. Changes in endogenous abscisic acid levels during dormancy release and maintenance of mature seeds: studies with the Cape Verde Islands ecotype, the dormant model of *Arabidopsis thaliana*. Planta 219:479-488.

Alliotte T, Engler TG, Peleman J, Caplan A, van Montagu M, and Inze D, 1988. An auxin-regulated gene of *Arabidopsis thaliana* encodes a DNA-binding protein. Plant Physiol 89:743–753.

Aloni R, Langhans M, Aloni E, and Ullrigh CI, 2004. Role of cytokinin in the regulation of root gravitropism. Planta 220:177-182.

Alonso LC, Fernandez-Serrano O, and Fernandez-Escobar J, 1991. The outset of a new oilseed crop: *Brassica carinata* with low erucic acid content. International Consultative Group on Rapeseed Congress A-21:170-176.

Babic V, Datla RS, Scoles GJ, and Keller WA, 1998. Development of an efficient *Agrobacterium*-mediated transformation system for *Brassica carinata*. Plant Cell Rep 17:183-188.

Baker CJ and Orlandi EW, 1995. Active oxygen in plant pathogenesis. Annu Rev Phytopathol 33:299-321.

Bangerth F, 1994. Response of cytokinin concentration in the xylem exudate of bean (*Phaseolus vulgaris* L.) plants to decapitation and auxin treatment, and relationship to apical dominance. Planta 194:439-442.

Bartel B, LeClere S, Magidin M, and Zolman BK, 2001. Inputs to the active indole-3-acetic acid pool: *de novo* synthesis, conjugate hydrolysis, and indole-3-butyric acid β-oxidation. J Plant Growth Regul 20:198-216.

Beffa R, Martin HV, and Pilet P, 1990. *In vitro* oxidation of indoleacetic acid by soluble auxin-oxidases and peroxidases from maize roots. Plant Physiol 94:485-491.

Bennett MJ, Marchant A, Green HG, May ST, Ward SP, Millner PA, Walker AR, Schulz B, and Feldmann KA, 1996. *Arabidopsis AUX1* gene: a permease-like regulator of root gravitropism. Science 273:948-950.

Berleth T, Krogan NT, and Scarpella E, 2004. Auxin signals – turning genes on and turning cells around. Curr Op in Plant Biol 7:553-563.

Beveridge CA, 2000. Long-distance signaling and a mutational analysis of branching in pea. Plant Growth Regul 32:193-203.

Beveridge CA, Symons GM, and Turnbull CGN, 2000. Auxin inhibition of decapitation-induced branching is dependent on graft-transmissible signals regulated by genes *Rms1* and *Rms2*. Plant Physiol 123:689-697.

Bialek K and Cohen JD, 1989. Free and conjugated indole-3-acetic acid in developing bean seeds. Plant Physiol 91:775-779.

Bianchi MW, Damerval C, and Vartanian N, 2002. Identification of proteins regulated by cross-talk between drought and hormone pathways in *Arabidopsis* wild-type and auxin-insensitive mutants *axr1* and *axr2*. Funct Plant Biol 29:55-61.

Blagoeva E, Dobrev PI, Malbeck J, Motyka V, Gaudinova A, and Vankova R, 2004. Effect of exogenous cytokinins, auxins and adenine on cytokinin *N*-glucosylation and cytokinin oxidase/dehydrogenase activity in de-rooted radish seedlings. Plant Growth Regul 44:15-23.

Bleecker AB, 1999. Ethylene perception and signaling: an evolutionary perspective. Trends Plant Sci 4:269-274.

Blilou I, Xu J, Wildwater M, Willemsen V, Paponov I, Friml J, Heldstra R, Aida M, Palme K, and Scheres B, 2005. The PIN auxin efflux facilitator network controls growth and patterning in *Arabidopsis* roots. Nature 433:39-44.

Borner GH, Lilley KS, Stevens TJ, and Dupree P, 2003. Identification of glycosylphosphatidylinositol-anchored proteins in Arabidopsis. A proteomic and genomic analysis. Plant Physiol 132: 568-577.

Boysen-Jensen P, 1913. Uber die leitung des phototropischen reizes in der Avenakoleoptile. Ber Deut Bot Ges 31:559-566.

Brandstatter I and Kieber JJ, 1998. Two genes with similarity to bacterial response regulators are rapidly and specifically induced by cytokinin in *Arabidopsis*. Plant Cell 10:1009-1019.

Brzobohaty B, Moore I, and Palme K, 1994. Cytokinin metabolism: implications for regulation of plant growth and development. Plant Mol Biol 26:1483-1497.

Burkhanova EA, Mikulovich TP, Kudryakova NV, Kukina IM, Smith AR, Hall MA, and Kulaeva ON, 2001. Heat shock pre-treatment enhances the response of *Arabidopsis thaliana* leaves and *Cucurbita pepo* cotyledons to benzyladenine. Plant Growth Regul 33:195-198.

Burkle L, Cedzich A, Dopke C, Stransky H, Okumoto S, Gillissen B, Kuhn C, and Frommer WB, 2003. Transport of cytokinins mediated by purine transporters of the PUP family expressed in phloem, hydathodes, and pollen of *Arabidopsis*. Plant J 34:13-26.

Campbell N, Mitchell L, and Reece J, 1997. Biology: Concepts and Connections, Benjamin/Cimmings Publishing Group, Don Mills, Ontario, p. 506.

Caplin SM and Steward FC, 1948. Effect of coconut milk on the growth of explants from carrot root. Science 108:655-657.

Chang C, Kwok SF, Bleecker AB, and Meyerowitz EM, 1993. *Arabidopsis* ethylene-response gene *ETR1*: similarity of product to two-component regulators. Science 262:539-544.

Chatfield PS, Stirnberg P, Forde BG, and Leyser O, 2000. The hormonal regulation of axillary bud growth in *Arabidopsis*. Plant J 24:159-169.

Chen AM and Melitz DK, 1979. Cytokinin biosynthesis in a cell-free system from cytokinin-autotrophic tobacco tissue cultures. FEBS Lett 107:15-20.

Chiwocha SDS, Abrams SR, Ambrose SJ, Cutler AJ, Loewen M, Ross ARS, and Kermode AR, 2003. A method for profiling classes of plant hormones and their metabolites using liquid chromatography-electrospray ionization tandem mass spectrometry: an analysis of hormone regulation of thermodormancy of lettuce (*Lactuca sativa* L.) seeds. Plant J 25:405-417.

Choi T, Aoki F, Makoto M, Yamashita M, Nagahama Y, and Kohmoto K, 1991. Activation of $p34^{cdc2}$ protein kinase activity in meiotic and mitotic cell cycles in mouse oocytes and embryos. Development 113: 789-795.

Christou P and Barton KA, 1989. Cytokinin antagonist activity of substituted phenethylamines in plant cell cultures. Plant Physiol 89:564-568.

Cline MG, 1996. Exogenous auxin effects on lateral bud outgrowth in decapitated shoots. Ann Bot 78:255-266.

Cohen DB and Knowles PF, 1983. Evaluation of *Brassica* species in California. In: GCIRC Proc 6th Int Rapeseed Cong, Paris, France, 17-19 May 1983, pp. 282-287.

Coruzzi G and Last RL, 2000. Amino acids. In BB Buchanan, W Gruissem, and RL Jones (Eds.), Biochemistry and molecular biology of plants (pp.358-401), Rockville, USA: American Society of Plant Physiologists.

Cousins HH, 1910. Jamaica Dept Agr Annual Report, 7.

Crosby KE, Aung LH, and Buss GR, 1981. Influence of 6-benzylaminopurine on fruit-set and seed development in two soybean *Glycine max* (L.) Merr. Genotypes. Plant Physiol 68:985-988.

Crozier A, Kamiya Y, Bishop G, and Yokota T, 2000. Biosynthesis of hormones and elicitor molecules. In BB Buchanan, W Gruissem, and RL Jones (Eds.), Biochemistry and molecular biology of plants (pp. 850-901), Rockville, USA: American Society of Plant Physioloists.

Dai Y, Michaels PJ, and Flores HE, 1993. Stimulation of ethylene production by catecholamines and phenylethylamine in potato cell suspension cultures. Plant Growth Regul 12:219-222.

Darwin CR, 1880. The power of movement in plants. London: Murray.

Datla RSS, Bekkaoui F, Hammerlindl JK, Pilate G, Dunstan DI, and Crosby WL, 1993. Improved high-level constitutive foreign gene expression in plants using an AMV RNA4 untranslated leader sequence. Plant Sci 94:139-149.

Datla, RSS, Hammerlindl JK, Panchuk B, Pelcher LE, and Keller W, 1992. Modified binary plant transformation vectors with the wild-type gene encoding NPTII. Gene 122:383-384.

De Vos CHR, Vonk MJ, Vooijs R, and Schat H, 1992. Glutathione depletion due to copper induced phytochelatin synthesis causes oxidative stress in *Silene cucubalus*. Plant Physiol 98:853-858.

De Vos CHR, Bookum WMT, Vooijs R, Schat H, and De Kok LJ, 1993. Effect of copper on fatty acid composition and peroxidation of lipids in the roots of copper tolerant and sensitive *Silene cucubalus*. Plant Physiol Biochem 31:151-158.

Dellaporta SL, Wood J, and Hicks JB, 1983. A plant DNA minipreparation: version II. Plant Mol Biol Rep 1:19-21.

Dengler NG and Kang J, 2001. Vascular patterning and leaf shape. Curr Op in Plant Biol 4:50-56.

Dharmasiri S and Estelle M, 2002. The role of regulated protein degradation in auxin response. Plant Mol Biol 49:401-409.

Doubt SL, 1917. The response of plants to illuminating gas. Bot Gaz 63:209-224.

Eagles CF, and Wareing PF, 1964. The role of growth substances in the regulation of bud dormancy. Physiol Plant 34:201–203.

Eklof S, Astot C, Blackwell J, Moritz T, Olsson O, and Sandberg G, 1997. Auxin-cytokinin interactions in wild-type and transgenic tobacco. Plant Cell Physiol 38:225-235.

Eklof S, Astot C, Sitbon F, Moritz T, Olsson O, and Sandberg G, 2000. Transgenic tobacco plants co-expressing *Agrobacterium iaa* and *ipt* genes have wild-type hormone levels but display both auxin- and cytokinin-overproducing phenotypes. Plant J 23:279-284.

Elstner EF, Konze JR, Selman BR, and Stoffer C, 1976. Ethylene formation in sugar beet leaves: evidence for the involvement of 3-hydroxytyramine and phenoloxidase after wounding. Plant Physiol 58:163-168.

Endress R, Jager A, and Kreis W, 1984. Catecholamine biosynthesis dependent on the dark in betacyanin-forming *Portulaca* callus. J Plant Physiol 115:291-295.

Fei H and Vessey JK, 2004. Further investigation of the roles of auxin and cytokinin in the NH_4^+-induced stimulation of nodulation using white clover transformed with the auxin-sensitive reporter *GH3:gusA*. Physiol Plant 121:674-681.

Friml J, 2003. Auxin transport – shaping the plant. Curr Opin Plant Biol 6:7-12.

Friml J and Palme K, 2002. Polar auxin transport – old questions and new concepts? Plant Mol Biol Rep 49:273-284.

Friml J, Wisnlewska J, Benkova E, Mendgen K, and Palme K, 2002. Lateral relocation of auxin efflux regulator PIN3 mediates tropism in *Arabidopsis*. Nature 415:806-809.

Friml J, Yang X, Michniewicz M, Weijers D, Quint A, Tietz O, Benjamins R, Ouwerkerk PBF, Ljung K, Sandberg G, Hooykaas PJJ, Palme K, and Offringa R, 2004. A PINOID-dependent binary switch in apical-basal PIN polar targeting directs auxin efflux. Science 306:862-865.

Galweiler L, Guan C, Muller A, Wisman E, Mendgen K, Yephremov A, and Palme K, 1998. Regulation of polar auxin transport by AtPIN1 in *Arabidopsis* vascular tissue. Science 282:2226-2229.

Gan S and Amasino RM, 1995. Inhibition of leaf senescence by autoregulated production of cytokinin. Science 270:1986-1987.

Garrison R, 1955. Studies in the development of axillary buds. Am J Bot 42:257-266.

Gaspar TH, Kevers C, Faivre-Rampant O, Crevecoeur M, Penel CL, Greppin H, and Dommes J, 2003. Changing concepts in plant hormone action. In Vitro Cell Dev Biol-Plant 39:85-106.

Getinet A, Rakow G, and Downey RK, 1996. Agronomic performance and seed quality of Ethiopian mustard in Saskatchewan. Can J Plant Sci 76:387-392.

Greb T, Clarenz O, Schafer E, Muller D, Herrero R, Schmitz G, and Theres K, 2003. Molecular analysis of the *LATERAL SUPPRESSOR* gene in *Arabidopsis* reveals a conserved control mechanism for axillary meristem formation. Gene Dev 17:1175-1187.

Guilfoyle TJ, Ulmasov T, and Hagen G, 1998. The ARF family of transcription factors and their role in plant hormone-responsive transcription. Cell Mol Life Sci 54:619-627.

Haver DL, Schuch UK, and Lovatt CJ, 2003. Exposure of petunia seedlings to ethylene decreased apical dominance by reducing the ratio of auxin to cytokinin. J Plant Growth Regul 21:459-468.

Hay A, Barkoulas M, and Tsiantis M, 2004. PINning down the connections:transcription factors and hormones in leaf morphogenesis. Curr Opin Plant Biol 7:575-581.
Hertel R, Thomson K-St, and Russo VEA, 1972. *In-vitro* auxin binding to particulate cell fractions from corn coleoptiles. Planta 107:325-340.
Hetherington AM, 2001. Guard cell signaling. Cell 107:711-714.
Heyl A and Schmulling T, 2003. Cytokinin signal perception and transduction. Curr Opin Plant Biol 6:480-488.
Higuchi M, Pischke MS, Mahonen AP, Miyawaki K, Hashimoto Y, Seki M, Kobayashi M, Shinozaki K, Kato T, Tabata S, Helariutta Y, Sussman MR, and Kakimoto T, 2004. *In planta* functions of the *Arabidopsis* cytokinin receptor family. Proc Natl Acad Sci USA 101:8821-8826.
Hirai N, Kondo S, and Ohigashi H, 2003. Deuterium-labeled phaseic acid and dihydrophaseic acids for internal standards. Biosci Biotechnol Biochem 67:2408-2415.
Hu Y, Xie Q, and Chua N-H, 2003. The Arabidopsis auxin-inducible gene *ARGOS* controls lateral organ size. Plant Cell 15:1951-1961.
Hwang I and Sheen J, 2001. Two-component circuitry in *Arabidopsis* cytokinin signal transduction. Nature 413:383-389.
Inoue T, Higuchi M, Hashimoto Y, Seki M, Kobayashi M, Kato T, Tabata S, Shinozaki K, and Kakimoto T, 2001. Identification of CRE1 as a cytokinin receptor from *Arabidopsis*. 409:1060-1063.
Jeffrey SW and Humphrey GF, 1975. New spectrophotometric equations for determining chlorophylls a, b, c1 and c2 in higher plants, algae, and natural phytoplankton. Biochem Biophys Phlanz 167:191-194.
Johnston GFS and Jeffcoat B, 1977. Effects of some growth regulators on tiller bud elongation in cereals. New Phytol 79:239-245.
John PCL, Zhang K, Dong C, Diederich L and Wightman F, 1993. P34 *cdc*2 related proteins in control of cell cycle progres-sion, the switch between division and differentiation in tissuedevelopment, and stimulation of division by auxin and cytokinin. Aust. J. Plant Physiol. 20:503–526
Johri MM and Mitra D, 2001. Action of plant hormones. Curr Sci 80:199-202.
Kaplinsky NJ and Barton MK, 2004. Plant acupuncture: sticking PINs in the right places. Science 306:822-823.
Kakimoto T, 1996. CKI1, a histidine kinase homolog implicated in cytokinin signal transduction. Science 274:982-985.
Kamisaka S, 1979. Catecholamine stimulation of the gibberellin action that induce lettuce hypocotyl elongation. Plant Cell Physiol 20:1199-1207.
Kato C, Kato H, Asami T, Yoshida S, Noda H, Kamada H, and Satoh S, 2002. Involvement of xylem sap zeatin-*O*-glucoside in cucmber shoot greening. Plant Physiol Biochem 40:949-954.
Kaur A and Thurkral AK, 1990. Effect of animal hormones on the growth, protein and sugar contents of *Vigna unguiculata* L. seedlings. Indian J Plant Physiol 33:259-261.
Kawano T, Pinontoan R, Uozumi N, Miyake C, Asada K, Kolattukudy PE, and Muto S, 2000. Aromatic monoamine-induced immediate oxidative burst leading to an

increase in cytosolic Ca^{2+} concentration in tobacco suspension culture. Plant Cell Physiol 41:1251-1258.
Kay R, Chan A, Daly M, and McPherson J, 1987. Duplication of CaMV 35S promoter sequences creates a strong enhancer for plant genes. Science 236:1299-1302.
Khurana JP, Tamot BK, Maheshwari N, and Maheshwari SC, 1987. Role of catecholamines in promotion of flowering in a short-day duckweed, *Lemna paucicostata* 6746. Plant Physiol 85:10-12.
Kleczkowsi K and Schell J, 1995. Phytohormone conjugates: nature and function. Crit Rev Plant Sci 14:283-298.
Koornneef M, van der Veen, JH, 1980. Induction and analysis of gibberellin sensitive mutants in *Arabidopsis thaliana* (L.) Heynh. Theor Appl Genet 58:257-263.
Koornneef M, Leon-Kloosterziel KM, Schwartz SH, and Zeevaart JAD, 1998. The genetic and molecular dissection of abscisic acid biosynthesis and signal transduction in *Arabidopsis*. Plant Physiol Biochem 36:83-89.
Kuklin AI and Conger BV, 1995. Catecholamines in plants. J Plant Growth Regul 14:91-97.
Langridge J, 1957. Effect of day-length and gibberellic acid on the flowering of *Arabidopsis*. Nature 180:36-37.
Lee TT, Starratt AN, and Jevnikar JJ, 1982. Regulation of enzymic oxidation of indole-3-acetic acid by phenols: structure-activity relationships. Phytochemistry 21:517-523.
Leyser HM, Lincoln CA, Timpte C, Lammer D, Turner J, and Estelle M, 1993. *Arabidopsis* auxin-resistance gene *AXR1* encodes a protein related to ubiquitin-activating enzyme E1. Nature 364:161-164.
Leyser O, 2002. Molecular genetics of auxin signaling. Annu Rev Plant Biol 53:377-398.
Ljung K, Bhalerao RP, and Sandberg G, 2001. Sites and homeostatic control of auxin biosynthesis in *Arabidopsis* during vegetative growth. Plant J 28:465-474.
Livak KJ and Schmittgen TD, 2001. Analysis of relative gene expression data using real-time quantitative PCR and the $2^{-\Delta\Delta C_{(T)}}$ method. Methods 25**:**402-408.
Liscum E and Reed JW, 2002. Genetics of Aux/IAA and ARF action in plant growth and development. Plant Mol Biol 49:387–400.
Luna CM, González CA, and Trippi VS, 1994. Oxidative damage caused by an excess of copper in oat leaves. Plant Cell Physiol 35:11-15.
Maher EP and Martindale SJB, 1980. Mutants of *Arabidopsis* with altered responses to auxins and gravity. Biochem Genet 18:1041-1053.
Mahonen AP, Bonke M, Kauppinen L, Riikonen M, Benfey PN, and Helariutta Y, 2000. A novel two-component hybrid molecule regulates vascular morphogenesis of the *Arabidopsis* root. Gene Dev 14:2938-2943.
Mantyla E, Lang V, and Palva ET, 1995. Role of abscisic acid in drought-induced freezing tolerance, cold acclimation, and accumulation of LT178 and RAB18 proteins in *Arabidopsis thaliana*. Plant Physiol 107:141-148.
Marchant A, Kargul J, May ST, Muller P, Delbarre A, Perrot-Rechenmann C, and Bennett MJ, 1999. AUX1 regulates root gravitropism in *Arabidopsis* by facilitating auxin uptake within root apical tissues. EMBO J 18:2066-2073.

Marchler-Bauer A, Anderson JB, DeWeese-Scott C, Fedorova ND, Geer LY, He S, Hurwitz DI, Jackson JD, Jacobs AR, Lanczycki CJ, 2003. CDD: A curated Entrez database of conserved domain alignments. Nucleic Acids Res 31:383-387.

Marcroft SJ, Purwantara A, Salisbury PA, Potter TD, Wratten N, Khangura R, Barbetti MJ, and Howlett BJ, 2002. Reaction of a range of *Brassica* species under Australian conditions to the fungus, *Leptosphaeria maculans*, the causal agent of blackleg. Aust J Exp Agric 42:587-594.

Miller CO, Skoog F, von Saltza MH, and Strong FM, 1955. Kinetin, a cell division factor from deoxyribonucleic acid. J Am Chem Soc 77:1392.

Mitchell JW, Skaggs DP and Anderson WP, 1951. Plant growth stimulating hormones in immature bean seeds. Science 114:159-161.

Morris DA, 2000. Transmembrane auxin carrier systems — dynamic regulators of polar auxin transport. Plant Growth Regul 32:161-172.

Müller A, Guan C, Gälweiler L, Tänzler P, Huijser P, Marchant A, Parry G, Bennett M, Wisman E, and Palme K, 1998. *AtPIN2* defines a locus of *Arabidopsis* for root gravitropism control. Embo J 17:6903-6911.

N^6-benzylaminopurine (cytokinin b). <http://www.chemicalland21.com/lifescience/agro/6-BENZYLAMINOPURINE.htm>, viewed July, 2005.

Naderi M, Caplan A, and Berger PH, 1997. Phenotypic characterization of a tobacco mutant impaired in auxin polar transport. Plant Cell Rep 17:32-38.

Napoli C, 1996. Highly branched phenotype of the petunia *dad1-1* mutant is reversed by grafting. Plant Physiol 111:27-37.

Neljubow DN, 1901. Uber die horizontale nutation der stengel von Pisum sativum und einiger anderen. Pflanzen Beitrage und Botanik Zentralblatt 10:128-139.

Neuteboom LW, Ng JMY, Kuyper M, Clijdesdale OR, Hooykaas PJJ, and van der Zaal BJ, 1999. Isolation and characterization of cDNA clones corresponding with mRNAs that accumulate during auxin-induced lateral root formation. Plant Mol Biol 39:273-287.

Nishimura C, Ohashi Y, Sato S, Kato T, Tabata S, and Ueguchi C, 2004. Histidine kinase homologs that act as cytokinin receptors possess overlapping functions in the regulation of shoot and root growth in *Arabidopsis*. Plant Cell 16:1365-1377.

Nooden LD and Letham DS, 1993. Cytokinin metabolism and signaling in the soybean plant. Aust J Plant Physiol 20:639-653.

Nordstrom A, Tarkowski P, Tarkowska D, Norbaek R, Astot C, Dolezal K, and Sandberg G, 2004. Auxin regulation of cytokinin biosynthesis in *Arabidopsis thaliana*: a factor of potential importance for auxin—cytokinin-regulated development. Proc Natl Acad Sci USA 101:8039-8044.

Normanly J and Bartel B, 1999. Redundancy as a way of life – IAA metabolism. Curr Opin Plant Biol 2:207-213.

Nowacki J and Bandurski RS, 1980. *Myo*-inositol esters of indole-3-acetic acid as seed auxin precursors of *Zea mays* L. Plant Physiol 65:422–427.

Ohkuma K, Lyon JL, Addicott FT, and Smith OE, 1963. Abscisin II, an abscission-accelerating substance from young cotton fruit. Science 142:1592–1593.

Ohtani N, Goto T, Waeber C, and Bhide PG, 2003. Dopamine modulated cell cycle in the lateral ganglionic eminence. J Neurosci 23:2840-2850.

Oka M, Miyamoto K, Okada K, and Ueda J, 1999. Auxin polar transport and flower formation in *Arabidopsis thaliana* transformed with indoleacetamide hydrolase (*iaaH*) gene. Plant Cell Physiol 40:231-237.

Oota Y, 1974. Removal of the sugar inhibition of flowering in *Lemna gibba* G3 by catecholamines. Plant Cell Physiol 15:63-68.

Oota Y and Kondo T, 1974. Removal by cyclic-AMP of the inhibition of duckweed flowering due to ammonium and water-treatment. Plant Cell Physiol 15:403-411.

Ori N, Juarez MT, Jackson D, Yamaguchi J, Banowetz GM, and Hake S, 1999. Leaf senescence is delayed in tobacco plants expressing the maize homeobox gene *knotted1* under the control of a senescence-activated promoter. Plant Cell 11:1073-1080.

Otsuga D, DeGuzman B, Prigge MJ, Drews GN, and Clark SE, 2001. *REVOLUTA* regulates meristem initiation at lateral positions. Plant J 25:223-236.

Paal A, 1918. Uber phototropische. Reizleitung Jahrb Wiss Bot 58:406-458.

Palni LMS, Burch L, and Horgan R, 1988. The effect of auxin concentration on cytokinin stability and metabolism. Planta 174:231-234.

Pasternak T, Miskolczi O, Ayaydin F, Meszaros T, Dudits D, and Feher A, 2000. Exogenous auxin and cytokinin dependent activation of CDKs and cell division in leaf protoplast-derived cells of alfalfa. Plant Growth Regul 32:129-141.

Pfaffl MW, 2001. A new mathematical model for relative quantification in real-time RT-PCR. Nucl Acids Res 29:2003-2007.

Phillips AL, 1998. Gibberellins in *Arabidopsis*. Plant Physiol Biochem 36:115-124.

Polce MJ and Wesdemiotis C, 2002. Introduction to mass spectrometry of polymers. In: Mass spectrometry of polymers. Montaudo G and Lattimer RP (eds.). CRC Press, Boca Raton, Florida, USA.

Popolo M, McCarthy DM, and Bhide PG, 2004. Influence of dopamine on precursor cell proliferation and differentiation in the embryonic mouse telencephalon. Dev Neurosci 26:229-244.

Protacio CM, Dai Y, Lewis EF, and Flores HE, 1992. Growth stimulation by catecholamines in plant tissue/organ cultures. Plant Physiol 98:89-96.

Radley M, 1956. Occurrence of substances similar to GA in higher plants. Nature 178:1070-1071.

Rakow G and Getinet A, 1998. *Brassica carinata* an oilseed crop for Canada. Proc Int Symp on Brassicas, pp 419-426, Eds Gregoire T and Monteiro A.

Rapparini F, Tam YY, Cohen JD, and Slovin JP, 2002. Indole-3-acetic acid metabolism in *Lemna gibba* undergoes dynamic changes in response to growth temperature. Plant Physiol 128:1410-1416.

Ribnicky DM, Cohen JD, Hu W-S, and Cooke TJ, 2002. An auxin surge following fertilization in carrots: a mechanism for regulating plant totipotency. Planta 214:505-509.

Richards DE, King KE, Ait-ali T, and Harberd NP, 2001. How gibberellin regulates plant growth and development: a molecular genetic analysis of gibberellin signaling. Annu Rev Plant Physiol Plant Mol Biol 52:67-88.

Richmond AE, 1957. Effect of kinetin on protein content and survival of detached Xanthium leaves. Science 125:650-651.

Robertson JG, Adams GW, Medzihradszky KF, Burlingame AL, and Villafranca JJ, 1994. Complete assignment of disulfide bonds in bovine dopamine β-hydroxylase. Biochemistry 33:11563-11575.

Roshchina VV, 1989. Biomediators in chloroplasts of higher plants. 1. The interaction with photosynthetic membranes. Photosynthetica 23:197–206.

Roshchina VV, 1990. Biomediators in chloroplasts of higher plants. 4. Reception by photosynthetic membranes. Photosynthetica 24:539–549.

Rodrigues-Pousada R, Caeneghem WV, Chauvaux N, Van Onckelen H, Van Montagu M, and Van Der Straeten D, 1999. Hormonal cross-talk regulates the *Arabidopsis thaliana* 1-aminocyclopropane-1-carboxylate synthase gene *1* in a developmental and tissue-dependent manner. Physiol Plant 105:312-320.

Rulcova J and Pospisilova J, 2001. Effect of benzylaminopurine on rehydration of bean plants after water stress. Biol Plantarum 44(1):75-81.

Romanov GA, 2002. The phytohormone receptors. Russ J Plant Physiol 49:552-560.

Sakai HS, Aoyama T, and Oka A, 2000. *Arabidopsis* ARR1 and ARR2 response regulators operate as transcriptional activators. Plant J 24:703-711.

Sakai H, Honma T, Aoyama T, Sato S, Kato T, Tabata S, and Oka A, 2001. ARR1, a transcription factor for genes immediately responsive to cytokinins. Science 294:1519-1521.

Sambrook J and Russell DW, 2001. Molecular cloning: a laboratory manual. (pp. 5.12-5.17; pp. 6.39-5.68), Cold Spring Harbor, New York, USA: Cold Spring Harbor Laboratory Press.

Scanlon MJ, 2003. The polar auxin transport inhibitor *N*-1-napthylphthalamic acid disrupts leaf initiation, KNOX protein regulation, and formation of leaf margins in maize. Plant Physiol 133:597-605.

Schenk RU and Hildebrandt AC, 1972. Medium and techniques for induction and growth of monocotyledonous and dicotyledonous plant cell cultures. Can J Bot. 50:199-204.

Schmitz G, Tillmann E, Carriero F, Fiore C, Cellini F, and Theres K, 2002. The tomato Blind gene encodes a MYB transcription factor that controls the formation of lateral meristems. Proc Natl Acad Sci USA 99:1064-1069.

Schroeder JI, Allen GJ, Hougovieux V, Kwak JM and Waner D, 2001. Guard cell signal transduction. Annu Rev Plant Physiol Plant Mol Biol, 52:627-658.

Schurr U, Gollan T, Schulze E-D, 1992. Stomatal response to soil drying in relation to changes in the xylem sap composition of *Helianthus annuus*. II. Stomatal sensitivity to abscisic acid imported from the xylem sap. Plant Cell Environ 15:561–567.

Sieberer T, Hauser M, Seifert GJ, and Luschnig C, 2003. *PROPORZ1*, a putative *Arabidopsis* transcriptional adaptor protein, mediates auxin and cytokinin signals in the control of cell proliferation. Curr Biol 13:837-842.

Skoog F and Miller CO, 1957. Chemical regulation of growth and organ formation in plant tissues cultured *in vitro*. Symp Soc Exp Biol 11:118-130.

Smith TA, 1977. Phenethylamine and related compounds in plants. Phytochemistry 16:9-18.

Snow M and Snow R, 1942. The determination of axillary buds. New Phytol 41:13-22.

Snowdon RJ, Kohler W, Friedt W, and Kohler A, 1997. Genomic in situ hybridization in *Brassica* amphidiploids and interspecific hybrids. Theor Appl Genet 95:1320-1324.

Sorefan K, Booker J, Haurogne K, Goussot M, Bainbridge K, Foo E, Chatfield S, Ward S, Beveridge C, Rameau C, and Leyser O, 2003. *MAX4* and *RMS1* are orthologous dioxygenase-like genes that regulate shoot branching in *Arabidopsis* and pea. Gene Dev 17:1469-1474.

Stirnberg P, van de Sande K, and Leyser HMO, 2002. *MAX1* and *MAX2* control shoot lateral branching in *Arabidopsis*. Development 129:1131-1141.

Sun W, Kieliszewski MJ, and Showalter AM, 2004. Overexpression of tomato LeAGP-1 arabinogalactan-protein promotes lateral branching and hampers reproductive development. Plant J 40:870-881.

Sussex IM, 1955. Morphogenesis in *Solanum tuberosum* L.: apical structure and developmental pattern of the juvenile shoot. Phytomorphology 5:253-273.

Suzuki M, Yamaguchi S, Iida T, Hashimoto I, Teranishi H, Mizoguchi M, Yano F, Todoroki Y, Watanabe N, and Yokoyama M, 2003. Endogenous α-ketol linolenic acid levels in short day-induced cotyledons are closely related to flower induction in *Pharbitis nil*. Plant Cell Physiol 44:35-43.

Swarup R, Friml J, Marchant A, Ljung K, Sandberg G, Palme K, and Bennett M, 2001. Localization of the auxin permease AUX1 suggests two functionally distinct hormone transport pathways operate in the *Arabidopsis* root apex. Genes Dev 15:2648-2653.

Sweidrych A, Lorenc-Kukula K, Skirycz A, and Szopa J, 2004. The catecholamine biosynthesis route in potato is affected by stress. Plant Physiol Biochem 42:593-600.

Symons GM, Ross JJ, and Murfet IC, 2002. The *bushy* pea mutant is IAA-deficient. Physiol Plant 116:389-397.

Szopa J, Wilczynski G, Fiehn O, Wenczel A, and Willmitzer L, 2001. Identification and quantification of catecholamines in potato plants (*Solanum tuberosum*) by GC-MS. Phytochemistry 58:315-320.

Taiz L and Zeiger E, 1998. Plant Physiology, 2nd ed., Massachusetts, USA: Sinauer Associates.

Tam YY, Epstein E, and Normanly J, 2000. Characterization of auxin conjugates in Arabidopsis. Low steady-state levels of indole-3-acetyl-glutamate, and indole-3-acetyl-glucose. Plant Physiol 123:589-595.

Tamura K, Liu H, and Takahash H, 1999. Auxin induction of cell cycle regulated activity of tobacco telomerase. J Biol Chem 274:20997-21002.

Tantikanjana T, Yong JWH, Letham DS, Griffith M, Hussain M, Ljung K, Sandberg G, and Sundaresan V, 2001. Control of axillary bud initiation and shoot architecture in *Arabidopsis* through the *SUPERSHOOT* gene. Gene Dev 15:1577-1588.

Taya Y, Tanakay Y, and Nishimura S, 1978. 5'-AMP is a direct precursor of cytokinin in *Dictyostelium discoidum*. Nature 271:545-547.

Turnbull CG, Booker JP, and Leyser HM, 2002. Micrografting techniques for testing long-distance signaling in Arabidopsis. Plant J 32:255-262.

Uchacz TM, 2000. Isolation and characterization of induced defense genes from *Brassica carinata*. MSc thesis. University of Saskatchewan.

Ueguchi C, Sato S, Kato T, and Tabata S, 2001. The *AHK4* gene involved in the cytokinin-signaling pathway as a direct receptor molecule in *Arabidopsis thaliana*. Plant Cell Physiol 42:751-755.

Ueno E and Shinozaki M, 1999. Effects of the inhibitors of biosynthesis and degradation of catecholamines on photoperiodic induction of flowering in *Pharbitis nil*. J Plant Physiol 155:332-337.

Ulmasov T, Hagen G, and Guilfoyle TJ, 1997a. ARF1, a transcription factor that binds to auxin response elements. Science 276:1865-1868.

Ulmasov T, Murfett J, Hagen G and Guilfoyle TJ, 1997b. Aux/IAA proteins repress expression of reporter genes containing natural and highly active synthetic auxin response elements. Plant Cell 9:1963-1971.

Vandenbussche F and Van Der Straeten D, 2004. Shaping the shoot: a circuitry that integrates multiple signals. Trends Plant Sci 9:499-506

Vandesompele J, De Preter K, Pattyn F, Poppe B, Van Roy N, De Paepe A, and Speleman F, 2002. Accurate normalization of real-time quantitative RT-PCR data by geometric averaging of multiple internal control genes. Genome Biol 3:1-11.

Vartanian N, 1981. Some aspects of structural and functional modifications induced by drought in root systems. Plant and Soil 63:83-92.

Vartanian N, Marcotte L, and Giraudat J, 1994. Drought Rhizogenesis in *Arabidopsis thaliana*. Differential responses of hormonal mutants. Plant Physiol 104:761-767.

Velasco L, Nabloussi A, De Haro A, and Fernandez-Martinez M, 2004. Allelic variation in linolenic acid content of high erucic acid Ethiopian mustard and incorporation of the low linolenic acid trait into zero erucic acid germplasm. Plant Breeding 123:137-140.

Verelst W and Asard H, 2004. Analysis of an *Arabidopsis thaliana* protein family, structurally related to cytochromes *b*561 and potentially involved in catecholamine biochemistry in plants. J Plant Physiol 161:175-181.

Vicente-Agullo F, Rigas S, Desbrosses G, Dolan L, Hatzopoulos P, and Grabov A, 2004. Potassium carrier TRH1 is required for auxin transport in *Arabidopsis* roots. Plant J 40:523-535.

Vogel JP, Schuerman P, Woeste K, Brandstatter I, and Kieber JJ, 1998. Isolation and characterization of Arabidopsis mutants defective in the induction of ethylene biosynthesis by cytokinin. Genetics 149:417-427.

Walker GC and Leonard NJ, 1974. The mode of incorporation of 6-benzylaminopurine into tobacco callus transfer ribonucleic acid: A double labeling determination. Plant Physiol 54(5):737-743.

Wang X and Below FE, 1996. Cytokinins in enhanced growth and tillering of wheat induced by mixed nitrogen source. Crop Sci 36:121-126.

Wang H, Qi Q, Schorr P, Cutler AJ, Crosby WL, and Fowke LC, 1998. ICK1, a cyclin-dependent protein kinase inhibitor from *Arabidopsis thaliana* interacts with both Cdc2a and CycD3, and its expression is induced by abscisic acid. Plant J 15:501-510.

Wang H, Fowke LC, and Crosby WL, 1997. A plant cyclin-dependent kinase inhibitor gene. Nature 386: 451-452.

Went FW, 1926. On growth-accelerating substances in the coleoptile of *Avena sativa*. Proc Kon Ned Akad Wet 30:10-19.

Werner T, Motyka V, Strnad M, and Schmulling T, 2001. Regulation of plant growth by cytokinin. Proc Natl Acad Sci USA 98:10487-10492.

Werner T, Motyka V, Laucou V, Smets R, Van Onckelen H, and Schmulling T, 2003. Cytokinin-deficient transgenic *Arabidopsis* plants show multiple developmental alterations indicating opposite functions of cytokinins in the regulation of shoot and root meristem activity. Plant Cell 15:2532-2550.

Wichers HJ, Visser JF, Huizing HJ, and Pras N, 1993. Occurrence of L-DOPA and dopamine in plants and cell cultures of *Mucuna pruriens* and effects of 2,4-D and NaCl on these compounds. Plant Cell Tiss Org 33:259-264.

Williams W, 1960. The effect of selection on the manifold expression of the `suppressed lateral' gene in the tomato. Heredity 14**:**285-296.

Wilson AK, Pickett FB, Turner JC, and Estelle M, 1990. A dominant mutation in *Arabidopsis* confers resistance to auxin, ethylene and abscisic acid. Mol Gen Genet 222:377-383.

Wilson RN, Heckman JW, and Somerville CR, 1992. Gibberellin is required for flowering in *Arabidopsis thaliana* under short days. Plant Physiol 100:403-408.

Yabuta T and Sumiki Y, 1938. Communication to the editor. J. Agric. Chem. Soc. 14:1526.

Yamada H, Hanaki N, Imamura A, Ueguchi C, and Mizuno T, 1998. An *Arabidopsis* protein that interacts with the cytokinin-inducible response regulator, ARR4, implicated in the His-Asp phosphorelay signal transduction. FEBS Lett 436:76-80.

Yamaguchi S, Yokoyama M, Iida T, Okai M, Tanaka O, and Takimoto A, 2001. Identification of a component that induces flowering of *Lemna* among the reaction products of α-ketol linolenic acid (FIF) and norepinephrine. Plant Cell Physiol 42:1201-1209.

Yamamoto M and Yamamoto KT, 1998. Differential effects of 1-naphthaleneacetic acid, indole-3-acetic acid and 2, 4-dichlorophenoxyacetic acid on the gravitropic response of roots in an auxin-resistant mutant of Arabidopsis, *aux1*. Plant Cell Physiol 39:660–664.

Yang SW, Jin E, Chung IK, and Kim WT, 2002. Cell cycle-dependent regulation of telomerase activity by auxin, abscisic acid and protein phosphorylation in tobacco BY-2 suspension culture cells. Plant J 29:617-626.

Zenser N, Ellsmore A, Leasure C, and Callis J, 2001. Auxin modulates the degradation rate of Aux/IAA proteins. Proc Natl Acad Sci USA 98:11795-11800.

Zheng Z, Uchacz TM, and Taylor JL, 2001. Isolation and characterization of novel defence-related genes induced by copper, salicylic acid, methyl jasmonate, abscisic acid and pathogen infection in *Brassica carinata*. Mol Plant Pathol 2:159-169.

9. APPENDICES

```
AAC62613        -EQNSAMASSSSSLLILAVACFVSLISPAISQ-----------QACKSQNLNSAGPFDS 47
CIL1            ------MASNASLTLVLAVACFVSLISPAIS-------------QTCSTQNVT--GDFKN 39
AAM65781        -------MDSSYLRISLSFLFWALLLSPAVSQS-----------SSCSSQTFSGVKSYPH 42
NP_566763       ------MSSSSSVRISLSFIFLALLISPAVSQT------------CKSQTFSGDKTYPH 41
BAB09428        ----MFLSSRTIFVGLCFLFVLAPCFTRATTNE---------VQVSCDSHNFNNGKHFRS 47
NP_191466       ----MSLSSRATLVVLCCLFMLIPSFTTAATEQGLH------ARSRCESYSFNNGKSFRS 50
AAL57706        MSNHMSIMKFLNQILCLSLILSISMTTLSFAQT------------CSKYKFSSNNVFDS 47
NP_199564       ----MAISS--NLLLCLSLFIFI-ITKSALAQK------------CSNYKFSTNRLFES 40
AAM64730        ----MD-RTQSPKTALFAVLATLLVLTVNGQSL------------CNTHRFTNNLAFAD 42
CAC37356        ----MDTKLLTSNLVLFSSILLTLFTFSYGQN-------------CSTHQFTNNNLFST 42
AAM61181        ---------MATLILSFLLLLLATKLPESLAG--------------HCTTTTATKSFEK 36
BAC01247        -MARAG--AVLVVVLAAASVLLAPWAATAQTSSCD---------DALPP-ALAGNYSGLA 47
NP_191734       -MKTLVGFYILCFLIGQDLPFLAADDVNVINDSTQNLCFANRLSDFLPP-PYSNISDNMP 58
NP_566313       -MKLYSVSIIIFVLIALSTIVNAQQAA---TDSCN---------STLPLNDLTFNTSLLQ 47


AAC62613        CEDLPVLNSYLHYTYNSSNSSLSVAFVATPSQANGGWVAWAINPTG-TKMAGSQAFLAYR 106
CIL1            CMDLPVLDSFLHYTYDAANSSLSVAFVATPPRS-GDWVAWGINPTG-TKMIGSQAFVAYS 97
AAM65781        CLDLPDLKAILHYSYDASNTTLAVVFSAPPSKP-GGWIAWAINPKS-TGMAGSQALVASK 100
NP_566763       CLDLPQLKAFLHYSYDASNTTLAVVFSAPPAKP-GGWIAWAINPKA-TGMVGSQTLVAYK 99
BAB09428        CVDLPVLDSFLHYSYVRETGVLEVAYRHTNIES-SSWIAWGINPTS-KGMIGAQTLLAYR 105
NP_191466       CTDLLVLNSYLHFNYAQETGVLEIAYHHSNLES-SSWISWAINPTS-KGMVGAQALVAYR 108
AAL57706        CNDLPFLDSFLHYTYESSTGSLHIAYRHTKLTS-GKWVAWAVNPTS-TGMVGAQAIVAYP 105
NP_199564       CNDLPVLDSFLHYTYDSSSGNLQIAYRHTKLTP-GKWVAWAVNPTS-TGMVGAQAIVAYP 98
AAM64730        CSDLSALGSFLHWTYNEQNGTVSIAYRHPGTSA-SSWVAWGLNPSS-TQMVGTQALVAFT 100
CAC37356        CNPLPVLNSFLHWTYHPDNHTVDLAYRHGGVTE-SSWVAWALNLDG-TGMAGCQSLIAFR 100
AAM61181        CISLPTQQTSIAWTYHPHNATLDLCFFGTFISP-SGWVGWGINPDSPAQMTGSRVLIAFP 95
BAC01247        CRPVWN--NFVLRYAQGKDNVLRVVISSMYSTG---WVGMGFSKDG--MMVGSSAMVGWV 100
NP_191734       CTPLWN--TFVLRYSENRDNVMTIIVSALYTTG---WVGIGFSKEG--RMVGSSAMIGWI 111
NP_566313       CTEAWTPQNFILRYARTAENTWSFILSAPDSSA---FIGIGFSTNG--QMIGSSAIVGWI 102
                *         :            .            ::. ...  .   * *   ::.

AAC62613        SGGGAAPVVKTYNISSYSS-LVEGKLA--FDFWNLRAESLS--GGRIAIFNR-----TVK 156
CIL1            PRAGARPEVNTYNISSYS--LSAGRLT--FDFWNLRAESMA--GNRIVIYT------SVK 145
AAM65781        DPSTGVASVTTLNIVSYSS-LVPSKLS--FDVWDVKAEEAANDGGALRIFA------KVK 151
NP_566763       DPGNGVAVVKTLNISSYSS-LIPSKLA--FDVWDMKAEEAARDGGSLRIFA------RVK 150
BAB09428        NSTSGFMRAYTSSINGYTPMLQEGPLS--FRVTQLSAEYLN---REMTIFA------TMV 154
NP_191466       NSTSGVMRAYTSSINSYSPMLQESPLS--LRVTQVSAEYSN---GEMMIFA------TLV 157
AAL57706        QSDG-TVRVYTSPIRSYQTSLLEGDLS--FNVSGLSATYQN---NEIVVLA------SLK 153
NP_199564       QSDG-TVRAYTSPISSYQTSLLEAELS--FNVSQLSATYQN---NEMVIYA------ILN 146
AAM64730        NTTTNQFQAYTSSVSSYGTRLERSSLS--FGVSGLSATLVS---GEVTIFA------TLE 149
CAC37356        NSSG-QIHAYTSPIAGYGTTLTEGALS--FGVPRISAEFVR---SEMIIFA------TLE 148
AAM61181        DPNSGQLILLPYVLDSSVKLQKGPLLSRPLDLVRLSSSSASLYGGKMATIRNGASVQIYA 155
BAC01247        GKTG-LSHVKQFSLRGKTPSQVVADEG---FLQSKDHDHTVVVQQAKIYLA--------- 147
NP_191734       SKKG-HAKIKQYYLQGTERDQVVPDQG---ELQLQKVPPVVALHGAMIYLA--------- 158
NP_566313       PSDGGSGTVKPYLLGGKSPGEVNPDQG---DLTIVNGSLKIESVSSRLYMR--------- 150
                          : .              .

AAC62613        VPAGRDS---VNQVWQIGGNVT-NGRPGVHPFGPDNLGSHRVLSFT----EDAAPGSAPS 208
CIL1            VPAGADS---VNQVWQIGGNVT-GGRPGPHPMTPANLASTRMLRLTGSDAPSSAPGSAPS 201
AAM65781        VPADLAASGKVNQVWQVGPGVS-NGRIQAHDFSGPNLNSVGSLDLTGTTPGVPVSGGGGA 210
NP_566763       VPADLVAKGKVNQVWQVGPELGPGGMIGRHAFDSANLASMSSLDLKGDNSGGTISGGD-E 209
BAB09428        WP---SNTTVVNHLWQDGPLKE-GDRLGMHAMSGNHLKSMANLDLLS-GQVMTTKAA--- 206
NP_191466       LP---PNTTVVNHLWQDGPLKE-GDRLGMHAMSGDNLKSMASLDLLS-GQVTTTKSV--- 209
AAL57706        LAQDLGNGGTINTVWQDGSMS--GNSLLPHPTSGNNVRSVSTLNLVS-GVS-AAAGG-AG 208
NP_199564       LP--LANGGIINTVWQDGSLS--GNNPLPHPTSGNNVRSVSTLNLVS-GASGSTSTG-AG 200
AAM64730        LS---PNLITANQLWQVGPVV--NGVPASHQTSGDNMRSSGRIDFRT-GQASAGGGG--- 200
CAC37356        LP---INRTSFTQVWQNGQVS--EQALRVHQTSGDNMRSVGTVDFAS-GQTSAGAGGGIS 202
AAM61181        SVKLSSNNTKIHHVWNRGLYVQ-GYSPTIHPTTSTDLSSFSTFDVTSGFATVNQNSG--- 211
BAC01247        FQLRFQSPLRRQQVLLAFGNA--IPVN--DRLTEHQGKTSFTFDFTTGS--SSGSSY--- 198
NP_191734       FQVKFAVRVPRRAVILAFSTA--YPSKL-GRLTKHDDKTTVIVDFSKASGATSIKTT--- 212
NP_566313       FQL--TATLPRQSLLYAVGPAGFFPSSPDFRLREHRFVTTTTINYNTGSQSVVKVSP--- 205
                          :                          :   .

AAC62613        --PGSAPS--PGSAP------------------------------APGTSG------- 225
CIL1            SGPGSAPSSGPGSAPGS----------------------------VPGSAEGPTTPDA 231
AAM65781        GNSRIHKRNIHGILNAVSWGLLFPIGAMIARYMRIFESADPAWFYLHVSCQFSAYAIGVA 270
NP_566763       VNAKIKNRNIHGILNAVSWGILFPIGAIIARYMRVFDSADPAWFYLHVSCQFSAYVIGVA 269
BAB09428        NDNMLLVKSIHGLVNAVCWGIFIPIGVMAARYMRTYKGLDPTWFYILIL----------- 255
NP_191466       NRNMLLVKQIHAIVNALSWGILMPIGVMAARYMKNYEVLDPTWFYIHVVCQTTGYFSGLI 269
AAL57706        GSSKLRKRNIHGILNGVSWGIMMPLGAIIARYLRVAKSADPAWFYIHVFCQASAYIIGVA 268
```

```
NP_199564       GASKLRKRNIHGILNGVSWGIMMPIGAIIARYLKVSKSADPAWFYLHVFCQSSAYIIGVA 260
AAM64730        SGDRLRKRNTHGVLNAVSWGVLMPMGAMMARYMKVF--ADPTWFYLHIAFQVSGYVIGVA 258
CAC37356        ASARQRRRNIHGVLNAVSWGVLMPMGAIFARYLKVFKSANPAWFYLHAGCQTVAYAVGVA 262
AAM61181        ---SRALKVTHGVVNAISWGFLLPAGAVTARYLRQMQSIGPTWFYIHAAIQLTGFLLGTI 268
BAC01247        ---PDGLKRAHGALNLFAWGVLLPIGAIIARYCR---RWDPLWFYLHAGIQLVGFILGLA 252
NP_191734       ---TSTEKTKHGVMAILGWGFLLPVGAILARYLR---HKDPLWYYLHIGFQFTGFIFGLA 266
NP_566313       ---HSKLKKTHGLMNMFGWGILIIVGAIVARHMK---QWDPTWFYAHIALQTTGFLLGLT 259
                          .

AAC62613        STTPGTAAGGPGNAGSLTRNVNFGVNLGILVLLGSIFIF---------------------- 264
CIL1            STTPG-QAGSPGNAGSMTTSVNFGVNFGILVMLASVFIF---------------------- 269
AAM65781        GWATGLKLGSESKGIQYNTHRNIGISLFSIATLQMFAMLLRPRKDHKFRFVWNIYHHGVG 330
NP_566763       GWATGLKLGNESEGIRFSAHRNIGIALFTLATIQMFAMLLRPKKDHKYRFYWNIYHHGVG 329
BAB09428        ------------------------------------------------------------
NP_191466       GGLGTAIYMARHTGMRTTLHTVIGLLLFALGFLQILSLKARPNKDHKYRKYWNWYHHTMG 329
AAL57706        GWATGLKLGGDSPGIQYSTHRAIGIALFSLATVQVFAMFLRPKPEHKHRLYWNIYHHTIG 328
NP_199564       GWATGLKLGNESAGIQFTFHRAVGIALFCLATIQVFAMFLRPKPEHKYRVYWNIYHHTVG 320
AAM64730        GWATRIKLGNDSPGTSYSTHRNLGIALFTFATLQVFALLVRPKPDHKYRTYWNVYHHTVG 318
CAC37356        GWGTGLKLGSDSVGIRFDTHRNIGITLFCLGTLQVFALLLRPKPDHKFRLYWNIYHHVTG 322
AAM61181        GFSIGIVLGHNSPGVTYGLHRSLGIATFTAAALQTLALLFRPKTTNKFRRYWKSYHHFVG 328
BAC01247        GIVAGVSLYNKIQA-DVPAHRGLGIFVLVLGILQILAFFLRPHKDSKYRKYWNWYHHWVG 311
NP_191734       AVILGIQLYNRIQP-DIPAHRGIGIFLLVLSTLQVLAFFARPQKETKMRRYWNWYHHWIG 325
NP_566313       GVICGLVLENRLKANNVSKHKGLGITILVMGVLQMLALLARPDKQSKYRKYWNWYHHNIG 319


AAC62613        ------------------------------------------------------------
CIL1            ------------------------------------------------------------
AAM65781        YSILILGIINVFKGLSILNPKHTYKTA-YIAVIGTLGGITLLLEVVTWVIVLKRKSAKST 389
NP_566763       YAILTLGIINVFKGLNILKPQDTYKTA-YIAVIAVLGGIALLLEAITWVVVLKRKSNNSM 388
BAB09428        ------------------------------------------------------------
NP_191466       YIVIVLSIYNIYKGLSILQPGSIWKIA-YTTIICCIAAFAVVMEILQFKKRWARLFFKKS 388
AAL57706        YTIIILGVVNVFKGLGILSPKKQWKNA-YIGIIVVLAIVATLLEAFTWYVVIKRR----- 382
NP_199564       YSVIILAVVNVFKGLDILSPEKQWRNA-YTAIIVVLGIVAVVLEGFTWYVVIKRG----- 374
AAM64730        YTTIILSIVNIFKGFDILDPEDKWRWA-YIGILIFLGACVLILEPLTWFIVLRRKSRGGN 377
CAC37356        YTVIILSIINVFEGFDALNGQKNWKKA-YIGVIIFLGAIAVLLEAITWFIVIKRK----- 376
AAM61181        YACVVMGVVNVFQGFEVLREGRSYAKLGYCLCLSTLVGVCVAMEVNSWVVFCRKAKEEKM 388
BAC01247        RLALFFAAINIVLGIKVG-AAGNSWKIGYGFNLAILLITIITLEVLLWTRWKNNNSS-SM 369
NP_191734       RISLFFGAVNIVLGIRMADNGGDGWKIGYGFVLSVTLLAFVVLEIFRIRGTIGSPSSRSP 385
NP_566313       RLLIILAISNIFYGIHLA-KAGTSWNGGYGFAVAVLALTAIGLEVRKFLKK--------- 369


AAC62613        ------------------------------------------------------------
CIL1            ------------------------------------------------------------
AAM65781        KPLKA------------------------------------------------------- 394
NP_566763       KPLRT------------------------------------------------------- 393
BAB09428        ------------------------------------------------------------
NP_191466       KDVEADQPTVSVDVIGETEKAERKKASGGIEIQIENYNITKNFMIPSVFVISYPHTSPPL 448
AAL57706        KLEA--KTAQHGASNGTRSQYA--------------------------------------- 402
NP_199564       KAEASAKTSQR-VGNDGRSLYV--------------------------------------- 395
AAM64730        TVAAPTSSKYSNGVNGTTTTGPHHQDA---------------------------------- 404
CAC37356        KTSVSDKYPHGNGTNGYASR-SHDQTA---------------------------------- 402
AAM61181        KRDGLTGVDRCSGSHS-------------------------------------------- 404
BAC01247        PTY--------------------------------------------------------- 372
NP_191734       PSFETHPSSSTSV----------------------------------------------- 398
NP_566313       ------------------------------------------------------------


AAC62613        ------------------
CIL1            ------------------
AAM65781        ------------------
NP_566763       ------------------
BAB09428        ------------------
NP_191466       LAFHSYHHPSTSIAATAA 466
AAL57706        ------------------
NP_199564       ------------------
AAM64730        ------------------
CAC37356        ------------------
AAM61181        ------------------
BAC01247        ------------------
NP_191734       ------------------
NP_566313       ------------------
```

Figure 9.1 Multiple sequence alignment (ClustalW) of possible dopamine binding domains, based on the publication of Verelst and Asard (2004). AIR12 accession number AAC62613. The NP_191734, NP_566313, AAL57706, NP_199564, AAM64730, AAM65781, NP_566763, NP191466, AAM61181, BAB09428 amino acid sequences from *Arabidopsis thaliana*, the CAC37356 amino acid sequence from *Solanum tuberosum*, the BAC01247 amino acid sequence from *Oryza sativa*, and the CIL1 amino acid sequence from *Brassica carinata* were compared in the alignment.

"-" Regions of an amino acid sequence that did not align to the consensus.
"*" Residues are identical in all sequences in the column.
":" Conserved amino acid substitutions observed in the column.
"." Semi-conserved substitutions present in the column.

A.

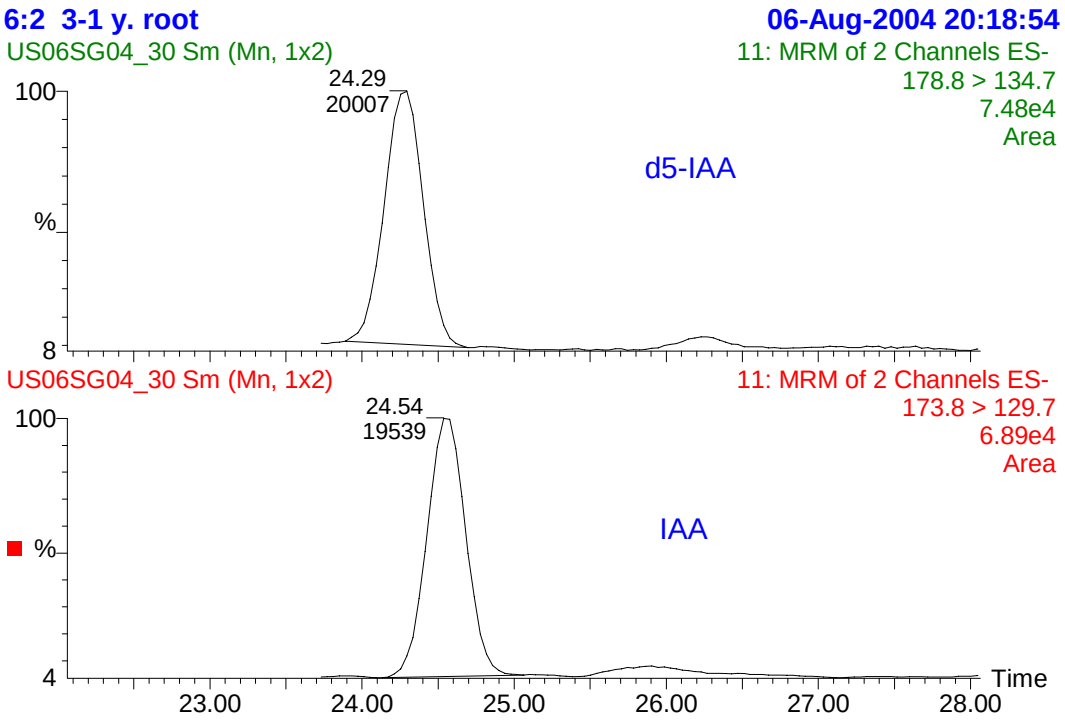
6:2 3-1 y. root
06-Aug-2004 20:18:54
US06SG04_30 Sm (Mn, 1x2)
11: MRM of 2 Channels ES-
178.8 > 134.7
7.48e4
Area
24.29
20007
d5-IAA
100
%
8
US06SG04_30 Sm (Mn, 1x2)
11: MRM of 2 Channels ES-
173.8 > 129.7
6.89e4
Area
24.54
19539
IAA
100
%
4
Time
23.00
24.00
25.00
26.00
27.00
28.00

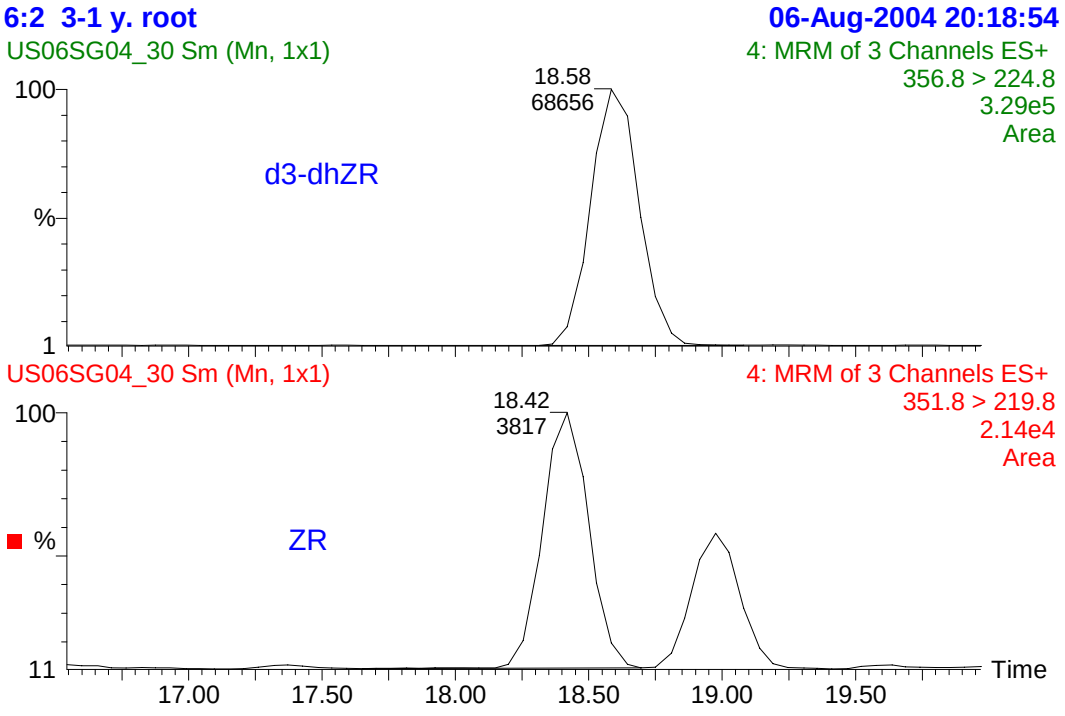
6:2 3-1 y. root
06-Aug-2004 20:18:54
US06SG04_30 Sm (Mn, 1x1)
4: MRM of 3 Channels ES+
356.8 > 224.8
3.29e5
Area
18.58
68656
d3-dhZR
100
%
1
US06SG04_30 Sm (Mn, 1x1)
4: MRM of 3 Channels ES+
351.8 > 219.8
2.14e4
Area
18.42
3817
ZR
100
%
11
Time
17.00
17.50
18.00
18.50
19.00
19.50

B.

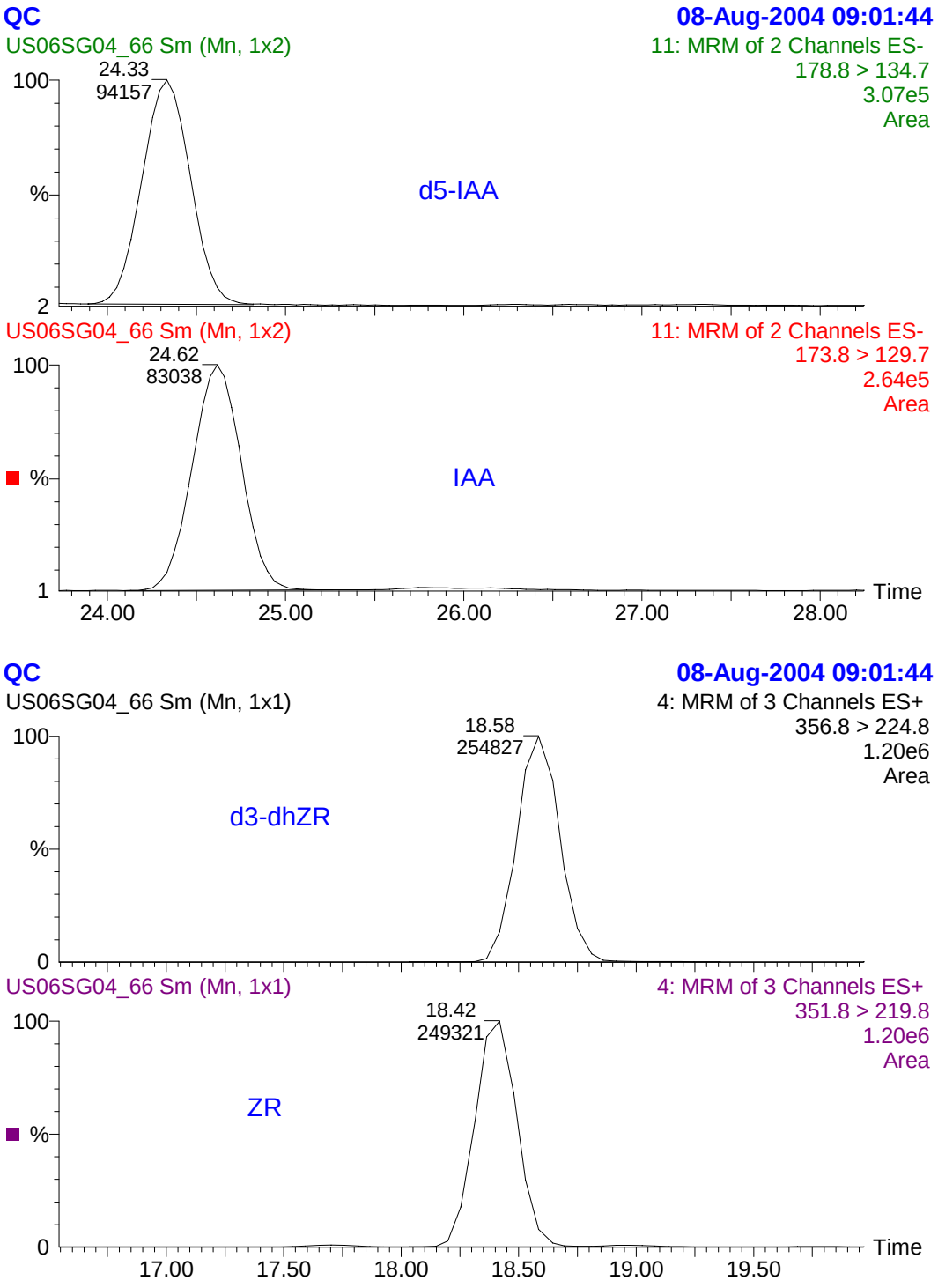

Figure 9.2 Chromatograms demonstrating typical mass spectra for d_5-IAA, IAA (upper panels in A, B) and for d_3-DHZR, DHZR in both 31 day-old root samples or quality control samples.

Table 9.1 Values used to construct the phytohormone profiling graphs. All values were measured ng/g dry weight.

A.

Indole-3-acetic acid			Mean	STDEV	SE
Non-transformed		1st leaf	199.33	71.06	41.03
		Stem	703.67	129.83	74.96
		Root	895.67	303.65	175.32
		LM	38.21	3.60	2.08
		SAM	23.25	2.00	1.15
Line 2		1st leaf	170.00	34.12	19.70
		Stem	628.33	267.87	154.66
		Root	338.33	28.02	16.18
		LM	50.90	31.93	18.44
		SAM	45.96	14.30	10.11
Line 3		1st leaf	243.00	46.70	26.96
		Stem	694.33	119.14	68.79
		Root	434.00	78.26	45.18
		LM	24.94	0.00	0.00
		SAM	29.54	5.04	3.56
Line 5		1st leaf	165.00	26.85	15.50
		Stem	25.77	7.83	5.54
		Root	12.52	7.98	5.64
		LM	39.18	23.46	16.59
		SAM	29.78	4.48	3.17
Line 6		1st leaf	230.00	19.67	11.36
		Stem	278.33	67.52	38.98
		Root	236.33	48.58	28.05
		LM	38.54	13.94	9.86
		SAM	27.01	10.37	7.34
Line 10		1st leaf	154.00	0.00	0.00
		Stem	519.00	113.21	65.36
		Root	220.67	42.19	24.36
		LM	32.73	4.28	2.47
		SAM	22.92	0.00	0.00
Line 13		1st leaf	166.67	16.77	9.68
		Stem	761.00	88.61	51.16
		Root	607.00	267.28	154.31
		LM	20.61	4.84	2.79
		SAM	22.34	1.81	1.05

B.

Zeatin Riboside (not logarithmically corrected)		Organ	Mean	STDEV	SE
Non-Transformed		1st leaf	8.60	0.42	0.2500
		Stem	140.0	21.21	12.25
		Root	34.75	17.47	10.08
		LM	13.47	5.59	3.220
		SAM	14.13	2.91	1.68
Line 2		1st leaf	9.35	0.90	0.52
		Stem	15.05	7.03	4.06
		Root	8.50	1.91	1.10
		LM	10.80	7.27	4.20
		SAM	118.07	64.46	37.21
Line 3		1st leaf	8.15	0.24	0.14
		Stem	22.83	10.32	5.96
		Root	20.23	4.74	2.74
		LM	320.93	295.31	170.50
		SAM	195.04	154.74	89.34
Line 5		1st leaf	9.16	0.73	0.42
		Stem	110.54	28.25	16.31
		Root	5.02	2.50	1.44
		LM	22.34	5.25	3.03
		SAM	346.55	89.84	51.87
Line 6		1st leaf	8.71	0.24	0.14
		Stem	8.00	0.02	0.01
		Root	11.97	0.71	0.41
		LM	22.33	11.34	6.55
		SAM	172.27	34.17	19.73
Line 10		1st leaf	3.72	0.84	0.49
		Stem	20.00	10.04	5.80
		Root	11.22	1.62	0.93
		LM	11.53	1.33	0.77
		SAM	154.34	18.99	10.96
Line 13		1st leaf	9.07	0.25	0.14
		Stem	203.00	33.78	19.50
		Root	16.25	8.70	5.02
		LM	9.95	3.94	2.27
		SAM	201.06	212.20	122.52

C.

Abscisic Acid		Organ	Mean	STDEV	SE
Non-Transformed		1st Leaf	584.50	4.95	42.58
		Stem	589.67	80.08	36.74
		Root	295.50	13.44	7.31
		LM	2127.73	433.82	306.75
		SAM	2731.56	575.57	406.99
Line 2		1st Leaf	413.33	73.76	27.91
		Stem	975.00	63.64	115.55
		Root	70.60	12.66	21.20
		LM	685.22	263.97	152.40
		SAM	1472.86	396.69	229.03
Line 3		1st Leaf	384.00	39.96	2.86
		Stem	238.00	48.28	46.23
		Root	110.80	37.41	7.76
		LM	843.41	13.61	7.86
		SAM	1748.01	757.14	437.14
Line 5		1st Leaf	456.50	95.46	23.07
		Stem	572.43	288.92	166.81
		Root	190.27	90.93	52.50
		LM	1836.87	625.27	361.00
		SAM	1783.63	432.60	249.76
Line 6		1st Leaf	719.33	94.13	55.11
		Stem	564.00	83.50	77.17
		Root	184.50	41.72	37.60
		LM	1126.17	418.64	241.70
		SAM	1897.90	181.51	104.80
Line 10		1st Leaf	156.99	22.61	13.06
		Stem	745.33	133.66	27.87
		Root	139.95	65.12	21.60
		LM	788.65	130.07	75.10
		SAM	1399.41	43.72	25.24
Line 13		1st Leaf	410.67	48.34	54.35
		Stem	756.33	200.14	48.21
		Root	149.00	36.72	24.09
		LM	901.39	31.59	18.24
		SAM	1487.96	163.07	94.15

D.

Dihydrophaseic Acid		Organ	Mean	STDEV	SE
Non-Transformed		1st Leaf	1129.67	155.73	89.91
		Stem	6823.33	1410.30	814.23
		Root	2786.67	991.68	572.55
		LM	2553.28	200.89	142.05
		SAM	8255.73	1910.58	1350.98
Line 2		1st Leaf	1097.33	139.00	80.25
		Stem	3646.67	427.82	247.00
		Root	643.00	371.94	214.74
		LM	2701.57	314.10	222.10
		SAM	10180.73	4586.18	2647.83
Line 3		1st Leaf	1886.67	400.04	230.96
		Stem	1800.00	304.47	175.78
		Root	1836.67	476.48	275.10
		LM	4308.01	2944.18	1699.83
		SAM	7921.23	2326.84	1343.40
Line 5		1st Leaf	1080.00	186.82	107.86
		Stem	8995.52	4898.93	2828.40
		Root	539.86	558.35	394.81
		LM	4921.94	4027.39	2325.21
		SAM	12957.12	7539.50	4352.93
Line 6		1st Leaf	640.33	130.22	75.18
		Stem	1833.33	388.12	224.08
		Root	1315.00	289.91	167.38
		LM	3348.28	1460.60	843.28
		SAM	7779.03	3422.23	1975.83
Line 10		1st Leaf	3421.31	194.65	137.64
		Stem	2113.33	340.34	196.50
		Root	1373.00	717.01	413.96
		LM	3828.59	22.45	15.88
		SAM	8070.81	5622.38	3246.08
Line 13		1st Leaf	1003.00	405.46	234.09
		Stem	1463.33	219.39	126.67
		Root	1425.00	388.91	224.54
		LM	3097.17	1114.31	787.94
		SAM	13516.00	485.93	343.60

IAA = Indole-3-acetic
ZR = Zeatin riboside
ABA = Abscisic acid
DPA = Dihydrophaseic acid
1st Leaf = 21-day old first leaf
Stem = 31-day old stem
Root = 31-day old root
LM = 31-day old lateral meristem
SAM = 31-day old shoot apical meristem

Table 9.2 High Performance Liquid Chromatography conditions used in phytohormone experiments.

Compound	Acetonitrile	H_2O	Glacial Acetic Acid 5% H_2O	Methanol	
Time (min.)	A%	B%	C%	D%	Flow (mL min^{-1})
0.00	2.0	94.2	0.8	3.0	0.200
2.00	2.0	94.2	0.8	3.0	0.200
10.00	5.3	85.9	0.8	8.0	0.200
10.10	8.0	85.9	0.8	5.3	0.200
14.50	13.2	73.2	0.8	12.8	0.200
36.75	26.4	55.2	0.8	17.6	0.200
45.75	34.1	42.5	0.8	22.6	0.200
45.95	60.0	0.0	0.8	39.2	0.350
48.95	60.0	0.0	0.8	39.2	0.350
49.15	2.0	94.2	0.8	3.0	0.200
57.15	2.0	94.2	0.8	3.0	0.200